Recycling of Composite Materials using Fluidised Bed Processes

Neal Fenwick

AMIMechE   MSc   BEng

CONTENTS

Chapter 6 Composite Scrap Thermal Decomposition Model 55

ABSTRACT

Lightweight engineering plastics have been increasingly used in automotive applications[3], this tends toward more fuel efficient vehicles[1]. Glass reinforced plastics commonly include thermosetting polymers. These cannot be re-moulded, unlike thermoplastics, thus thermoset scrap is currently disposed of in landfill. This is increasingly targeted by legislation[14] and is becoming more expensive. This thesis describes work to maximise resource recovery from scrap thermoset composites.

A review of relevant literature identified thermal processes for treating scrap thermoset composites. Combustion is particularly suitable for the mixed and contaminated materials arising from end of life vehicles. The literature showed that heating glass fibres reduced their properties, which is a concern for any thermal recycling process.

The methodology of this work is to recover energy from the composite polymer and reuse the incombustible residues. Two experimental processes are reported:

Fluidised Bed Co-combustion of Thermoset Composites with Coal.
The common composite filler of calcium carbonate captures the sulphur emissions from the coal combustion. Results show that scrap composites can successfully be burned in a commercial scale fluidised bed. Retention of the sulphur from the coal by the composite filler was up to 75% of the input. Although a technical success, economic analysis shows this disposal to be unviable compared with similar desulphurisation via crushed limestone.

Fluidised Bed Thermal Processing Rig for Recovering Glass Fibres.
The incombustible constituents of a crushed Sheet Moulding Compound were released from processing above 400°C in the fluidised bed test rig. The reinforcing glass fibres were elutriated as monofilaments, suitable for use in a veil product, and recovered from the flue gases. Scanning Electron Microscopy showed that the fibres were intact. The tensile strength of fibres from 450°C processing was reduced by approximately 50% and by 90% from 650°C[73]. Strength was also found to reduce with increasing time at a temperature[76].

Flue gas analysis showed that carbon monoxide and hydrocarbons were present. This

indicated that full combustion did not take place and the associated heat energy lost. Measured nitrogen oxides and sulphur dioxide concentrations were low.

After initial testing, the test rig was refined by the incorporation of a Rotating Screen Collector to separate the fillers and fibres. The fibre contamination was reduced by 50% via this novel equipment. Fibre recovery rates of up to 57% were achieved.

Resin Decomposition Model.

Results indicate that the resin endothermic energy of decomposition maintained the temperature of the Sheet Moulding Compound significantly below the bed temperature.

ACKNOWLEDGEMENTS

GLOSSARY

Arrhenius:	decay applied to chemical and physical reactions
BMC:	Bulk Moulding Compound
Ca/S:	calcium to sulphur ratio, used to rate sorbent performance
CFRP:	carbon fibre reinforced plastics
DMC:	Dough Moulding Compound
elutriation:	process of carrying material out of fluidised bed with fluid
EC:	European Community
ERCOM:	German company that markets recyclate
freeboard:	region above fluidised bed
FID:	Flame Ionisation Detection
FRP:	fibre reinforced plastics
GRP:	glass reinforced plastics
leachate:	liquid effluent extracted from landfill by ground water
micrograph:	photograph taken of a Scanning Electron Microscope screen
NO_x:	nitrogen oxides
PAF:	primary air-fuel ratio
PMMA:	Polymethyl methacrylate
ppm:	parts per million
PU:	polyurethane
RRECOM:	Recycling and Recovery from Composite Materials
SMC:	Sheet Moulding Compound
STP:	standard temperature and pressure
thermoset:	polymer type that does not melt on application of heat
thermoplastic:	polymer type that can be remelted
Weibull analysis:	a statistical technique used for fitting a characteristic value to a data range

NOMENCLATURE

A:	pre-exponential factor	s^{-1}
Bi:	Biot number	
C_d:	discharge coefficient	
Cp:	specific heat capacitance	J/kg.K
CV:	calorific value	kJ/kg
d_{CaO}:	density of CaO grain	kg/m^3
d:	particle diameter	m
D:	cyclone diameter	m
E:	activation energy	kJ/mol.K
F:	fraction of range failed in Weibull analysis	
Fo:	Fourier number	
FR:	feed rate	kg/s
g:	gravitational acceleration	m/s^2
h:	heat transfer coefficient	$W/m^2.K$
k:	thermal conductivity	W/m.K
K:	reaction rate constant	s^{-1}
L:	characteristic dimension	m
m:	mass	kg
n:	order of reaction	
N_{st}:	Stokes number	
ΔP:	pressure difference	Pa
Q:	heat (input)	kJ
Qp:	endothermic energy	kJ/kg
R:	universal gas constant	kJ/kmol.K
Re:	Reynold's number	
r_g:	radius of CaO grain within calcine particle	m
s:	tensile strength	GPa
$R\eta$:	retained Weibull Modulus	GPa
S_g:	specific surface area	m^2
T:	temperature	°C
ΔT:	temperature difference (to ambient)	°C
t:	time	s

Δt:	time increment	s
u:	cyclone inlet velocity	m/s
U:	fluidising velocity	m/s
x:	distance	m
Δx:	node spacing	m
Z:	Cyclone pressure coefficient	
%:	percentage composition	%

α:	fraction decomposed	
β:	heating rate	°C/s
	and Weibull shape parameter	
ε:	bed void fraction	
η:	efficiency	%
	and Weibull Modulus	GPa
μ:	dynamic viscosity	kg/m.s
ϱ:	density	kg/m^3
ϕ:	sphericity of a particle	

Subscripts:

c:	coal
cn:	carbon
CO_2:	carbon dioxide
f:	cyclone fines
g:	gas
s:	surface or solid
sc:	scrap composite
l:	losses
mf:	minimum fluidising condition
N:	nitrogen
O:	oxygen
op:	operating fluidising condition
Orif:	orifice value
dist:	FB distributor value
R, r:	radiative
WV:	water vapour

Chapter 1
INTRODUCTION

1.0   Overview

This introduction presents the problem that will be addressed by this thesis and the justification for undertaking the work. As the thesis was completed as part of a larger research project, a brief description of that has been included as background. The chapter concludes with a preview of the contents of subsequent chapters.

1.1   The Problem Being Addressed

A method of recovering value, recycling in the broadest sense, from scrap composite thermoset plastic materials was required. The current method of disposal is to landfill the scrap. This problem is particularly applicable to the automotive industry, which has the potential to generate large quantities of thermoset waste when vehicles are scrapped.

1.2   Evidence for the Necessity of the Work

Plastics are attractive materials for construction of vehicles and have been increasingly used in automotive applications. This is due to cost savings on tooling during manufacture, leading to low volume marque production being more economic with polymeric components.

The use of lighter weight polymeric components leads to more fuel efficient vehicles[1]. This is of particular interest in light of recent UK Government figures[2], which show that fuel use for road transport has risen by nearly 20% since 1970, and currently accounts for 25% of total energy consumption.

1.2.1 Increasing use of polymers in automobiles

Figure 1.1 shows the growth in thermoset polymers used per car[3]. Cars containing such quantities of thermoset polymer can be profitably processed by metal reclamation companies, although concern has been expressed[4] about reduced profitability. Analysis of Figure 1.1 shows that the thermoset content of a car increased by 185% during the ten year period from 1980 to 1990. Over the same period the growth in composites was lower at 167%.
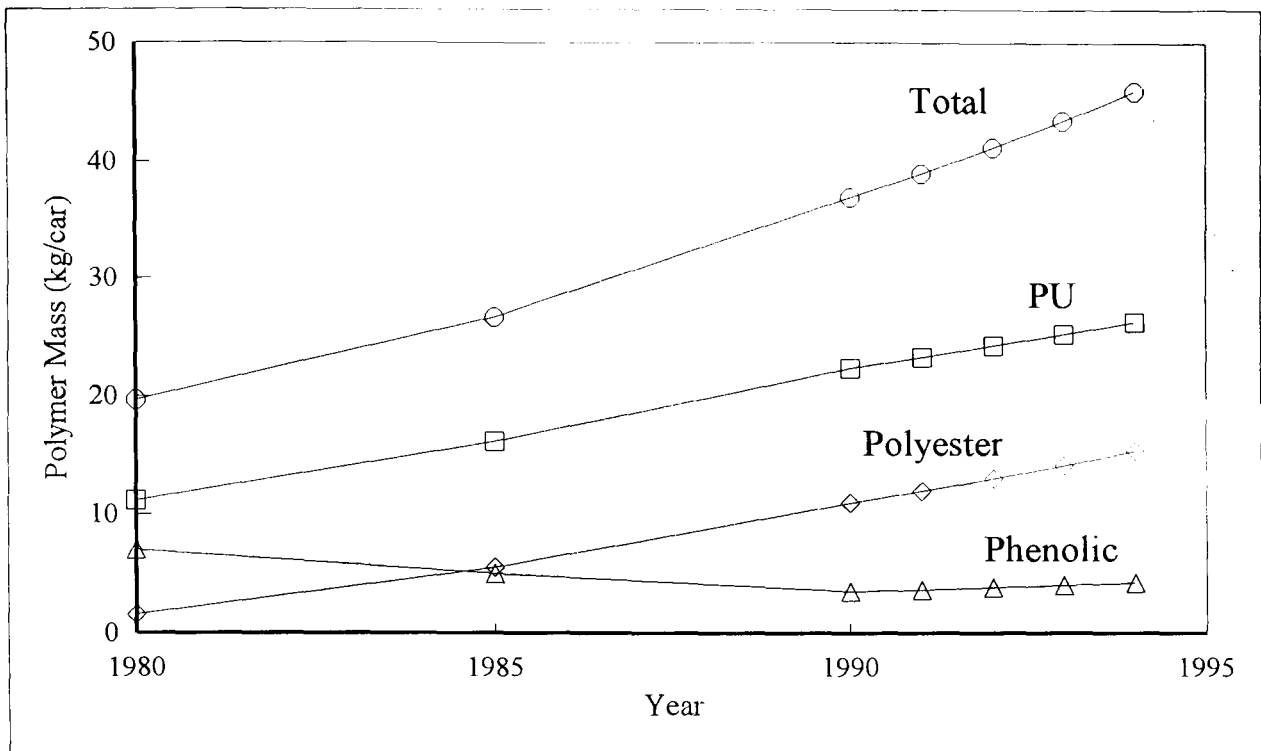
Figure 1.1   Changes in the Proportion of Thermoset Polymers in New Cars.
Showing the increased use of thermoset components in automotive construction over recent years.
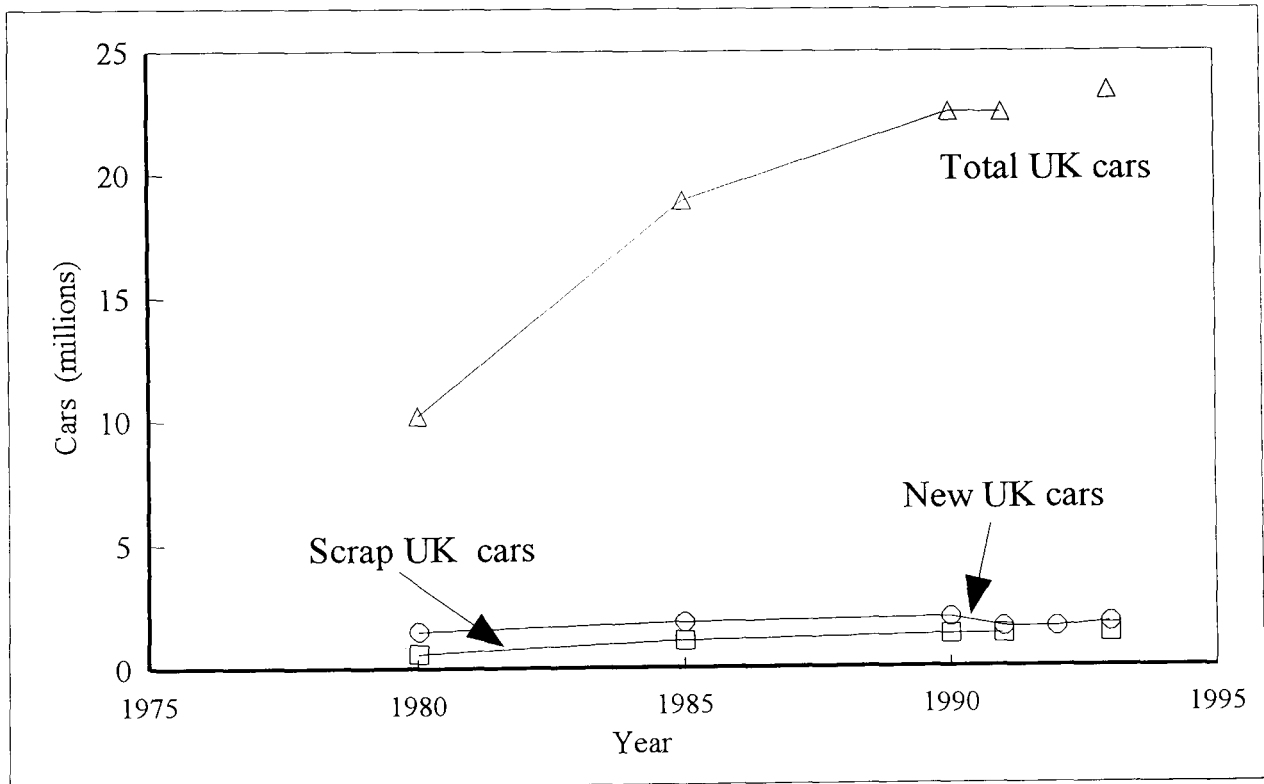
Figure 1.2   Changes in the Number of Cars in the UK.
The number of scrapped vehicles is consistently lower than the number of newly registered vehicles, resulting in the steady increase of vehicles on the road.

However, it must be remembered that the values in figure 1.1 are polymer masses and thus in the case of composites will only be a proportion, often 30% or less, of the total component mass. This is due to composites often being highly filled with a cheap finely divided mineral, in addition to the reinforcing fibres.

1.2.2 Growth in vehicle numbers

In 1991, 1.6 million new cars were registered[5], the UK had 22.5 million registered cars and 1.31 million vehicles were scrapped[6], see Figure 1.2. Assuming an average 10 year product life, then Table 1.1 shows a 170% increase in automotive thermoset scrap from 1991 to 2003. These figures show a compounded impact on thermoset polymer waste from automotive components, i.e. increased vehicle numbers with an increased proportion of thermoset components.

Table 1.1   Change in the Proportion of Automotive Thermosets over 10 Year Product Life Significantly Increases Thermoset Scrap.

Year		1981	1991	1993	2003
Thermoset content kg/car	manufactured	22		43.4	
	scrapped		22		43.4
New registrations (millions)		1.48	1.6	1.78	
Cars scrapped (millions)			1.31		1.46
Thermoset waste (10^6 kg)			28.8		63.4

1.2.3 Environmental benefits of polymeric materials in vehicles

Vehicle Emissions

Over the life of a car, the greatest energy consumption, including production, is during customer operation[7]. The use of lightweight materials has a significant impact on reducing the fuel consumption during this energy expensive period. Despite this, modern cars are increasing in weight due to having more comfort and safety features. Such weight increases have been reduced by the use of polymeric components. However, average car fuel economy has still fallen since 1987, despite improving by 20% from 1978 to 1987[8]. Currently, the emissions from cars account for 12% of European emissions of CO_2[8]. Any weight associated energy savings are not directly beneficial to the motor manufacturer, but may impact on sales

as environmentally-friendly attributes are increasingly key selling points.

Manufacturing production

The control of costs is vital to the survival of any company manufacturing large numbers of products. The majority of the literature suggests that the tooling for plastics forming is usually considerably cheaper than that required for metals[6]. This supports the business decisions resulting in the actual growth in the use of composites. However, one reference proposed that composites were not used at high levels because the manufacturing costs tended to be higher[9] for polymeric components.

1.2.4 Existing thermoset scrap disposal

Automotive scrap

The traditional disposal route for scrap vehicles depends on a market for the waste stream at each stage of the disposal from the final vehicle owner, via a breaker to final disposal at a metals reclamation company. This market demand ensures profitability for the individuals and companies involved at each stage. The charges incurred for disposing of non-recyclable scrap in landfill are a cost to the metals reclamation companies, reducing the revenue from the recycled metals. The existing disposal route is threatened at the metals reclamation stage by the increased use of polymeric materials and thermosets in particular. There is currently no market for thermoset scrap[9], so the disposal of this material is a direct cost, unless a recycling process can define a value for the non-metallic components. Table 1.2 shows the revenue from the shredding industry from the use of automotive polymeric components. This will increase with the UK landfill tax implementation in October 1996.

Table 1.2   Lost Revenue for the Metals Reclamation Industry due to Reduced Metallic Content and Disposal of Automotive Thermosets.

Steel scrap value lost if polymer component used[10]	£/kg	0.225
1995 Landfill disposal cost[11]	£/kg	0.016
Lost revenue	£/kg	0.241
1991 Mass of thermoset per vehicle	kg/car	22
1991 Vehicles scrapped	million vehicles per annum	1.31
Scrapped thermoset	10^6 kg/annum	28.8
1991 Lost revenue due to use of thermosets	£ million	6.94

Manufacturing scrap

Traditionally, manufacturing scrap has been landfilled and is thus subject to the same market forces as post consumer scrap. One alternative is grinding the well characterised scrap for use as a filler by companies like ERCOM Composite Recycling GmbH (see Chapter 2).

1.2.5 Research and design for scrap disposal

If car transportation is to continue as a major people mover, with reasonable sales growth, then enviro-economic pressures will require the increased use of polymers in new designs. But in order to get beyond the design stage, an acceptable scrap disposal route must be identified during design. Often, within large manufacturing companies, a Life Cycle Analysis must be completed prior to the release of a new product. Thus research into appropriate disposal methods has to be completed some 10 years before the volume disposal actually becomes a problem.

If research into recycling processes is not done then there will be pressure not to use materials, irrespective of any benefits, that cannot be recycled from post consumer scrap. This may already be the case with aluminium, an alternative lightweight material that has much less recycling problems. The growth in the use of aluminium is projected as 56% between 1991 and 2000[12] compared with 22% for composites from 1990 to 1994 despite more expensive tooling.

Thus, the increased utilisation of thermosets, without due consideration to final disposal, will distort the traditional disposal mechanism. The profit margin of the metals reclamation companies will be reduced, perhaps to an extent that the current market driven disposal route collapses. Then legislation will have to be used to enforce where the market cannot operate if a return to the abandoned car hulks of the 1950s is to be avoided.

1.2.6 Legislation changes

Europe

The European recycling effort has largely been driven by the threat of Draconian laws in Germany, that - it was assumed - would become the European Community standard. These have been held as consultation documents for a number of years and led to the formation of ERCOM in 1991. The actual German legislation was passed in 1994 and comes into effect in 1996, when a product's disposal will be the responsibility of the producer (not the material

supplier), i.e. if a material cannot be recycled it is unlikely to be specified for a component. The German automotive reuse and recovery goals are 20% polymers for 1997 and 80% by 2000[13]. This is the only European legislation to break automotive waste down by type, other countries specify reducing the proportion of material going to landfill.

UK landfill tax

This was introduced on 1 October 1996 and will add economic pressure to the reduction and recycling of all waste that has traditionally gone to landfill. The cost is projected as £ 7 per tonne for the standard rate[14] and £ 2 per tonne for inactive wastes, although very few materials will be classified as such. Such costs are still significantly cheaper than £ 10 to 41 per tonne for hazardous waste in Germany[15]. Recycling processes are currently more expensive than landfill charges. But, increasing landfill charges due to legislation changes could shift the economic balance to the commercial application of research.

1.3   Background to the Current Work

1.3.1 Project history

Research projects at The University of Nottingham have been investigating methods of disposing of scrap thermosets since 1988. Initially this work was funded by a consortium of companies[1]. In November 1994 a DTI and EPSRC supported LINK project was awarded jointly to Nottingham and Brunel Universities, supported by a larger group of companies[2].

1.3.2 Previous work at The University of Nottingham

The early work considered a wide range of disposal options for scrap thermosets reported in the PhD thesis of M.Benson[16]. Those relevant to the current work are:

Combustion

Combustion with heat recovery is a method of recovering the energy content of the polymer. It is suitable for large quantities of material and is not particularly sensitive to the purity of

---

1   Dow Plastics, DSM Resins, Ford Motor Company, GKN Technology, Jaguar Cars, Lotus Cars, Perstorp and PSA Citroën.

2   Alcan Chemicals, Autopress Composites (DSM), Balmoral Group, BIP Plastics, Cray Valley, Croxton and Garry, Dow Chemical, Filon Products, Ford Motor Company (including Jaguar Cars), GKN Technology, Laminated Profiles, Owens-Corning, Permali, Rover Group and Scott Bader.

the scrap. However, due to the high proportions of incombustible filler in composites, a high percentage of the original mass, typically 70%, remains as ash for subsequent disposal. Thus for an acceptable combustion disposal process, the fillers and fibres must be recycled in some way.

Traditionally, combustion has been considered throughout Europe as an unacceptable method of processing waste materials. Indeed, the standard disposal hierarchy has energy recovery as the last option before landfill. More recently, both technical and public opinion is beginning to see the advantages of combustion as a suitable and environmentally acceptable method of treating waste. A 1993 report[17] concluded that the incineration of waste ought to have an important and growing role in the strategy of waste management and incineration is sometimes less expensive compared with landfill.

Draft European legislation allows energy recovery only when recycling is not yet technically feasible or when recycling would create a heavier impact on the environment[18]. The latter may well be the case for thermosets, where one feasible method of recycling is via a combustion process.

Fluidised bed combustion

As a process medium, fluidised bed combustion is an efficient method of burning materials of low calorific value at modest temperatures. Literature also shows that fluidised bed processes can be used for the separation of mixtures (see Appendix 1). Thus, fluidised bed combustion was considered for simultaneous polymer combustion and material separation of composite scrap as the churning motion of the bed would aid the breakdown of the composite.

Crushed limestone is added to the bed in fluidised bed coal combustion plant to reduce the emissions of sulphur oxides in the flue gases. Thermosets containing calcium carbonate filler have the potential to act in the same way as limestone.

1.4   Overview of Thesis

The work presented in this thesis continues the previous research with fluidised bed combustion technology.

1.4.1 Objectives in this thesis

The objective of this work is to investigate the use of fluidised bed thermal processes to address the problem of recycling scrap thermoset composites. The scrap used in these investigations is comprised of a polyester resin matrix reinforced with E-glass fibre roving and filled with calcium carbonate. Two types of scrap are used, a Dough Moulding Compound (DMC) and a Sheet Moulding Compound (SMC). The composition of these materials is given in Chapter 3.

The simultaneous combustion of the polymer with recovery of the fillers and fibres is researched. Initially, the use of composites filled with calcium carbonate in place of limestone is investigated as a de-sulphurisation agent for coal combustion. Subsequently, a fluidised bed combustion test rig was designed and commissioned by the author to investigate the recovery of high quality glass fibres for reuse.

1.4.2 Chapter summary

Chapter 2

This Chapter reviews the relevant literature, including a survey of the current commercial methods of disposal of scrap composites. This is contrasted with the research work in the field.

Chapter 3

This Chapter presents commercial scale test work of the co-combustion of glass reinforced composite scrap with coal in a fluidised bed fired boiler. The work aims to use the calcium carbonate filler of crushed scrap Dough Moulding Compound (DMC) and Sheet Moulding Compound (SMC) as a de-sulphurisation agent for the gases evolved from combustion of the coal.

Chapter 4

This Chapter details the technical design of a fluidised bed test rig based on the findings of the work reported in Chapter 3. The equipment was designed for this study to investigate whether the glass reinforcing fibres could be recovered intact from the scrap SMC.

Chapter 5

This Chapter contains the strategy for testing the rig and the analysis techniques used for characterisation of recovered materials are described.

Chapter 6

This Chapter introduces a one dimensional model for predicting the thermal decomposition of a composite within a fluidised bed.

Chapter 7

This Chapter discusses the results from test work processing scrap composites in the fluidised bed rig compared with stated success criterion.

Chapter 8

This Chapter states the original aspects of this study and the conclusions before recommending further work.

Chapter 2
LITERATURE REVIEW

2.0   Introduction

This literature review was undertaken to identify the key aspects to be considered when devising a process to recycle scrap composites. The points that were investigated include:

- The current commercial methods that are used for thermoset disposal. These have traditionally been limited to landfilling the composite scrap after any other reclamation operations have been performed. More recently, other commercial recycling interests have arisen based on grinding scrap for use as a filler.

- Recycling processes identified in research studies; these are typically based on grinding the scrap for use as a filler or some form of thermal treatment.

- The effect of heating on the physical properties of glass fibres; a major consideration for a thermal recycling process.

Other literature reviews on specific technical studies are included as appendices and are referenced in later chapters. The concluding remarks in Section 2.4 define the experimental investigations of this thesis.

2.1   Current Disposal of Scrap Thermoset Plastics

Thermoset plastics, unlike thermoplastics, have the reputation of not being suitable for recycling, even within the plastics industry itself[19]. Automotive thermoset composites are currently left on the scrap vehicle and are landfilled along with other non-metallic materials after metal reclamation. This is a cost to the vehicle disposal industry which will increase with the proportion of polymers in automotive construction. It is worth re-iterating that successful recycling processes are required to stimulate growth in the use of thermoset composites.

2.1.1 Landfill

Disposal by landfill currently accounts for the bulk of automotive polymers which become scrap at the end of a vehicle's life. The composition of the mainly non-metallic residue remaining after metal reclamation is very variable, as indicated in Table 2.1. There are also quantities of heavy metals which are of concern to any disposal process, eg: cadmium (67 ppm), antimony (180 ppm), chromium (340 ppm) and cobalt (24 ppm)[6].

Table 2.1 Material Constituents of Automotive Waste after Metal Reclamation

This indicates the wide range of composition of the metal reclamation residue from three references.

Component	Mass range[7] (%)	Mass[20] (%)	Mass[21] (%)
metals	3 -14	5.2	8.1
plastics	4 -14	15.4 (0.5 composites)	19.3
linoleum	1 - 17	-	-
foam (etc)	2 - 4	8.5	2.2
rubber	2 - 6	22.5	5.3
wood	1 - 3	7.1	2.2
paper	1 - 9	3.8	6.4
textiles (inc carpet)	2 - 4	29.9	45.1
misc	3 - 40	0.2 (glass)	3.5 (glass), 2.1 (wiring), 5.8 (tar)
fines (size undefined)	30 - 45	7.5	-

The constituents of the metal reclamation residue are intimately mixed, very difficult to separate and often have low scrap values. If a recycling process was directed at a particular component or metal reclamation residue constituent, then the process must be able to cope with the rest of the residue as a contaminant. Alternatively - the targeted constituent must be separated from the waste stream before metal reclamation.

Lost material added value by landfill disposal of composites

Considering a component made from Sheet Moulding Compound (SMC) to represent a typical automotive thermoset composite. Then, the energy expended to produce the polymer for an automotive thermoset composite has been estimated as 45 MJ/kg[22]. Thus the scrap quantity of 3×10^6 kg (see 1.1.2) represents approximately 135×10^6 MJ material added value buried without return each year.

If the most basic recovery technique of combustion were applied to the 7×10^5 tonnes[6] metal reclamation residue sent to UK landfill per year, then the potential heat recovered could be 1×10^{10} MJ p.a. (at a mean calorific value of 14.6 MJ/kg[6]). The UK figure is only a third of the US and Canada value of 3.1×10^{10} MJ[22]. Of the UK total, 1.2×10^7 MJ[20] can be attributed to thermosets. This is small due to composites containing high proportions of incombustible filler. Thus for the thermoset waste stream, combustion alone is not an effective process as virtually the same volume remains as ash for landfilling. A process which recovered both energy and materials is more suitable and economical.

Discussion of disposal of automotive metal reclamation residue in landfill

Metal reclamation residue is used as a day-cover for landfill dumps to prevent loss of friable materials. A concern over such use is that the metal reclamation residue is often contaminated with heavy metals, oils and other automotive fluids which could leach into ground water[6]. Reference 6 reports earlier work by the Warren Spring Laboratory which found that toxic metals in metal reclamation residue leachate were at a similar level to that from domestic rubbish. However, the chemical oxygen demand of the leachate was higher than the level permitted for effluent in sewers.

For comparison, a review of metal reclamation residue in landfills by Day[23] showed that the concentrations of species in leachate is a function of the method of measurement. Further testing showed that metal reclamation residue could actually be used to fix lead compounds which would otherwise leach into ground water. Following a number of leachate tests, Day concludes that metal reclamation residue could be viewed as a potentially valuable resource to act as a decontaminant medium that could be used in landfill operations for its beneficial effect. However, 2%[24] of the lead was not fixed and may produce a cumulative problem. The metal reclamation residue component that acted as the lead fixative is not identified and thus the thermosets could be removed from the system without loss of lead fixation properties. While homing in on the beneficial property of retaining lead compounds, the other potentially harmful heavy metals were not considered. This debate may prove to be academic when facing a hostile public combined with increasing landfill costs and reducing landfill site availability.

2.1.2 Recycling thermoset composites

Regrind

One recycling method for thermosets which has commercial interest is the re-compounding of ground up composite scrap, termed recyclate, as a replacement for mineral filler. The physical form of the recyclate influences the properties of the resulting material. For example, if the recyclate is still fibrous, it can add reinforcement. If this is the case then the economics are more favourable as glass roving at £1.4 /kg[24] is significantly more expensive than calcium carbonate filler at £0.06-0.30 /kg[24]. Thus replacing a quantity of reinforcing material will make the recycling process more viable than replacing some of the filler. Many research studies have been carried out into recycling ground thermoset waste. Some recent studies are summarised in Table 2.2.

Table 2.2 <u>Summary of Work into the Re-compounding of Ground Thermoset Scrap</u>

This demonstrates the range of material properties obtained by different research studies using recyclate as a filler.

BMC = Bulk Moulding Compound

Regrind Material	New Material	Regrind Quantity	Change in Physical Properties Compared with Control		Ref
ERCOM	SMC	10% regrind	flexural modulus	-12.4%	25
			flexural strength	+3%	
SMC	SMC	13% of filler	flexural strength	-6.3%	26
			Izod impact	+6.5%	
	SMC, class A	25% of filler	flexural strength	-12.1%	
			Izod impact	+2.6%	
SMC (coarse ground)	BMC 35% total glass	5% of filler	flexural strength	-7.7%	27
		30% of filler	flexural strength	-30.8%	
SMC fine SMC	SMC / BMC	20% (class A)	no change		28
coarse	BMC	40%	no change		

The ERCOM ground material used in reference 25 contained fibres shorter than 0.5mm and could be expected to impart little reinforcement, but the flexural strength was increased by 3%. There appears to be some variability in the results reported in the literature. Despite the

use of large particles (1.25 to 5.0 mm) in reference 27, the physical properties were reduced. This may indicates that there were few free fibres present. The positive result of reference 25 was confirmed by Konig[29] where the flexural strength was found to increase to a maximum with 15% ERCOM regrind. However, the increase was only 7.7% compared with the control.

The mechanical properties of a SMC[26] incorporating regrind were reduced, but adequate for use as a roof inner rack on a Toyota vehicle. No details were given as to the physical form of the regrind. By comparison the roughly ground material of reference 28 contained unbroken glass fibres which could still function as reinforcement. Indeed this was seen by the physical properties being unchanged compared to the control.

Generally, the literature suggests a reduction in composite properties on incorporation of regrind. A few notable exceptions are presented: Kawamura[28] claims no change, even up to a level of 40% addition. Also, the impact strength measured by Kitamura[26] actually increases on replacing filler with recyclate. If this were reproducible in a production environment, it could certainly be exploited.

If all the waste thermoset were incorporated into new composite products at a typical rate of 20%, the industry would be unsustainable. Reuse of recyclate at these rates implies a new production growth of 500% over the lifetime of the product. Even for long lived products, e.g. a car at ten years, the sales growth between 1980 and 1990 was 40%. Very high sales growth are associated with relatively new products, e.g. the car sales in the 1940s and 1950s.

Commercial operations
Thermoset waste is used as a raw material in the following patented processes:

i) BIP Plastics

Granulated phenolic production scrap is marketed as shot blast media. It has been found to be of the correct hardness to clean surfaces without damaging 'softer' substrate materials.

ii) ERCOM

This is a commercial venture set up in Europe to exploit the regrind technology. The

company has a mobile crusher which reduces the bulk volume of the material on-site prior to transportation. The collected waste is subsequently ground to produce different size fractions for use as reinforcement and filler in new composites. Production began in 1991 at a rate of 2000 tonnes per year using mainly production scrap, with the capacity to uprate to 6000 tonnes per year[30]. This is a modest process capacity compared with 232,000 tonnes[3] of reinforced composites produced in Europe for the transportation sector alone in 1992.

ii) Phoenix Fiberglass[31]

This is a Canadian company which operates on a similar basis to ERCOM. The plastic scrap is shredded into approximately 80 mm square pieces. This is then pulverised by a fiberiser - a vertical shaft machine with a number of swinging hammers. The fiberiser separates the fibres from the resin without heat generation or fibre damage. After the pulveriser, a number of sequential screens grade the waste and return it to the pulveriser if required. The pulveriser and sieves are air swept to prevent reprocessing any fibres and thus unnecessarily damaging them. After the final sieve a mill produces a filler substitute.

The pilot plant processed a maximum of 820 kg SMC per hour with the optimal output achieved at 680 kg per hour. Unfortunately, due to the slow specification of composites containing recyclate by car manufacturers, the plant was shut down in April 1996.

2.2   Research Work into Disposal of Scrap Thermosets

The majority of the above work on regrind has been completed as part of research programmes and only a small number of companies exist that exploit this technology. The industry is far from maturity and research continues to optimise the techniques used.

2.2.1 Thermal processing

Thermal processes that have been applied to plastic scrap include: incineration, pyrolysis, gasification, hydrogenation and combustion. References 6 and 32 are comprehensive review papers of the success of a variety of thermal processes going back to the 1970s (see the summary in Table 2.3). Most combustion research has optimised the process at a high temperature for high thermal efficiency. This leaves a low value incombustible residue as a hard glassy slag which may be used for aggregate.

Table 2.3 Summary of Thermal Processes[6,32] used for Scrap Composites or Similar Waste Streams.

P = pyrolysis,   D = domestic rubbish,   MR = metal reclamation residue

Process or Developer	Feedstock Type	Procedure	Products	Development stage and Year reported
KWU Process	plastics with D	P, indirectly heated rotary kiln, 450-500°C	energy	3 tonnes/hr, plant, Germany. 1992
Otto Noell Process	MR	P, indirectly heated rotary kiln, 650-700°C	pyrolysis oils, gas	6 tonnes/hr, plant, Germany. 1992
Tsukishima Ebara		P, two fluidised beds, one oxidising	energy	4 tonnes/hr, Japan. 1992
Hamburg Process (1976)	plastics, tyres, MR, sewage sludge	P, indirectly heated fluidised bed, 600-900°C	pyrolysis oils, gas, soot	20-60 kg/hr, Hamburg University. 0.5 tonnes/hr, ABB 0.5 tonnes/hr, MAG
Rotopyr	plastics, MR, cable scrap	P, indirectly heated rotating drum, 650°C	pyrolysis oils	200 kg/hr, pilot plant, Germany. 1982
SMCAA	SMC scrap	P, pyrolysis reactor, 700-980°C	oil and gas	commercial scale trials, USA. 1991.
Ford (USA)	plastics	P,	fuel oil	1980
Voest-Alpine	waste oils, MR	Gasification combustion chamber, 1600°C	fuel gas	400 kg/hr, Austria. 1991
Kobe Steel[33]	CFRP scrap	P, 400-600°C	carbon fibres	laboratory rig, Japan. 1994
Mitsubishi Heavy Industries[34]	GRP scrap	Steam gasification, kiln, 700°C	glass fibres, fuel gas for process heat	2 tonnes/day, pilot plant, Japan. 1993/1994
Stevens Institute[35]	SMC	P, 400°C in air	oil and glass fibres	bench top, USA. 1993
Peninsula Copper[36] Industries	GRP scrap (epoxy), SMC	Indirectly heated (454-565°) rotating calciner	glass fibres and gaseous fuel	2.5 kg fibres/hr, pilot plant, USA. 1990/1991

For the greatest economic viability, any residues should be in as high a value state as possible. This may be achieved at lower temperatures, providing that the thermal efficiency is not compromised, resulting in a less economic overall process. This route has been investigated in Japan[33,34] and the US[35,36] with lower temperature processes, aiming to recover fibres in as good a condition as possible. In reference 33, pyrolysis was investigated to recover carbon fibres from Carbon Fibre Reinforced Plastic (CFRP). Although the method quoted was heating the plastic in a stream of air and thus not strictly pyrolysis. Testing at a

temperature of 400°C did not fully break down the epoxy resin matrix. An optimum temperature of 500°C was found to remove the resin but avoid oxidation of the fibres, see Table 2.4.

Table 2.4   Experimental Output from Pyrolysis[33] at Different Temperatures of Epoxy Composite Reinforced with Carbon Fibres

The yield percentage is calculated by dividing the residue mass by the mass of carbon fibres in the original composite

CFRP	Temperature °C	400	500	600
sample	Residue property			
T-300 /	format	sheet	fibres	fibres
Epoxy	yield (%)	130.4	100.6	30.1
T-40 /	format	sheet	fibres	fibres
Epoxy	yield (%)	119.8	100.2	97.5
T-300 /	format	sheet	part sheet	fibres
Phenol	yield (%)	-	113.7	95.5

Table 2.5   Tensile Properties of Thermally Recovered Carbon Fibres[33]

Fibre Sample	Temperature °C	Tensile Strength MPa	Tensile Modulus GPa
Virgin T-300	-	3660	241
Virgin M-40	-	3360	395
T-300	500	3370	194
(Epoxy)	600	2450	174
M-40	500	3130	355
(Epoxy)	600	3360	347
T-300	500	3500	212
(Phenol)	600	2600	175

The recovered fibres were assessed by tensile strength measurement. Table 2.5 shows that the fibres recovered at 500°C have strengths comparable with virgin fibres. No hardware details are given or any indication of the scale of the process development, other than the process being aimed at scrap laptop computer carcases.

The magazine type articles quoted as reference 34 describe a process as follows:

Scrap thermoset GRP from boats or ships is crushed into 100-150 mm^2 pieces and gasified with steam in a kiln at 700°C. The resin matrix gasifies to give hydrogen and carbon monoxide without coating the fibres with carbon, the fibres are then recovered in some unspecified way. The fuel gas is incinerated at 1000°C to provide the process heat for the kiln. The quoted pilot plant operates at 2000 kg/day.

Both the processes detailed in references 33 and 34 deal with contaminated post consumer composite waste streams. However, the composite waste was only of a single type. A number of processes[6,32] have been successful in treating mixed polymer wastes, including automotive metal reclamation residue. However, the processes have not produced any high grade residue for reuse.

The residue from pyrolysis of an SMC[35] was recompounded as a replacement filler in an epoxy resin system. The seven day tensile strength of the resulting composite was increased by 8.3% and 48% for residue filler loadings of 25% and 30% respectively. This demonstrates the benefits of a thermal process compared with direct regrind, where properties of the resulting material were often reduced.

Further work on recycling scrap composites is reported in references 37 and 38. Reference 37 is a review of the various recycling technologies either currently employed or under investigation. Significantly, it was reported that the Japanese Waste Recycling and Treatment Council did not consider a viable fibre recovery method to exist in 1993 and quoted the mechanical methods of ERCOM and Phoenix Fiberglass as being the most interesting. Also the use of thermally treated composite residues were addressed, due to the shortage of landfill sites in Japan. Composite scrap from ships (40% glass) was heated to 300°C in the absence of oxygen which yielded gas and pyrolysis oils. The residue was 52.4% of the input mass and contained carbon and glass. Thus, the process is less efficient than that of reference 34 which leaves the fibres free of carbon contamination.

A trailer mounted mobile pyrolysis system (operational by the end of 1993) is described which can process whole composite boats below 6 metres in length at 400°C. This has the advantage of volume reduction at source, similar to the ERCOM mobile shredder, but does not require the energy intensive size reduction step. However, the process does go on to shred

the pyrolysis residue prior to incineration in a mobile rotary kiln, thus the residue must again contain carbon contamination.

Details are given[39] of the decomposition products resulting from heating unsaturated polyester resin to different temperatures. The decomposition took place in a water vapour atmosphere at 400-500°C, to obtain phthalic acid for recycling into new resin. This is effectively direct recycling of the thermoset polymer. The decomposition took 5 minutes at 500°C but was not complete in 60 minutes at 350°C[39], thus demonstrating a strong temperature dependence. The product comprised: 11% solid, 25.8% oil (30% styrene) and 46% residue[40], mainly phthalic acid. The recovered acid was separated and reused in polyester resin. Table 2.6 shows that the resin using recycled phthalic acid had slightly reduced properties compared with virgin.

Table 2.6 Properties of Unsaturated Polyester Resin from Recycled Phthalic Acid[40]

Physical Properties		Recycled	Virgin
Deformation Temperature	°C	92	95
Flexural Strength	MPa	95.0	113.5
Flexural Modulus	GPa	2.93	2.95
Tensile Strength	MPa	67.2	77.2
Maximum Strain	%	2.01	2.56

As an alternative material recovery process, ash from the incineration of boat composite scrap was crushed and heated[38]. The temperature was maintained above 900°C for four hours to allow the formation of any crystal phases. The phases: Cristobalite (SiO_2), Anorthite ($CaAl_2SiO_8$) and Wollastonite ($CaSiO_3$) were found. Thermal analysis found exothermic oxidation of carbon contamination in the range 400 to 600°C and an endothermic reaction at 860°C corresponding to the E-glass softening point. Some success was achieved in forming a glassy material by heating the milled residue in sample trays. This implies that scrap composite ash could be used as a feedstock in the glass industry. However, the reuse of thermal residue in this way is of low cost benefit compared to direct fibre recycling. This is due to glass raw materials being cheap minerals (see above for calcium carbonate cost).

2.3   Strength of Heated Glass Fibres

Research into glass fibres revealed[41] that thermal processing may result in a significant

reduction in physical properties.

2.3.1 Reduction of physical properties

Reference 41 reports work on the marked effect on tensile strength of heat treating soda-silica glass fibres of various diameters, shown in Table 2.7. Also reported is that heating low alkali borosilicate glass for 24 hours at 580°C produced no effect on the glass strength.

Table 2.7 The Reduction of Fibre Strength due to Heat Treatment[41].

Fibre Diam. (μm)	Tensile Strength kg/mm²	
	unheated	15 min at 520°C
25	161	86
40	172	85
80	100	70
120	61	-
160	-	42

However, this comforting view of the strength of borosilicate glass is not supported by other literature. Thomas[42] reports a detailed experimental study of E-glass fibres. This finds that not only is the fibre strength reduced even at temperatures below 100°C but the effect is strongly time dependent; the strength decreasing rapidly up to 10 to 15 minutes. These results were confirmed by the testing of borosilicate glass fibres[43], which had significant tensile strength reductions after heating for one hour above 200°C. A reduction of 50% in strength was found after heating at 450°C for both 12 and 22 μm diameter fibres.

This trend was further confirmed by the pyrolysis testing of an SMC[44]. The report concludes that above 300°C the glass fibres undergo an (unspecified) irreversible embrittlement process which reduces the mechanical properties. Figure 2.1 shows the reduction in fibre physical properties with increasing process temperature and shows that increasing the time at a given temperature also reduces the fibre properties.

The combined temperature and time effect was further researched as part of the RRECOM project[45]. The strength of laminates containing glass cloth, heat cleaned for 20 minutes at 625°C, was reduced to approximately one quarter of the value for the laminate containing virgin glass cloth. It was found that the tensile strengths of mouldings incorporating glass

cloth heat cleaned at 500°C were higher than the corresponding results for 625°C. However, the 500°C strength decreased with time and for heating periods greater than 60 minutes, the strength reduced to that for fibres heat treated at 625°C. The tensile strengths of mouldings incorporating fibres heated at 375°C reduced with increasing cloth heating period. But these were higher than the corresponding results for 500°C and 625°C.
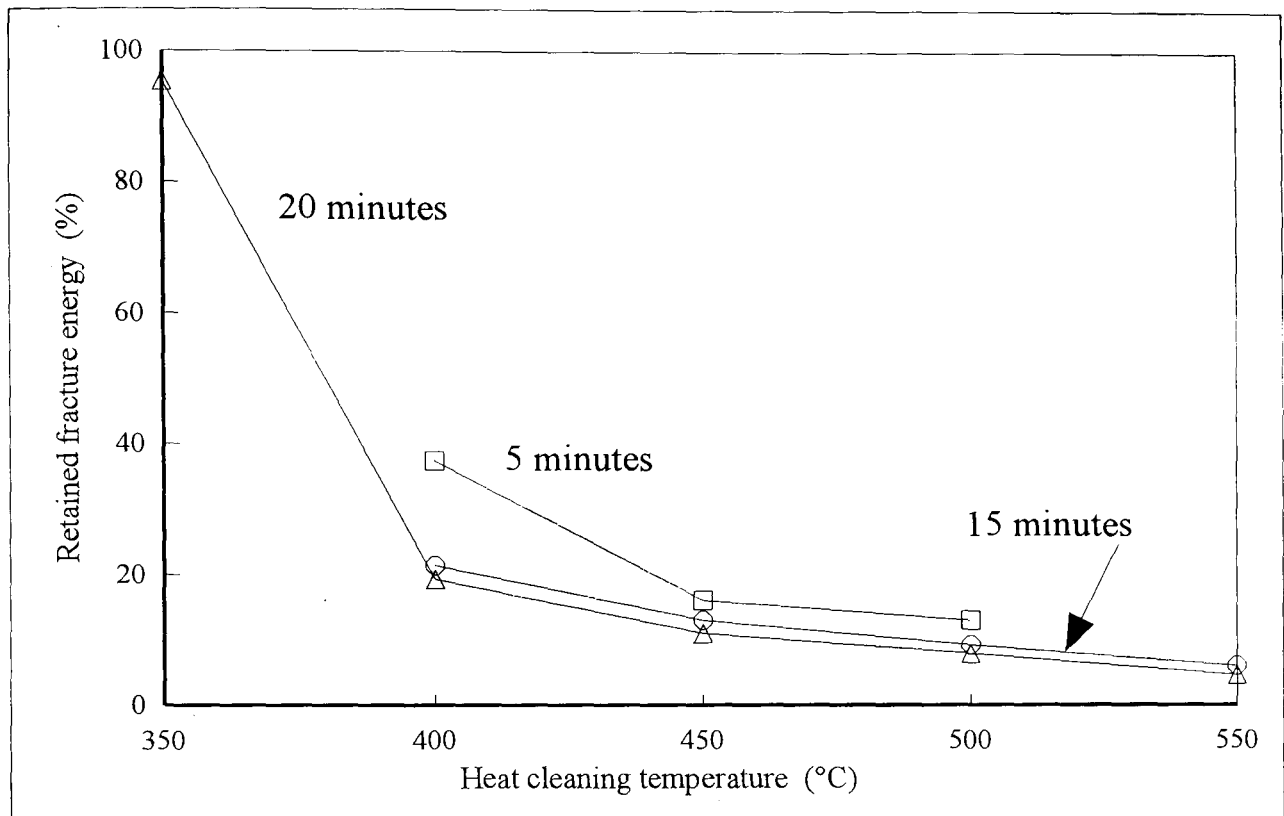
Figure 2.1   <u>Retained Glass fibre Specific Fracture Energy against Heat Cleaning Temperature Indicating Thermal Embrittlement of Fibres with Heat[44].</u>

The specific fracture energy is the area under the stress-strain curve produced during tensile test measurement. Values from heat cleaned fibres were compared with those from virgin fibres to give a retained percentage.

2.3.2 Cause of physical property change

Heat treatment of fibres is likely to influence any physio-chemical differences between the inner and surface of the fibre. Annealing is likely to reduce the surface compressive stress and make the fibre more susceptible to surface flaw formation. An increase in temperature is likely to make the metal ions more mobile within the silicon oxide structure that will tend to equalise any as-drawn chemical differences between the fibre surface and body. Also the ambient conditions during heating may be significant as water was found to leach fibres[46]. In fact, ion exchange occurs between a fibre and the water cooling spray during manufacture[47].

The strength reduction of soda-silica glass[41] was considered to be due to the diffusion of sodium ions to the surface. This produced surface flaws or increased the severity of existing ones. The quality of the surface layer is suggested as being key to the strength of glass. The quality of a glass surface layer and surface treatments is reviewed briefly in reference 41. Reference is made to earlier work which describes the etch removal of the surface layer, assumed to contain defects, by hydrofluoric acid. Table 2.8, shows the increase in borosilicate glass fibre strength obtained by such surface etching. This was found to be the case for both soda and borosilicate glasses.

Table 2.8 Effect of Acid Etch on Borosilicate Glass Fibres

The acid has etched away the surface of the fibres including the surface flaws that are understood to reduce fibre strength.

Fibre Diam. (μm)	Tensile Strength (kg / mm^2)	
	Untreated	2-10μm Surface Etch
20	160	320
100	50	170
200	30	120
500	23	70

The work done by Sakka[43] confirms the above results. Borosilicate glass fibres that had been heated were found to regain their original tensile strength on etching with 10% hydrofluoric acid for 3 minutes.

2.3.3 Re-use of heat-cleaned fibres

Some research work has recompounded heated or heat cleaned fibres into new composite structures[48,36,35,45]. A byproduct of testing annealed optical glass fibres in a PMMA matrix[48] was the flexural strength results shown in Figure 2.2. The fibres were heated for 0.5 hour and it is seen that an annealing temperature of 500°C reduces the reinforcing effect of the fibres virtually to zero. Similar trends were found during RRECOM project work[45].

This strength reduction was not found in the work reported by Hanson[36]. There, the glass fibres were heat cleaned at 454 to 565°C in a calciner and subsequently recompounded into nylon, phenolic and polyester composites. The physical properties obtained were comparable to composites containing unheated glass fibres. For example: a tensile strength value of 96.6

MPa at 17% fibre loading in nylon 6/6 was compared with manufacturers data at 75.9 to 151.8 MPa for virgin fibre loadings of 13 to 15%. Useful reinforcement was also obtained from an SMC pyrolysed at 400°C that was recompounded into an epoxy matrix[35]. However, the fibrous residue was used to replace filler and so the substantial increases in tensile strength were not unexpected.
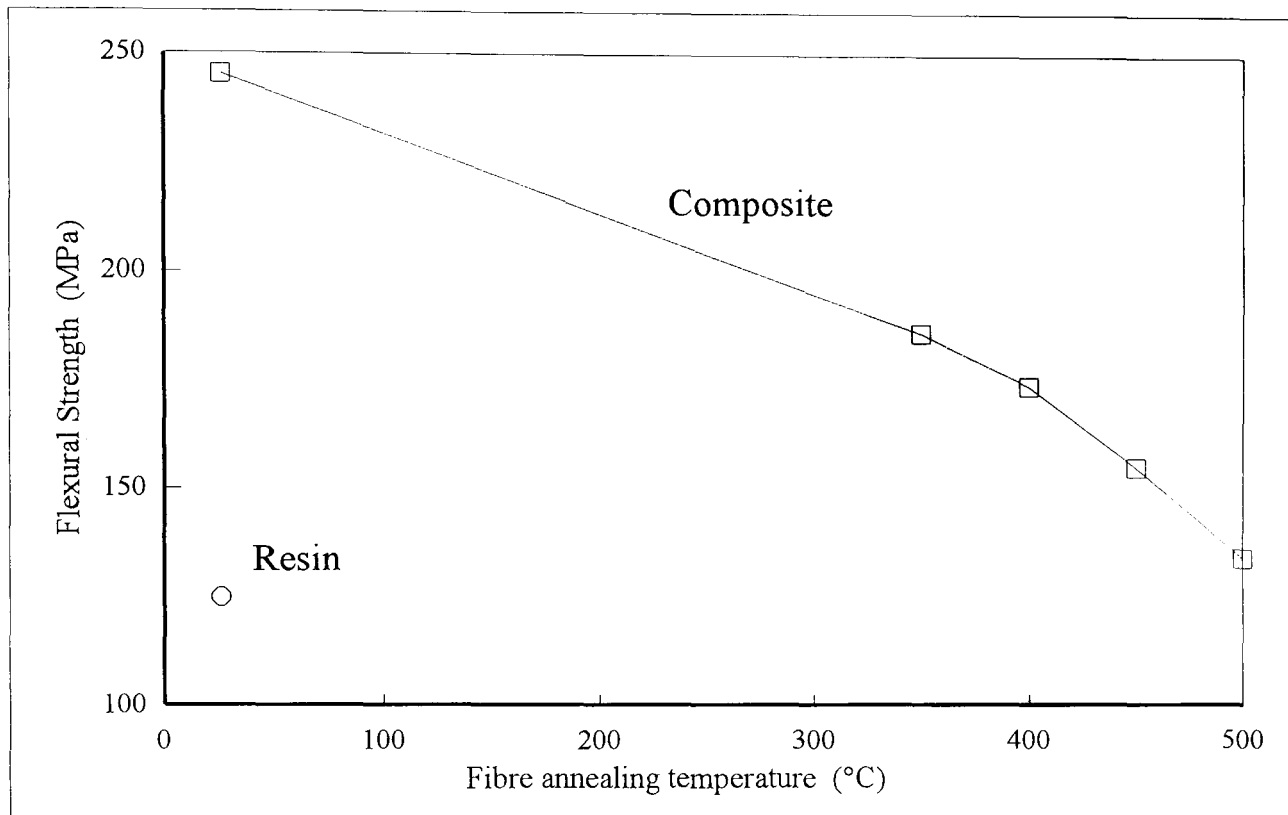
Figure 2.2   Flexural Strength of Annealed Optical Glass Fibres in a PMMA Matrix[48].

This shows the reduction in composite flexural strength with increasing fibre anneal temperature

2.4 Concluding Remarks

If a market or process existed for scrap thermosets, then the vehicle disposal industry would maintain its profitability. Also, thermoset composites could be used in greater abundance in vehicles, with the associated environmental benefits.

A recycling process must be tolerant of contamination if post consumer scrap is to be recycled without costly cleansing operations. A process which requires a pure waste stream as a starting medium requires a final product whose value is sufficient to balance the cost of initial dismantling.

2.4.1 Current scrap disposal

An existing collection, material sorting and reclamation industry exists for metals reclamation from vehicles. A composite recycling process which interfaces with and was complimentary to this business would be readily accepted and have a good economic viability.

A minimum improvement over the current situation should be the incineration of the metal reclamation residue prior to landfill.

2.4.2 Scrap recycling research

Four thermal processes[33,34,35,36] were found which achieved success in recovering fibres from composites at a quality sufficient for reuse directly as fibres. Thus a thermal process was chosen for further experimental investigation. Since the proportion of polymer is often small in composites, material as well as energy recovery is required for economic viability. The recovered fibres and fillers should be in as high a value form as possible. This implies that a process that can recover the reinforcing fibres intact is suitable.

The desirable direct recycling of the thermoset polymer[37,39] involves many processes beyond the initial decomposition step. It is therefore likely to be at a price disadvantage compared with virgin resin, unless legislation artificially weights the process economics.

2.4.3 Strength of heated fibres

The heating of glass fibres is widely reported to have a detrimental effect on the fibre strength[42,43,44,45,48], with the exception of the work by Hanson[36]. However, there is a lack of information in the literature on the actual strength loss mechanism. Potential influences are: the number of surface flaws, annealing of as drawn stress differences between the surface and centre and ion exchange between the fibre surface and the surroundings. The strength loss also seems to have a time and temperature dependency.

2.4.4 Investigations in this thesis

Fluidised beds have been used for processing composite scrap in a number of research studies. Fluidised bed combustion of scrap composites at The University of Nottingham has also proved successful (see Chapter 3). This literature review gives confidence that glass fibres may be recovered intact from fluidised bed combustion of scrap composites. However, such fibres are likely to have reduced strength compared to virgin fibres.

Chapter 3
USE OF COMPOSITE SCRAP IN COMMERCIAL COAL COMBUSTION PLANT

3.1 Introduction

Test work at the Coal Research Establishment[49] in 1991 had shown that calcium carbonate filled composites could be used to reduce sulphur oxide emissions from the fluidised bed combustion of coal. If composite scrap is added to the bed with the coal, the polymer burns to release useful energy and the filler calcines to calcium oxide which absorbs the sulphur dioxide formed during coal combustion. A literature review on the use of sulphur sorbents in fluidised bed combustion is presented in Appendix 1.

The work reported in this Chapter was a further trial to demonstrate the desulphurisation technique on a commercially operating boiler.

3.1.1 Aim of test

The aim of the test was to assess the effectiveness of filled composite scrap in reducing sulphur oxide emissions on a commercial scale. The test was limited to a few days to give an indication of the potential success of emissions control. Ideally a longer test, of several months duration, would be required if sufficient composite scrap were available. Such a test could investigate longer term factors, such as the ash deposition and fouling described in Appendix 1.

3.1.2 Commercial test in context

In some respects this chapter can be seen as a stand alone piece of work. However, the fluidised bed and material handling experience gained were essential at an early stage of the research.

More importantly, during size characterisation of the cyclone fines produced when burning the composite scrap, some short glass fibres were seen[50]. This indicated the potential to recover glass fibres from scrap composite materials with fluidised bed thermal processing. This led directly to the process development described in the rest of this thesis.

3.2 Boiler Plant Description

A suitable coal fired fluidised bed boiler (see figure 3.1) was available at the Faculty of Agricultural and Food Sciences, The University of Nottingham at the Sutton Bonington site. This boiler had been the subject of extensive research by the Coal Research Establishment on the use of limestone as a sorbent for sulphur dioxide from the fluidised bed combustion of coal[51].
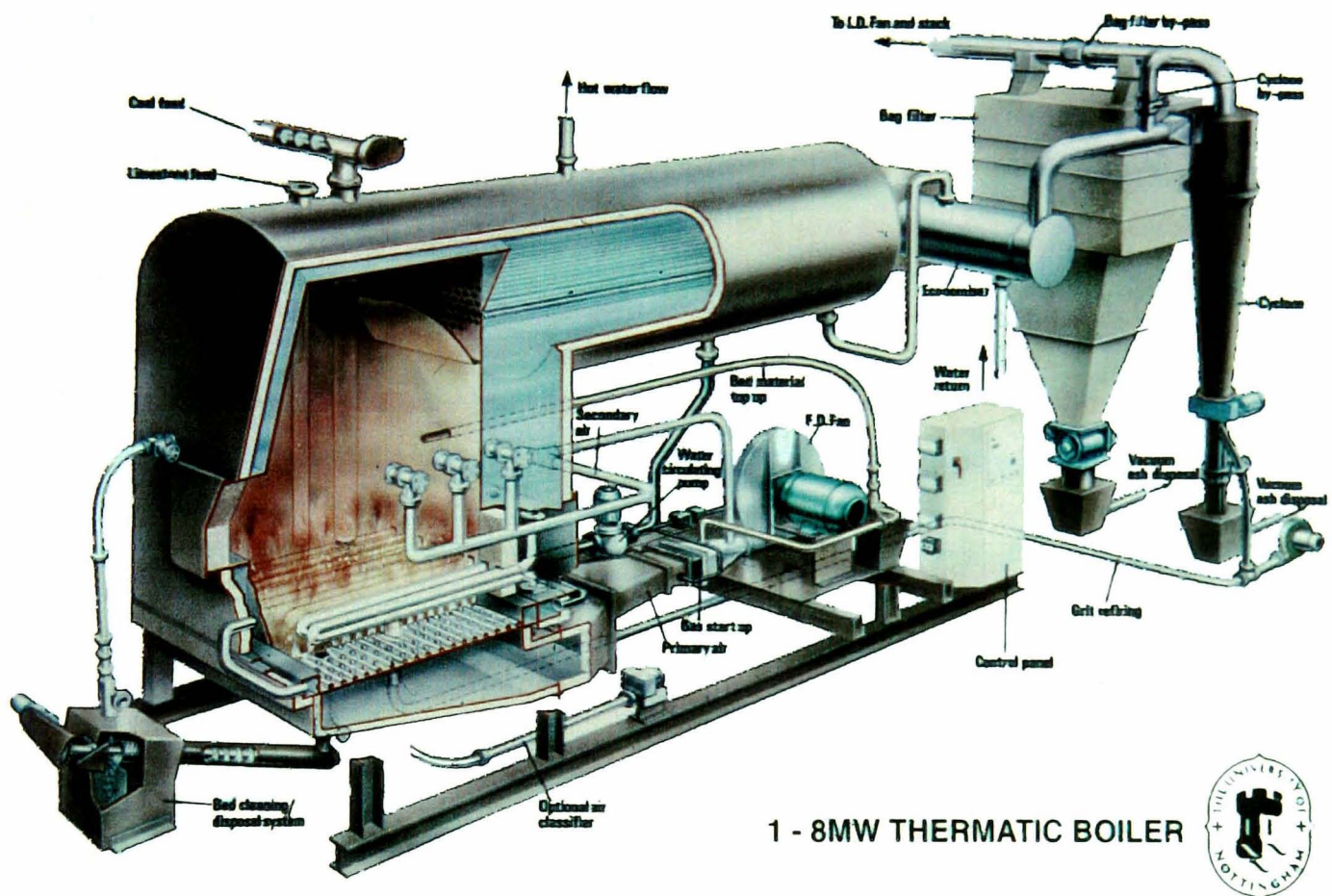
Figure 3.1   The Fluidised Bed Fired Boiler at Sutton Bonington Site

The fluidised bed boiler supplies low pressure hot water to the whole college site. The boiler is of a single pass shell and smoke tube construction. The combustion chamber has a vertical shell wall which forms the freeboard of the fluidised bed. The boiler is virtually automatic, operated via a programmable logic controller. This modifies combustion conditions in response to changes in boiler parameters. The bed target temperature has the narrow range of 835°C (low firing rate) to 839°C (high firing rate). This narrow range limits the formation

of nitrogen oxides (NO$_x$) and is only achievable due to the high thermal stability of the fluidised bed.

The fluidised bed has a plan area of 1.9 m^2 with a static height of approximately 0.1 m. It is supported on a water cooled base plate and horizontal water tubes provide in-bed heat removal. The bed is made up from silica sand graded between 0.5 to 1.5 mm. A regrading system automatically removes sand from the base of the bed via a water cooled screw. Oversize material is sieved and discarded; the remainder can be returned to the bed or fresh sand added to maintain the bed level. The fluidising air is supplied by a forced draught fan, while an induced draught fan maintains a slightly negative furnace pressure. A single cyclone removes particulate ash from the flue gas.

3.2.1 Hardware for test work

A method of feeding the composite scrap into the boiler was required. The author designed and commissioned a feed system based on a 70° hopper sited on top of the boiler to feed into the auxiliary drop tube, see figure 3.2.
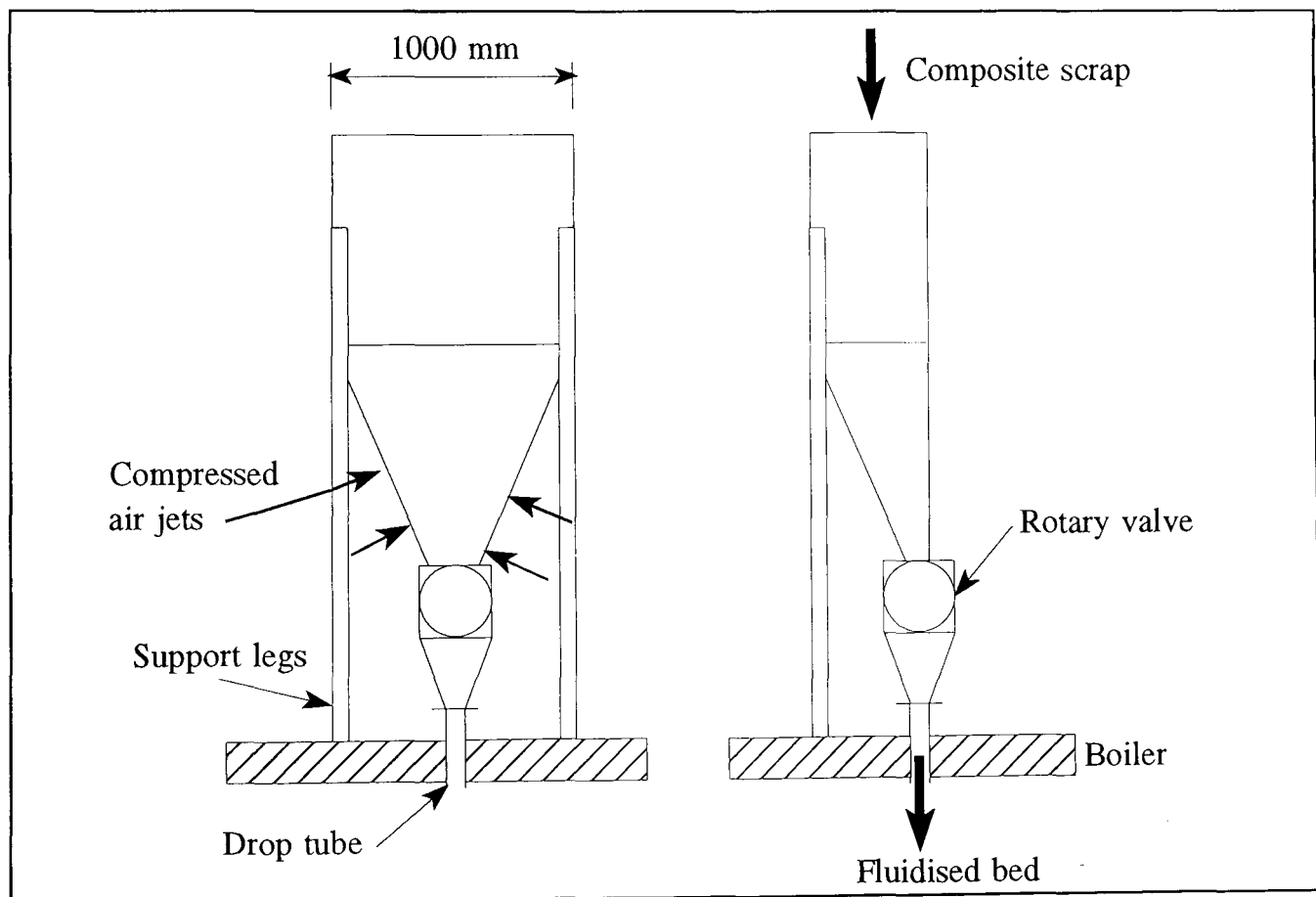
Figure 3.2   The Hopper and Rotary Value used to Feed Composite Scrap into the Fluidised Bed during Testing at Sutton Bonington Site.

27

The hopper outlet was sealed with a rotary valve that had been modified to have flexible tips on the vanes to prevent jamming. To prevent the scrap material bridging in the hopper, a number of pneumatic valves periodically released compressed air bursts into the hopper to keep the material free flowing.

3.3   Test Method

3.3.1 Composite scrap

The composite scrap used was of two different types, shown in Table 3.1. The Dough Moulding Compound (DMC) was similar to that of the pilot plant test and the Sheet Moulding Compound (SMC) was of significantly different composition for comparison. Both materials were production scrap meter boxes, crushed and sieved through a 25 mm aperture screen. The coal burnt during the test period was Calverton Singles, the normal fuel for the boiler, of 1.28% sulphur content.

Table 3.1   The Main Constituents of the Commercial Test Composite Scrap

Constituent		DMC	SMC
Resin	%	17	25
Calcium Carbonate	%	60	35
Glass	%	15	22
Alumina Trihydrate	%	-	15

3.3.2 Test procedure

The crushed scrap was not premixed with the coal, as in the rig test, but added to the bed through the limestone drop tube, see figure 3.1. The test was of four working days in duration and is summarised in Table 3.2.

Throughout the test days, boiler operation parameters were recorded on a data logger every eight seconds and averaged over five minute intervals. A day was monitored with no composite input to provide datum values for the boiler parameters.

Material and gas samples were taken before and after each test period and as often as

practicable during. The solid samples comprised: cyclone fines and sand from the bed regrading sieve (see Section 3.2). The flue gas measurements of sulphur dioxide and NO_x concentration were made using Dräger tubes.

Table 3.2 Summary of the Quantities of Materials Added to the Fluidised bed over the Duration of the Co-Combustion Test Work

Test Day		1	2	3	4
Period of Composite input	(hr)	2.9	7.7	7.3	6.8
Coal input	(kg)	573	1157	1338	1368
	(GJ)	17.4	35.2	40.7	41.6
DMC input	(kg)	160	220	-	-
	(GJ)	0.64	0.87		
SMC input	(kg)	-	60	150	140
	(GJ)		0.40	1.00	0.93

On the second test day, a mobile laboratory unit carried out continuous flue gas analysis and particulate analysis, to BS 3405, downstream from the cyclone. These results provided an accurate datum with which to calibrate the Dräger tube values.

3.3.3 Composite scrap material feed

Continuous 24 hour composite scrap input had been planned via the rotary valve linked to the boiler control system. However, problems were encountered in achieving a steady input feed rate. This was due to the suction created by the negative pressure within the boiler. Constant supervision was required to ensure operation and this limited the test periods to only part of a full day. Also, the scrap was fed in at a fixed mean rate, which varied the calcium (in the composite filler) to sulphur (in the coal) ratio as the coal input rate changed with heat demand.

3.4   Results and Discussion

Throughout the periods of composite scrap addition, the boiler operated normally, even though the control system had not been modified to increase the air flow for the extra fuel input. This implies that in commercial operation, the use of composite scrap as a sulphur

dioxide sorbent would require minimal control changes and be tolerant of a varied supply.

The as-measured sulphur dioxide concentrations in the flue gases were normalised to standard dry, 6% oxygen content, STP values.

3.4.1 Boiler efficiency

Figure 3.2 shows that, during composite scrap addition, the boiler efficiency increased slightly. This is indicative of the extra heat input from the combustion of the resin in the composite scrap. However, the flue gas analysis below shows that unburnt fuel was lost in the flue, i.e. the actual heat input is lower than that available. This indicates that the boiler controller should be modified to optimise the airflow for complete combustion of any composite scrap input.
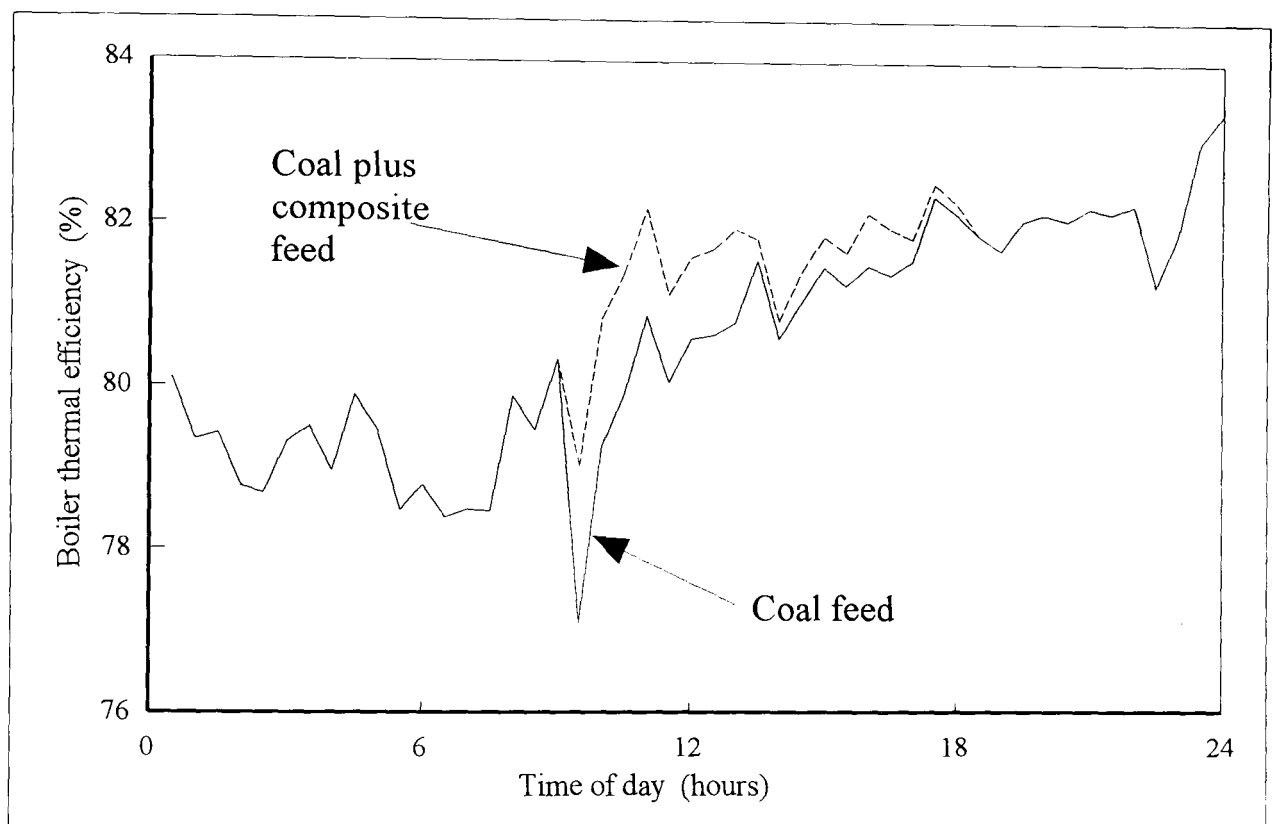
Figure 3.3   The Thermal Efficiency of the Boiler During a Day with Composite Scrap Input to the Fluidised Bed

The boiler efficiency values plotted in figure 3.3 were calculated by comparing the heat input less any losses with the heat input. The theoretical heat input is the mass feed rate multiplied by the calorific value for the coal and any composite scrap. The heat losses include: the unburnt carbon content in the cyclone fines and the sensible heat lost in water vapour and the combustion gas products. Radiation losses were estimated as 2% of the thermal output of the boiler.

The boiler efficiency was calculated as:

$$\eta = \frac{Q - Q_l - Q_R}{Q}$$

Where:

$$Q = (CV \times FR)_c + (CV \times FR)_{sc}$$

$$Q_l = \%_{Cn}.m_f.CV_{Cn} + m_{WV}.Cp_{WV}.\Delta T + ((m.Cp)_N + (m.Cp)_O + (m.Cp)_{CO_2}).\Delta T$$

$$Q_R = 0.02 \times 1.8 MW$$

3.4.2 Flue gas analysis

The minimum measured sulphur dioxide emissions during the period 12:00 to 12:30 on Day 2 was a very low 10 ppm, indicated in figure 3.4. This was consistent with the addition of DMC scrap at a high calcium to sulphur (Ca/S) input ratio of 9.18:1. This is the mean ratio of the calcium in the filler to the sulphur in the coal. The mean sulphur dioxide emission during the afternoon was 280 ppm, when calcium carbonate filler was added in the SMC scrap at a Ca/S input ratio of 0.98:1. Both results compare favourably with a mean sulphur dioxide output of 680 ppm during the datum day.

It was considered[50] that the boiler operated under non-steady state conditions, from variations in the flue gas concentrations, even though the coal firing rate was constant throughout the mobile laboratory test period on Test Day 2. This was probably due to the composite scrap feed problems, particularly the SMC, producing a variable composite scrap input rate.

Thermal plant of the size of the Sutton Bonington boiler (1.8MW) have a particulate emission limit of 3.4 kg/h, specified within the 1971 Clean Air Regulations. This limit was not exceeded during the mobile laboratory testing. However, the particulate burden did vary by a factor of 2.6 between 260 and 680 g/h, which is outside the factor of 1.5 limit required in BS 3405. This corresponds to a 2.4:1 variation in the feed rate of the SMC of during the particulate measurement period.

An average NO_x concentration of 765 mg/m³ was measured which was similar to previous testing on this boiler running on only coal. During the detailed flue gas analysis, larger than expected levels of carbon monoxide were noted (800 mg/m³) compared with previous

work on this boiler. Also, large fluctuations between 600 mg/m³ to 1200 mg/m³ were recorded.

The presence of carbon monoxide in flue gases is indicative of incomplete combustion of carbon and represents a loss of potential boiler heat input. Total flue gas hydrocarbon concentration varied between 20 and 130 mg/m³ with an average of 30 mg/m³. This is indicative of poor combustion conditions. There may have been poor mixing of the air and hydrocarbon gases from the coal and resin in the freeboard resulting in incomplete combustion.

Such emissions would be controlled during any future commercial operation by modifying the boiler control system to allow for the input of auxiliary fuel. Also, modifications to the composite scrap feed system could be made to ensure a constant input rate.

3.4.3 Daily sulphur balance

The sulphur input from the coal has three final destinations: as sulphur dioxide in the flue gas, in solid particulates in the flue gases extracted by the cyclone and in solids retained in the bed. Sulphur input and output balances over each test day are shown in Table 3.3.

Table 3.3   Daily Sulphur Mass Balances

This table compares the sulphur input to the boiler in the coal feed with the sulphur outputs from the boiler: as calcium sulphate in the cyclone fines or as sulphur dioxide in the flue gases.

Test Day	Sulphur					
	Input (kg)	Output (kg)			Input less output (kg)	Output as a % difference from input
		Flue gas SO_2	Cyclone Fines	Sum		
1	54.2	39.7	3.8	43.7	10.5	-19.4
2	54.6	32.1	7.6	40.0	14.6	-26.7
3	52.8	41.4	4.6	46.0	6.8	-12.9
4	41.9	33.1	4.3	38.6	3.3	- 7.9

The largest discrepancies in the sulphur mass balances are those for Days 1 and 2 when DMC

was added at a high Ca/S ratio. Day 2, which has the most information due to the mobile laboratory analysis and should therefore have the most reliable figures, has the worst balance. Assuming that the flue gas sulphur dioxide and fines sulphur measurements are correct, then this implies that sulphur was likely to have been retained in the bed by analogy to the rig test[56].

The retention of sulphur in the bed was not detected by the indirect method of sampling from the bed sand regrading system. By comparison, sulphur retention in the bed was detected after the earlier rig testing at the Coal Research Establishment. Then, the whole bed was weighed before and after the test and homogeneous samples taken for chemical analysis[49]. The results from that work are compared with the commercial test below.

3.4.4 Hourly sulphur balance

Figures 3.4 and 3.5 show comparisons of sulphur input in the coal with sulphur output of flue gas sulphur dioxide for the first two test days. Figures 3.4 and 3.5 are hourly averages, based on Dräger tube measurement and the detailed Day 2 flue gas analysis.
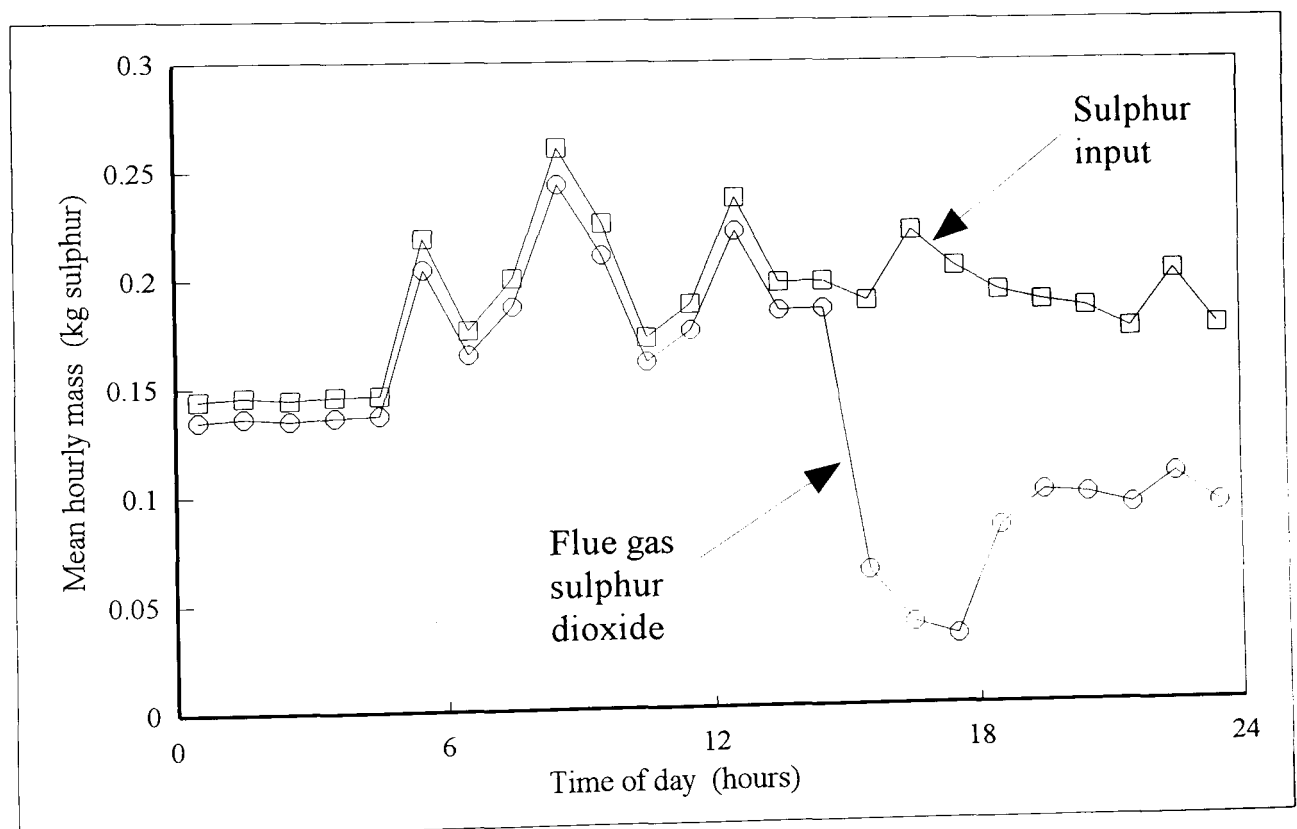
Figure 3.4   Sulphur Balance for the Boiler for the First Test Day

This compares the sulphur input in the coal with the sulphur output as sulphur dioxide in the flue gases.

33

Figure 3.4 shows very little sulphur retention during the morning of Day 1, when the boiler was running on just coal. However, a significant reduction is seen after the addition of DMC between 14:15 and 17:10. The sulphur dioxide output does not recover to its original proportion of input throughout the rest of the day. This may be indicative of calcium remaining in the bed at the low firing rate and continuing to remove sulphur dioxide from the flue gas. The Day 1 to Day 2 overnight period was operated at low fire conditions and the difference between the sulphur input and output may have been due to transient bed retention. This was not seen on subsequent days due to regular switching of the boiler to high fire. At the high fire rate, any calcium retained in the bed may well have been elutriated.
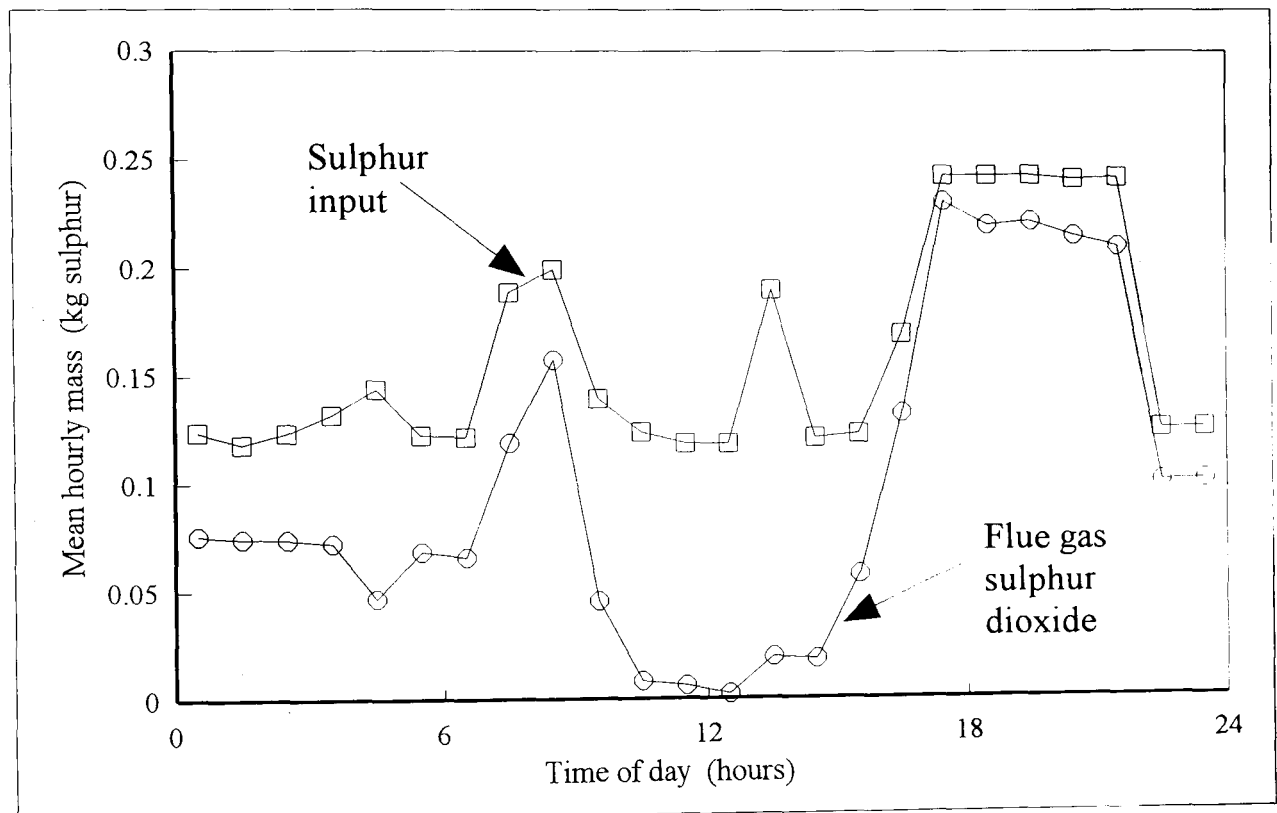
Figure 3.5   Sulphur Balance for the Boiler for the Second Test Day

This compares the sulphur input in the coal with the sulphur output as sulphur dioxide in the flue gases. The sorbent material was added at a lower Ca/S ratio than during the first day.

Figure 3.5 shows that the Day 2 sulphur dioxide output reduced further with composite scrap input during the period 09:20 to 17:50. After this, the sulphur in the flue gas, as a proportion of input, increased nearly to early Day 1 levels. Over the afternoon there was a less significant reduction in sulphur dioxide output. This was due to the addition of crushed SMC,

with a lower proportion of filler than the DMC at a lower input rate, resulting in a reduced calcium to sulphur ratio.

3.4.5 Sulphur retention

Figures 3.6 and 3.7 show the variation in sulphur retention as a function of input Ca/S ratio for the cyclone fines and overall values respectively.
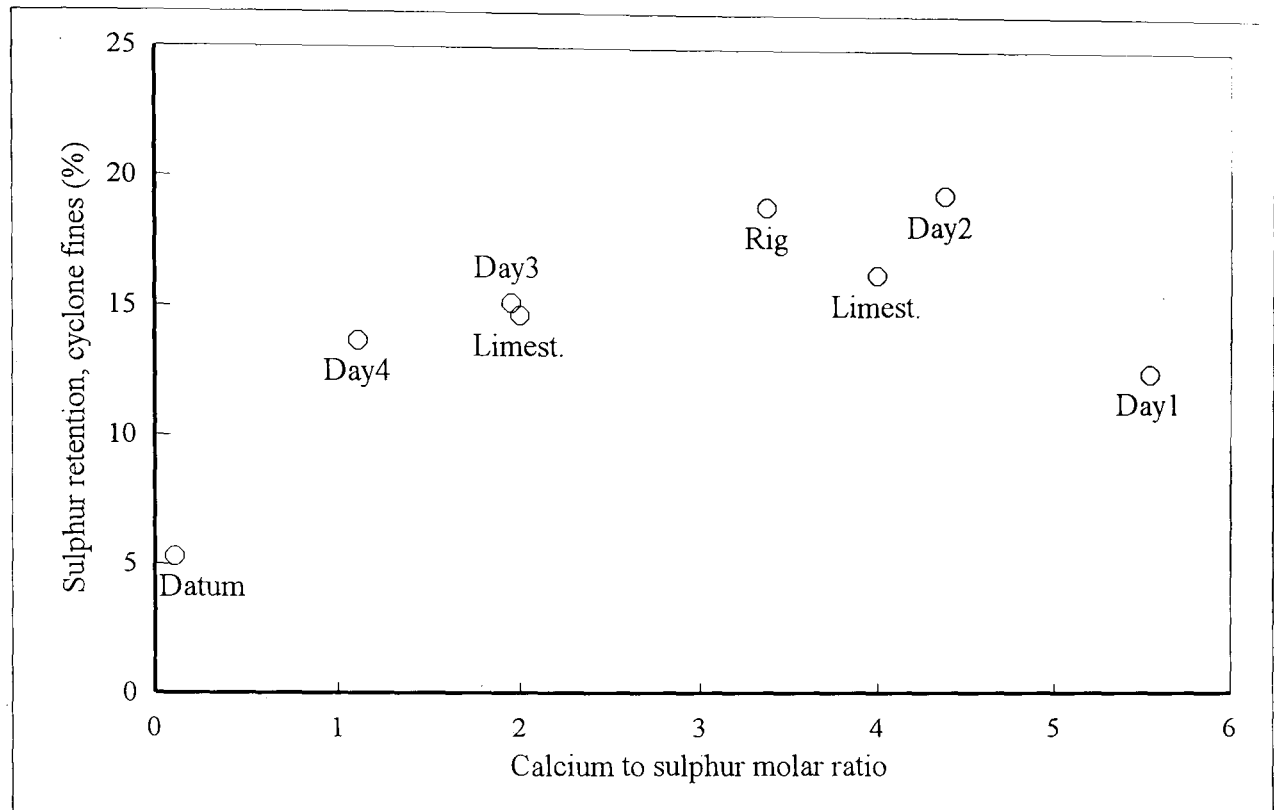
Figure 3.6   Fines Sulphur Retention, During Sorbent Addition as a Function of Calcium to Sulphur Ratio

This graph compares the retention of coal sulphur in the cyclone fines with previous test work. The fines sulphur was calculated from chemical analysis of fines samples and the fines accumulation rate.

Cyclone fines sulphur retention

Figure 3.6 shows the 19.4% fines sulphur retention for Day 2 during composite scrap addition to be comparable with the value of 18.9% obtained from the rig test[49]. The rig result was achieved at a Ca/S ratio of 3.38:1 compared with an average of 4.38:1 over the DMC and SMC addition on Day 2 of the boiler test.

The data points for the sulphur retention in the fines fall on a diminishing returns curve, similar to those found in the literature[52]. The fines sulphur retention from the earlier rig

testing appears to fit in with the boiler testing data. Also, points are plotted from the original Coal Research Establishment work at Sutton Bonington with a crushed limestone sorbent[51].

Overall Sulphur Retention

No sulphur retention in the bed could be detected from the bed samples taken during co-firing the boiler with composite scrap. However, the plots of figures 3.4 and 3.5 show that it did not exit the boiler as sulphur dioxide. As a comparison with the total rig[49] and limestone sorbent[51] values, retention values are plotted in figure 3.6 based on sulphur not emitted as sulphur dioxide during this test work.
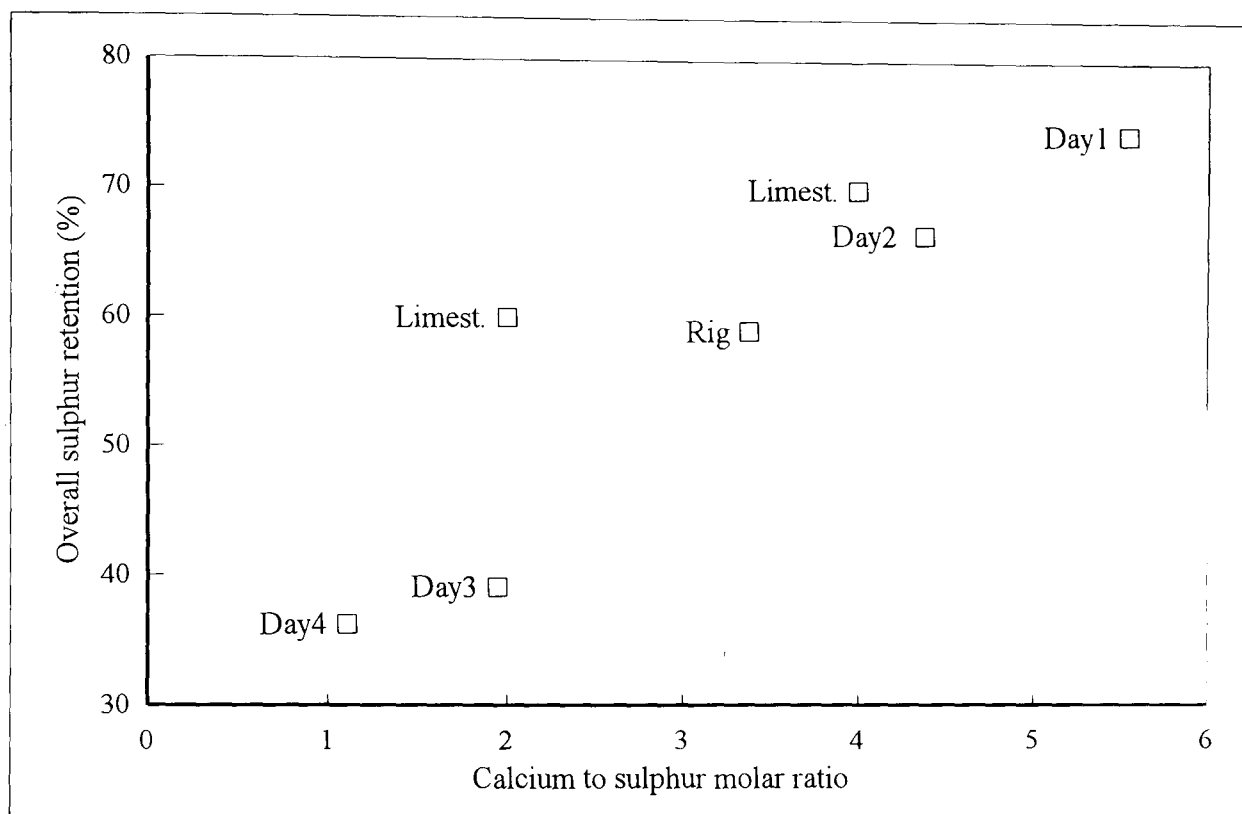
Figure 3.7 Total Sulphur Retention, During Sorbent Addition as a Function of Calcium to Sulphur Ratio

This graph compares the overall retention of coal sulphur with previous test work. The sulphur retention was calculated from the difference between the sulphur input and the measured sulphur dioxide output in the flue gases.

The data in figure 3.7 appears to lie on a similar curve to the tests by Coal Research Establishment. The rig bed was found to retain 40.1% of input sulphur, giving a total retention of 59%. The original limestone testing at Sutton Bonington had 50 to 60% sulphur retention in the bed, giving a total retention of 60 to 70%.

If sulphur retention did occur within the bed, as was expected from previous work and the

literature, it would account for the discrepancies in the sulphur balances in Table 3.3. A longer test would be desirable to allow the calcium levels at different positions within the system to achieve steady state.

3.5 Economic Analysis

Technically, the use of composite scrap can be seen to be comparable to limestone in the reduction of flue gas sulphur dioxide. But limestone is a very cheap raw material and so the value recovered from the scrap plastic can be considered to be low. Indeed it may be so low as to cause this disposal route to be uneconomic. Table 3.4 shows a simple cost comparison of the testing carried out, this is based on a heating equivalent of one tonne of coal. The comparative cost is made up of the costs of the: coal, sulphur dioxide sorbent and ash disposal. This is detailed in full in Appendix 2.

Table 3.4   The Comparative Cost of Different Sulphur Dioxide Sorbents.

The values in this table are comparative only, comprising the costs of the: coal, sorbent and ash disposal. All the other plant costs were assumed to be the same, irrespective of the sorbent type. As the composite scrap contains energy, the costing is calculated for the equivalent of one tonne of coal heat input.

Combustion plant feedstock	Cost (£ per tonne of coal equivalent heating value)		Sulphur dioxide output (kg)
	Low landfill	High landfill	
Coal alone	51.73	54.15	25.6
Coal and limestone	55.49	73.34	7.94
Coal and composite scrap	66.76	80.06	7.46

Table 3.4 shows that at low landfill costs, typical of the UK, the use of composite scrap as a sorbent costs 20.3% more than for an equivalent sulphur retention by limestone. Even applying a high landfill charge, typical of Germany, this difference only reduces to 9.2%. The main problem is the high cost of crushing the composite scrap, although this would

37

probably reduce with economies of scale.

Interestingly, if the glass fibres seen in the cyclone fines (see 3.1.2) were removed from the waste stream, then the value of £80.06 for the high landfill costing reduces to £63.26 and becomes cheaper than desulphurisation via limestone. The separation, collection and characterisation of reinforcing glass fibres from composite scrap forms the remainder of this thesis.

3.6   Conclusions

- The sulphur dioxide emissions from a coal fired fluidised bed boiler were reduced by using calcium carbonate filled scrap thermoset composites as an auxiliary fuel[53]. Up to 75% of the sulphur in the coal was retained, based on the reduction in sulphur dioxide output. However, the actual retention could not be precisely defined, due to the apparent absence of sulphur in the samples taken of the bed material.

  Such a disposal procedure is an example of the combined energy recovery and material reuse that has been identified previously as being vital for the economic recycling of composite scrap. As this was achieved in existing combustion plant, then considerable advantages could be gained in terms of acceptance, implementation and economic viability.

- The equilibrium conditions needed to assess accurately the sulphur balance of the boiler combustion system were not reached. This was due to: non-steady plant operation meeting the site heating demands, the irregular composite scrap input and as the test duration was only a few days. The composite scrap feed system would require development if continuous trouble free operation were to be achieved.

- No significant problems were encountered with the composite scrap combustion and plant operation. This was encouraging as the test was carried out during normal operation of the boiler. However, a longer test would be desirable to assess the long term operational impact on the boiler of this method of scrap disposal.

- The economics of composite scrap disposal by this method depend on the cost of

crushing the scrap, the proportion of incombustible content and the prevailing landfill charges.

- Glass fibres were found in the cyclone fines. This indicated the potential to recover the glass fibres from scrap composites via fluidised bed thermal processing. Recovering the fibres would improve the economic viability of the disposal route even before the fibres were recycled in some way.

Chapter 4
FLUIDISED BED THERMAL PROCESSING
TEST RIG - DESCRIPTION

4.0   Introduction

Analysis of the fines elutriated from the previous fluidised bed combustion trial indicated that reinforcing fibres could be recovered from scrap thermoset composites. As the value of the reinforcement is much higher than the other incombustible constituents, a test rig was designed by the author to investigate this phenomenon further.

This chapter describes the fluidised bed rig that was designed and commissioned for the combustion and separation of composite materials. In the initial Phase 1 design, cyclones were used to recover the fibres and fillers from the flue gases. An improved, low contamination, fibre collection system was developed in Phase 2. Appendices 3, 4 and 5 contain: a literature review of fluidisation as a separation technique, the design theory of the fluidisation chamber of the test rig and the rig safe operating procedure, respectively.

4.1   Test Rig Brief

Test equipment was required to operate both as thermal process plant and as a material separator for combustion residues. The test rig had to have the ability to operate off the design point, to determine the optimal conditions for a high rate of fibre recovery and quality of recovered fibres. A fluidised bed design was chosen as previous work[49] had shown this to be an effective combustion medium for the polymer component of composite materials and a means of recovering reinforcing fibres. The literature review of Appendix 3 indicated that the churning motion of the fluidisation would aid the breakdown of the composite, once the polymer had been burnt off.

4.2   Rig Hardware Description

Figures 4.1 and 4.2 show the Phase 1 fluidised bed test rig. The rig receives air at relatively low pressure, but high flow rate. This is heated by, electric resistance element, duct heaters.
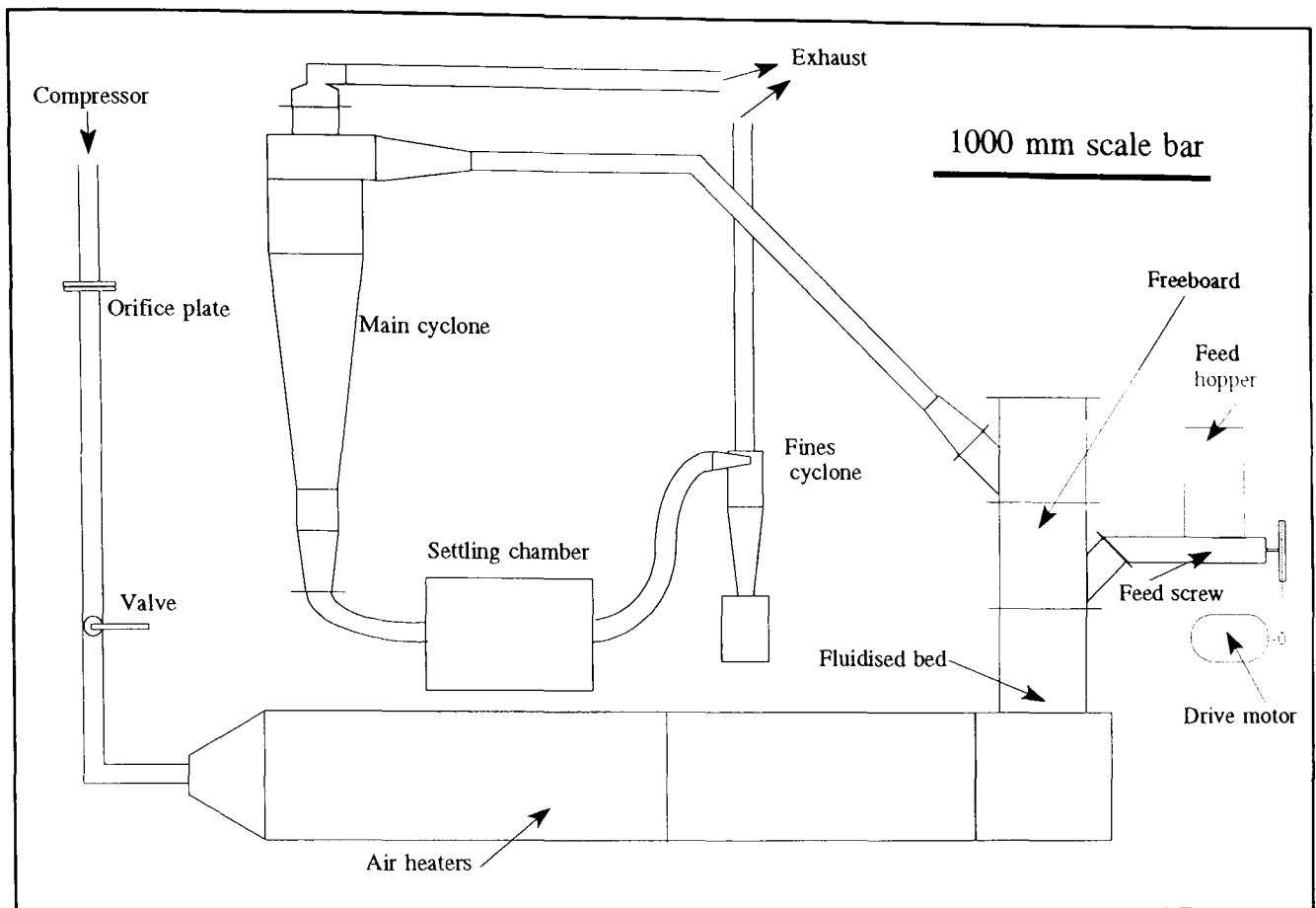
Figure 4.1   Phase 1 Fluidised Bed Test Rig
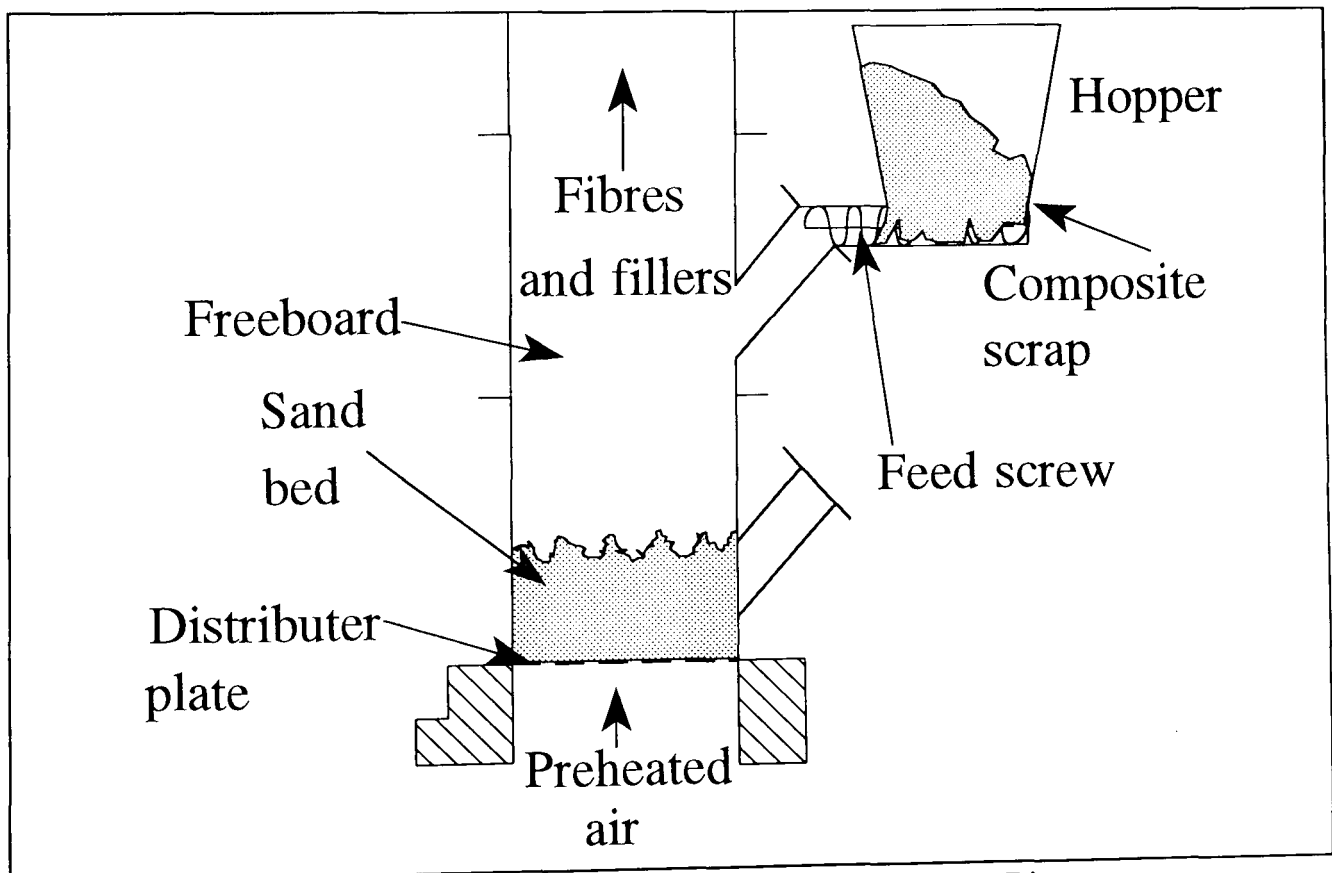
Figure 4.2   Expand Detail of Phase 1 of the Fluidised Bed Test Rig

The air then passes through a 90° duct before entering the sand bed that sits on a mesh air distributor. Scrap composite is fed by a screw into the freeboard from a hopper bolted to a barrel side-arm. Everything entering the freeboard (elutriated solids and combustion gases) passes into a cyclone that removes the solids from the hot gases. A bleed flow from the base of the cyclone transports the solids into a gravity settling bin. The bleed flow then passes into a small high efficiency cyclone to remove fine particles.

4.2.1 Fluidising air inlet

The airflow rate was measured with an orifice plate to BS 1042. This plate was sited above the inlet valve in standard 50 mm diameter pipe work. The inlet valve was of a globe type. Downstream of this was a pressure relief valve set to 1.2 bar.

4.2.2 Electric air preheater

Electricity was chosen as the preheating medium for the test rig for the simplicity and accuracy of temperature control. Also, the fluidising air would not be contaminated with combustion products from a preheat fuel. Two heaters were used of 15 kW and 28 kW rating, supplied by Kanthal Ltd, see Table 4.1. The heaters had full Proportional, Integral and Differential temperature control via a Watlow series 965 temperature controller. Heater element over-temperature control was via two Watlow series 141 on-off temperature controllers. A low air flow monitor was via an adjustable differential pressure switch across the orifice plate. The heaters were locked out until this switch was activated.

Table 4.1   Test Rig Heaters Specifications

	15 kW	28 kW
Internal dimensions (mm)	250 x 250 x 1300	250 x 250 x 1250
Elements	3 mm Kanthal AF	2.5 mm Kanthal AF
Insulation	75 mm ceramic fibre	75 mm microtherm® & ceramic fibre

4.2.3 Fluidised bed and freeboard

The test rig comprised three 2.64 mm wall thickness stainless steel flanged tubes with instrument and access ports. The tubes were 312 mm internal diameter and 400 mm long. These were insulated externally with ceramic fibre blanket. The tubes were bolted together

to form a continuous cylinder. The fluidised bed was at the base of the cylinder, the remainder forming the freeboard.

The bed of 150 mm depth by 312 mm in diameter ensured a realistic representation of a commercial plant. The bed was made up of the same silica sand (graded larger than 0.5 mm and smaller than 1.0 mm) that was used commercially at the Sutton Bonington plant (see Chapter 3). The air distributor for the bed was simply two sheets of stainless steel perforated plate (see Appendix 4). The plates sandwiched a layer of fine mesh to prevent the bed sand falling through. The fluidising velocity design point was 1.5 m/s, similar to a commercial unit. This value was varied by changing the air flow rate and bed temperature.

The bed and freeboard assembly sat on a supporting duct of mild steel, internally insulated with ceramic fibre. The duct received the air from the electric air pre-heaters and changed the direction from horizontal to vertical.

4.2.4 Material feed unit and test material

The feed mechanism for the input of composite scrap benefitted from the experience gained during the coal co-combustion test. The material feed was via a centre-less 10 mm wire diameter pig-tail screw, of 70 mm overall diameter. This was driven, within a feed tube of 89 mm internal diameter at the bottom of the feed hopper, by a 1.5 kW motor. This design avoided the jamming problems encountered with a positive displacement rotary valve during the commercial scale test. The feed hopper was sealed to prevent exit of the process gas through the feed material. A compressed air bleed into the feed tube prevented the crushed composite bridging in the hopper and provided a positive airflow into the freeboard. The air bleed also prevented the feed tube overheating.

The test work was performed with the same Sheet Moulding Compound (SMC) that was used in the above co-combustion testing. This had been processed in a knife type shredding mill at Birds Ltd (later Allied Metals) and sieved to be less than 20 mm in size. The SMC main constituents were: 25% resin, 22% glass fibre, 35% calcium carbonate filler and 15% alumina trihydrate.

4.2.5 Cyclone separators

The main cyclone was produced by Van Tongeren Ltd, a high efficiency type AC850 / 300

unit. The design air flow rate was 0.15 cubic metres per second at ambient temperature with a particulate loading of 0.25 g fibre/s.

In commissioning trials the Van Tongeren cyclone had been compared to one manufactured from a textbook design, see Appendix 4. This was a small diameter, high efficiency design in which it was assumed the particles to be collected were spherical (clearly not the case in this application). Initial commissioning showed that the high speed internal vortex, resulting from the small diameter, broke down any collected fibres. Thus the arrangement shown in figure 4.1 was used, where the large cyclone separated the fibres from the exhaust stream and the small cyclone collected the finer filler particles that were swept through the collection box.

The decoupling of a cyclone vortex from the collected material is usually achieved by a rotary valve. In this case, such a positive device was avoided to prevent damage to recovered fibres. An air bleed from the base of the cyclone, said to improve efficiency[54], was used for pneumatic transportation of the collected fibres into the collection bin. This was effectively a gravity settling chamber to remove the fibres from the bleed air flow.

4.2.6 Test rig - Phase 2 hardware

The second phase of the test rig was implemented after testing the original design. This recovered the reinforcing fibres heavily contaminated with mineral filler. Such contamination prevented wet out of the fibres for subsequent reuse. The main change in the Phase 2 test rig, shown in figures 4.3 and 4.4, is a rotating filter to separate reinforcing fibres from the fillers.

The fibres and fine fillers are elutriated from the fluidised bed into the freeboard. At the top of the freeboard is a coarse filter of 1.2 mm aperture. The fillers are swept through the filter with the exhaust gases for collection by the small cyclone. However, the fibres, being much longer are trapped on the underside of the filter. If this were static, the filter would quickly choke with fibres and block the outlet of the freeboard. However, the filter is continuously rotating about the freeboard axis. Once a region of filter passes a diametral split across the freeboard, a second reverse airflow blows the fibres off the sieve (see figure 4.4). These are then collected in a galvanised tank and immediately protected by a spray of size solution. The size used for this work was Cellosize® hydroxyethyl cellulose diluted to 20 g/m^3 in water.

44

The rotating filter is formed from two thin rings of stainless steel bolted together to frame a stainless steel mesh. This assembly has a central drive shaft powered by a DC motor that rotates the filter over a speed range of 0-480 rpm.
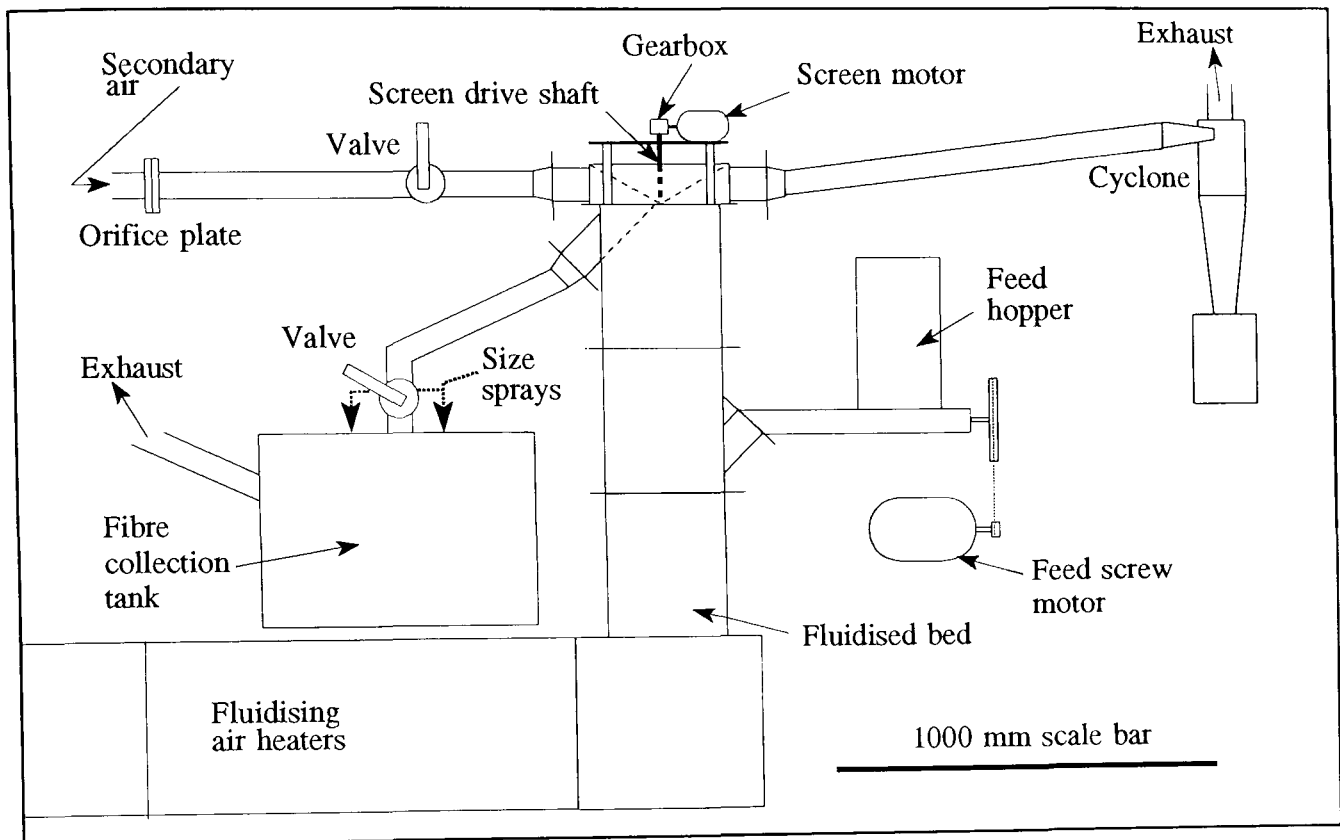
Figure 4.3   Phase 2 Fluidised Bed Test Rig
This shows the incorporation of the Rotating Screen Filter, designed to separate the fibres from the fillers after elutriation.
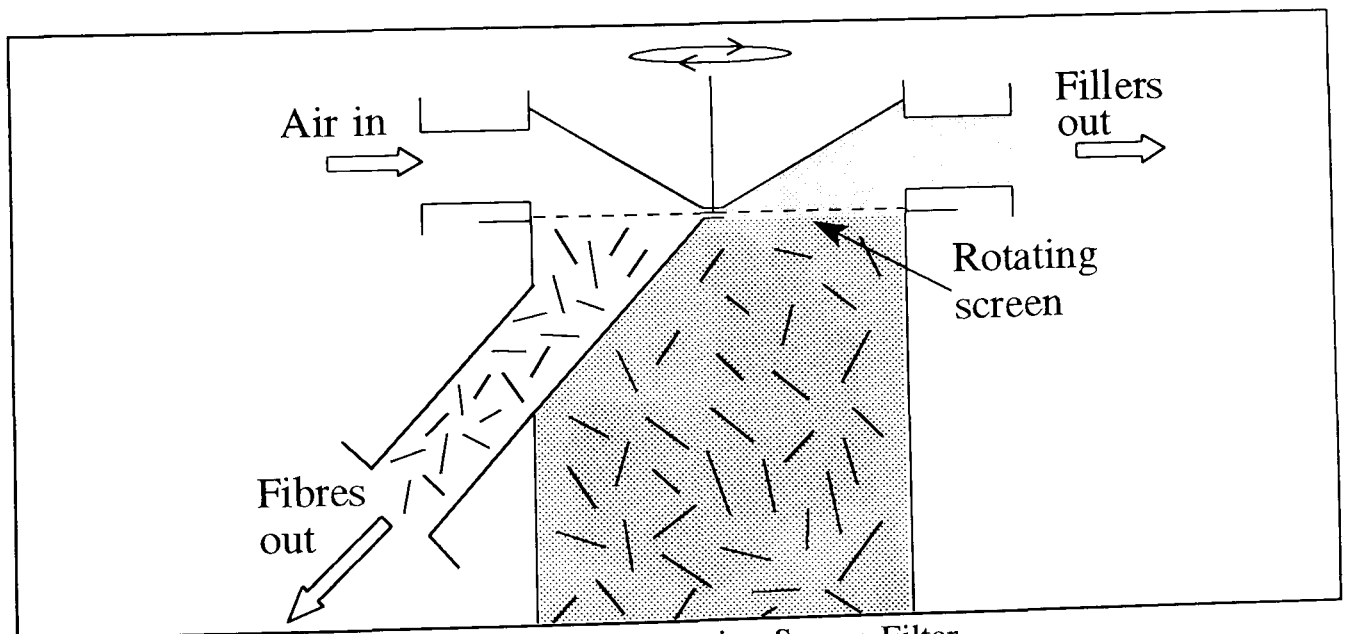
Figure 4.4   Schematic Diagram of the Rotating Screen Filter
This describes the operation of the filter. The elutriated fillers are swept through the filter while the fibres are caught on the underside. The filter rotates and the fibres are blown off by a secondary air flow.

45

The filter rotates within a stainless steel housing having inlet and outlet ports. The freeboard split was created by modifying one of the original freeboard barrels. The second (cold) air stream is controlled and measured by the same method as the fluidisation air.

A further hardware modification was to decouple the vortex at the base of the small cyclone cone. To avoid the use of a powered device, a cylindrical section containing five vertical truncated vanes was incorporated. This effectively choked the cyclone vortex from entering the collection pot without hindering the passage of particulates.

4.2.7 Instrumentation and gas analysis

The instrumentation of the two phases of the test rig is shown schematically in figures 4.5 and 4.6. Standard mineral insulated K-type thermocouples were used to measure temperatures at the positions shown.
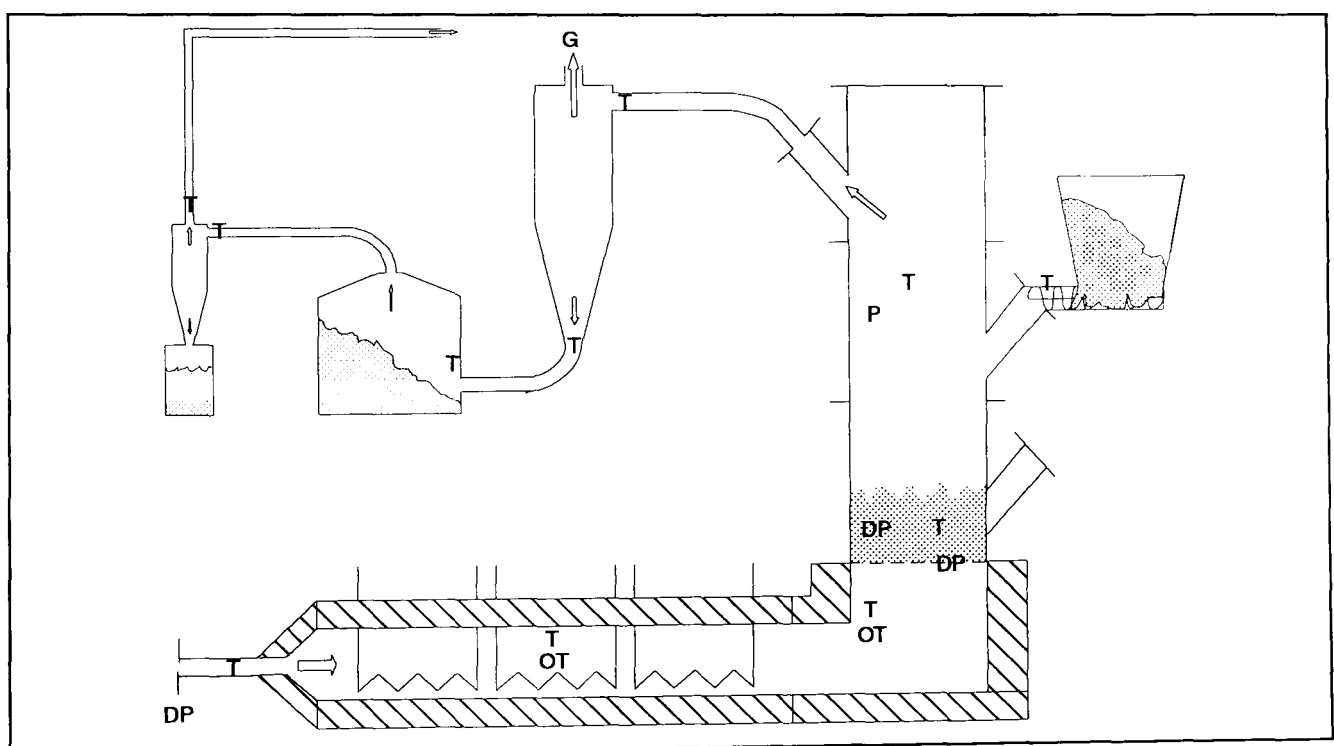
Figure 4.5   The Instrumentation on the Phase 1 Test Rig
    Key: T: Thermocouple
        DP: Differential pressure
        OT: Over temperature monitor
        G: Gas analysis point

Pressure measurement

A Furnace Instruments FCO16 pressure transducer was used for differential pressure measurement across the fluidising orifice plate. This single device was also used on Phase 2,

46

via a switching box, for setting the sieve cold air flow rate and differential pressure across the two halves of the sieve. Low pressure sensors from RS were used to monitor: the pressure drop across the distributor and bed and the gauge pressure in the freeboard over-pressure monitor.

The output from these devices was logged every 6 seconds by a Campbell Scientific 21 × Datalogger, which was down loaded periodically to an Akhter® personal computer.

Figure 4.6   The Instrumentation on the Phase 2 Test Rig
Key: T: Thermocouple
       DP: Differential pressure
       OT: Over temperature monitor
       G: Gas analysis point

Electrochemical gas analysis

The analysis of species in the flue gases was carried out with a Quintox electrochemical gas analyser from Kane International. This had been programmed by the manufacturers to output at three second intervals. The analyser was capable of detecting: oxygen, carbon monoxide, carbon dioxide, NO_x and SO_2. These gas concentrations indicated the quality of the resin combustion.

Flame Ionisation Detection (FID) of hydro-carbons

A Signal 3030 portable hydrocarbon analyser was used (on Phase 2 of the rig) to quantify the unburnt resin decomposition products at different conditions. Thus indicating the quality of

combustion of the resin.

4.3   Concluding Remarks

This chapter has described the test equipment. The next chapter details the method and assessment techniques applied to the recovered material obtained from the test rig.

Chapter 5

FLUIDISED BED THERMAL PROCESSING TEST RIG
- TEST STRATEGY AND ANALYSIS TECHNIQUES

5.0   Overview

The recovery of materials from composite scrap, in a high value form is vital for the economic viability of any recycling process. The most valuable recoverable material is the fibre reinforcement. Characterisation of the recovered material and the test rig combustion efficiency at different operating conditions would define the optimum processing conditions for a scrap composite.

This chapter has two subjects: the strategy behind the rig testing and the assessment methods for the incombustible material recovered from the fluidised bed test rig. Different assessment methods were applied to the two phases of the rig due to equipment and techniques becoming available during the progress of the project.

Rig Phase 1 - assessment techniques:

- Scanning Electron Microscopy.
- Strength characterisation of recovered glass fibres carried out by J. Kennerley[73, 76].
- Assessment of fibre surface contamination.
- Measurement of combustion gas concentrations via an electrochemical analyser.

Rig Phase 2 - assessment techniques:

- Phase 1 assessment techniques.
- The efficiency of combustion of the resin was monitored following the purchase of a hydrocarbon analyser.

The assessment techniques that were employed are described here, the results being discussed in Chapter 7. This chapter ends with a criterion for the success of the recycling process, with which results will be compared.

5.1   Testing Strategies

An inspection of the test rig parameters that influence the operating conditions is given in Table 5.1. This shows that the only independent variables were bed temperature and fluidising air flow rate. However, to change the bed fluidising velocity - the air mass flow rate must be varied. Thus, for experiment planning purposes, the test variables were: bed temperature and fluidising velocity, controlled by the air flow rate.

Table 5.1   Test Rig Parameters that Influence the Rig Operating Conditions
This inspection of the rig operating parameters defined those that could be varied to change the processing conditions.

Test Rig Variable	Comments
Duration of test	This influences the quantity of material processed and therefore the quantity of material recovered.
Fluidised bed temperature	An independent variable.
Fluidising velocity	A function of fluidising air flow rate and bed temperature.
Fluidising air flow rate	An independent variable.
Process material bed residence time	A function of fluidising velocity and bed temperature, independent of test duration.
Freeboard off take position	This may influence residence time conditions.

Initial commissioning trials proved that fibres were liberated and could be collected from processing composites in a heated fluidised bed. The trials also helped define the limits to the rig operation, as:

i)   The minimum realistic bed temperature to release fibres from the Sheet Moulding Compound (SMC) being investigated was 450°C.

ii)   The maximum bed temperature, limited by the preheater element temperature, was 750°C.

iii)   Commercial fluidising velocities are typically 1 to 2 m/s. Initial work showed little collection at 1 m/s and sand was carried out of the bed at a fluidising velocity of 1.7 m/s. This defined the upper and lower limits for testing.

iv)   To avoid a potentially self igniting mixture of volatile products in air, the SMC feed rate was limited to less than 1 g/s. Thus to recover just 0.5 kg of fibres required a test of 38 minutes duration.

5.1.1 Test methodology - Phase 1

The information gained from the commissioning trials and the rig parametric inspection was used to define the operating conditions for the test series matrix shown in Table 5.2.

Table 5.2   The Phase 1 Rig Conditions that were Tested with SMC Scrap

Bed Temperature (°C)	Density of air in bed. (kg/m³)	Mass flow rate in kg/s for a range of three test bed fluidising velocities:		
		1.3 (m/s)	1.5 (m/s)	1.7 (m/s)
450	0.481	0.0478	0.0552	0.0625
550	0.423	0.0420	0.0485	0.0550
650	0.377	0.0375	0.0432	0.0490

The actual experimental method used is detailed in the rig safe operating procedure in Appendix 5.

5.1.2 Test methodology - Phase 2

The Phase 2 test work was carried out to optimise the secondary airflow to the Rotating Screen Collector and assess the anticipated contamination reduction. The test work was carried out at 450°C and 1.3 m/s bed conditions, defined from Phase 1 test work (see chapter 7). Slightly higher temperatures were also tested for comparison, as the elutriated fibres were quickly quenched and thus the heat exposure period would be less than Phase 1. Also, an evaluation of total hydrocarbons was undertaken after delivery of the hydrocarbon analysis equipment.

Initial commissioning showed that for fibres to exit the Rotating Screen Collector housing into the tank, then a secondary air mass flow of at least the fluidising flow was required. This is un-surprising when considering the relative volumetric air flows. As the freeboard gas flow is nominally at 400°C, then the freeboard volumetric flow is more than twice that of the secondary airflow at approximately 20°C.

The pressure difference and thus any leakage flow between the hot and cold chambers of the Rotating Screen Collector was considered an important factor in the cross contamination of fillers and fibres. The original intent was to have a small bleed of secondary clean air counter to the movement of fibres to prevent both fillers and combustion products been carried into the tank. However, during initial commissioning this mode of operation also inhibited the movement of fibres. To enable fibre collection, a small bleed flow from hot to cold controlled by the tank valve was required to aid fibre movement. Thus the secondary air flow was fixed early in the test work at approximately the same mass flow as the fluidising air. This flow was sufficient to remove the fibres from the screen, but no higher, to avoid retarding the movement of the fibres past the Rotating Screen Collector split line.

5.2   Recovered Material Quality

5.2.1 Scanning Electron Microscopy

The surface quality of recovered fibres is important because the strength of glass is governed by surface flaws acting as stress raisers. The appearance of a fibre surface can give information on the quality of the recovered fibres. The large depth of field available on an Electron Microscope compared with an optical microscope was found to be very useful when looking at samples of overlapping fibres. As a first level of assessment, the micrographs produced were found to be ideal for qualitative comparison of fibres recovered from processing at different conditions.

The micrographs in this thesis were produced by the author on a JEOL JSM 35C machine. Samples of glass fibres were mounted on one side of a double sticky sided disk of carbon that was fixed to a larger aluminium specimen disk. The whole assembly was then gold plated. This deposited a very thin conducting layer without influencing the surface resolution.

Great care was required during sample preparation to ensure a thin scattering of fibres that were wholly in contact with the carbon disk. Any loose fibres or ones only partially secured would become charged by the electron beam and move about on the view screen as they discharged. By trial and error, an accelerating voltage of 12 kV was found to produce the best micrographs. A beam current of 0.1×10^{-10} A was used as this gave a narrow electron beam, leading to better surface definition particularly at higher magnifications. As small a beam aperture as possible was used as this produced a parallel electron beam. This improved the

depth of field and was especially useful for overlapping fibres.

The Electron Dispersive X-Ray elemental analysis facility of the Electron Microscope was tried on recovered fibres. This was performed across a fibre diameter, checking for variation in composition. However, the sample preparation and polishing were found to smear the mounting resin across the fibre, confusing the results. Thus the method was not pursued.

5.2.2 Contamination

It was important to know the quantity of material contaminating the recovered glass fibres. This was vital for defining a use for the recovered fibres, as any reuse would be likely to be governed by surface quality.

During trials to make samples of glass fibre veil from recovered fibres by a paper making type process, it was found that dispersing the fibres in a water slurry washed virtually all the visual contamination off. Thus the assessment of fibre contamination was built around washing the fibres (see the flow chart in figure 5.1).
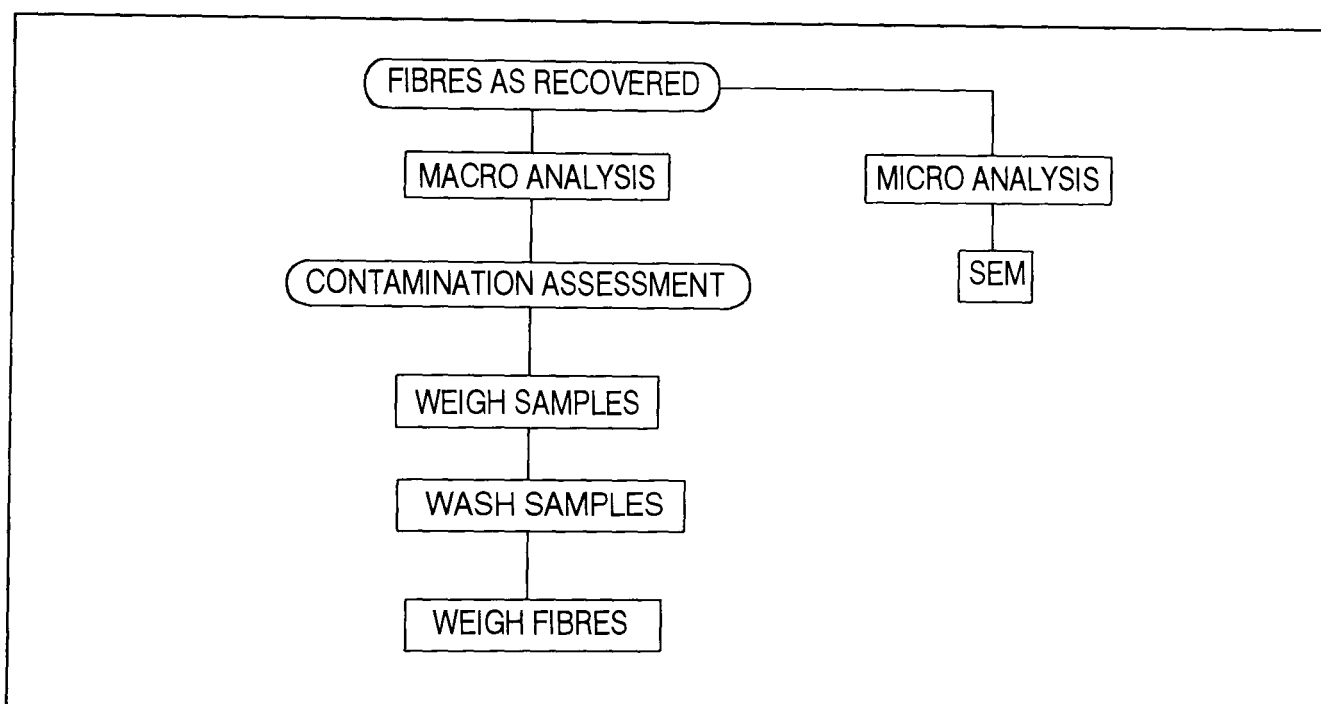
Figure 5.1   Surface Contamination Assessment for Recovered Fibres

5.2.3 Individual fibre tensile strength

As part of the RRECOM project the tensile strength of recovered fibres was measured by Kennerley[73,76].

53

Individual glass fibre tensile test method

The recovered glass fibres were individually glued onto paper frames to give a 10 mm gauge length. The fibre diameters were measured on a travelling microscope. Once mounted in the tensile test machine, the paper was burnt away. Fibre tensile strength was measured on an Instron 1195 machine. The results of this investigation are reviewed with the other results in Chapter 7 and used to optimise the rig Phase 1 process conditions.

5.3 Recycling Process Rig Success Criterion

The first consideration for the fluidised bed process is whether the incombustible material is released from the resin matrix and if fibres are in a reusable form. Given the achievement of this goal, the following are considered to define a successful process.

a) Recovery of the incombustible fraction of the composite in a form with the highest value possible, i.e. relatively unbroken fibres with high physical properties. Also, a high rate of incombustible material recovery is vital for the overall economic viability.

b) The efficient recovery of heat from the combustion of the polymer matrix of the composite. However, this could not be assessed on the test rig as no heat exchanger was included. The completeness of combustion was measured by analysis of the flue gases.

c) The output into the atmosphere should be within the regulations for the size of combustion plant. The scale of the test rig defines the output to atmosphere as being negligible.

5.4 Concluding Remarks

This chapter has described: the fluidised bed combustion rig test strategy, the assessment techniques applied to the recovered materials and a success criterion for the recycling process. Chapter 7 reports and discusses the results obtained from running the fluidised bed test rig.

Chapter 6

COMPOSITE SCRAP THERMAL DECOMPOSITION MODEL

6.0   Overview

The literature survey of Section 2.3 showed that there is a reduction in the strength of glass fibres on exposure to heat. This depends upon the temperature-time history of the fibres. Thus the time-temperature history of any recovered fibres was vital to understand the recovered material characterisation.

The test rig instrumentation and flow rates gave information on the environment of the fibres, once elutriated. However, the thermal breakdown of composite scrap within the fluidised bed could not be monitored directly. Thus a modelling technique was developed to gain an appreciation of the likely temperature-time history of the fibres in the fluidised bed process. The thermal breakdown of the composite is governed by the heat conducted into the matrix from the surface. Thus the problem is one of heat transfer. Once validated, the model could be used as a predictive tool to aid optimisation of the process conditions for a given thermoset type.

6.1   Model Assumptions

6.1.1 One dimensional heat transfer

To keep the modelling task manageable within the scope of these investigations, a one dimensional through thickness heat transfer model was developed. The crushed Sheet Moulding Compound scrap used in this work had a mean length to thickness ratio of less than 7:1. Thus, the assumption of one dimensional heat transfer required validation with experimental results.

6.1.2 Symmetry of composite scrap plates

The plates of crushed composite scrap were considered to be symmetrical about their mid-planes, see figure 6.1. Thus only the heat transfer from the surface to the centre, through the plate thickness, requires consideration.

55

6.1.3 Composite thermo-physical properties

The composite was assumed homogeneous, the density and specific heat capacity were calculated in the mass ratio of the constituents. Table 6.1 shows the data values used in the model. As the composite decomposed, the contribution of the resin to the overall material property was adjusted in proportion to the fraction of the resin remaining.
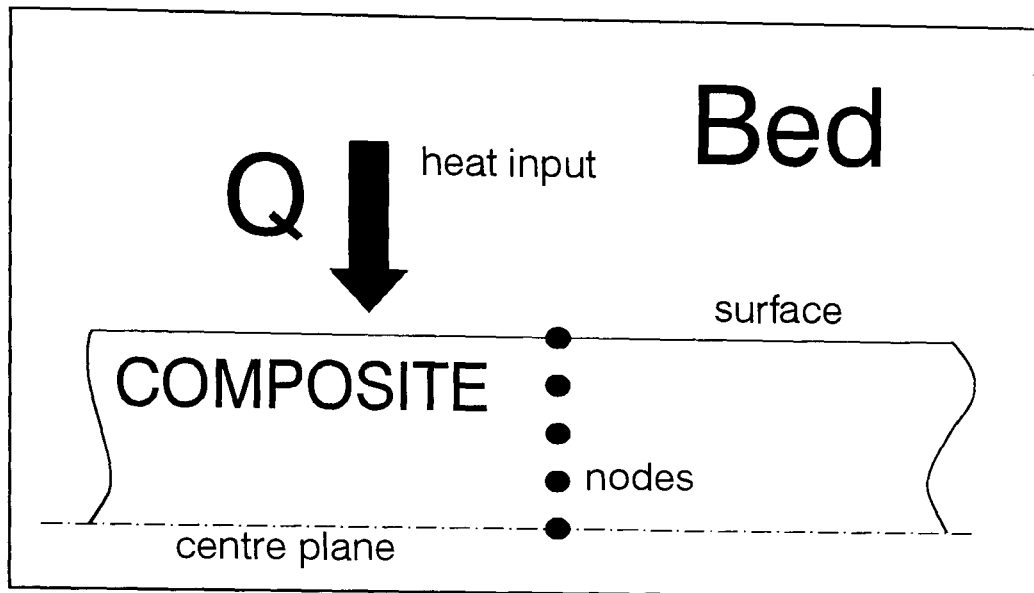
Figure 6.1   One Dimensional Model for the Thermal Decomposition of Composite Scrap within a Fluidised Bed.

Table 6.1   Assumed Material Thermo-physical Bulk Properties

The quoted properties were measured at: a: 20°C, b: 20-300°C, c: 200°C, d: 22°C. The estimated properties for alumina trihydrate were arrived at by a review of available data for other minerals.

Composite Constituent	Material Property					
	Density		Specific Heat Capacity		Thermal Conductivity	
	(kg/m³)	Ref.	(J/kg.K)	Ref.	(W/m.K)	Ref.
Polyester Resin	1100	55	1800	56	0.2	56
Calcium Carbonate	2700[a]	57	900[a]	57	2.7[b]	58
Alumina trihydrate	2400	59	900	est.	2.2	est.
E-Glass (bulk)	2565	60	1034[c]	60	1.154[d]	60

Thermal conductivity

The overall thermal conductivity of a composite structure cannot be calculated in simple proportion to the mass or volume of constituents and many experimentally validated models exist for its derivation[61]. An in depth study and comparison of the methods to calculate the thermal conductivity of a composite is beyond the scope of this investigation. Table 6.1 indicates that the thermal conductivity value will lie between 0.2 and 2 W/m.K, the values for resin and filler respectively. An experimental measurement of the thermal conductivity of a composite, from reference 61, is shown in Table 6.2.

Table 6.2   Measured Thermal Conductivity of a Composite[61]

The conductivity values were measured for a composite, containing polyester resin and uni-directional glass roving (66% by weight). The higher in plane conductivity is due to heat being conducted along glass fibres rather than across them.

Property	Temperature	0°C	160°C
Through plane conductivity (W/m.K)		0.35	0.4
In plane conductivity (W/m.K)		0.56	0.61

The resin decomposition curves calculated by the model for three different values of thermal conductivity are compared with experimental data in figure 6.2. (The model details are described below, in Section 6.2). This shows the sensitivity of the model to thermal conductivity of the composite within the material range shown in Table 6.1. A thermal conductivity of 0.3 W/m.K fits the experimental data and is consistent with the through plane values from the literature in Table 6.2. Thus a composite thermal conductivity of 0.3 W/m.K is used in the model.

Resin decomposition

The endothermic energy of decomposition of polyester resin, see Section 6.2.1, was assumed to be 2.34 MJ/kg. This was taken from similar modelling work at The University of Newcastle-upon-Tyne[62].

The resin decomposition activation energy and pre-exponential factor were calculated from

57

Thermo-gravimetric analysis of cured polyester resin, see Section 6.3. This reaction was assumed to be first order.

Decomposition of alumina trihydrate filler

The effect of decomposition of any alumina trihydrate filler was assumed to start at 200°C, be a maximum at 300°C and have finished at 400°C[58]. The associated endothermic decomposition energy of the filler was assumed to be 150 kJ/mol[59].
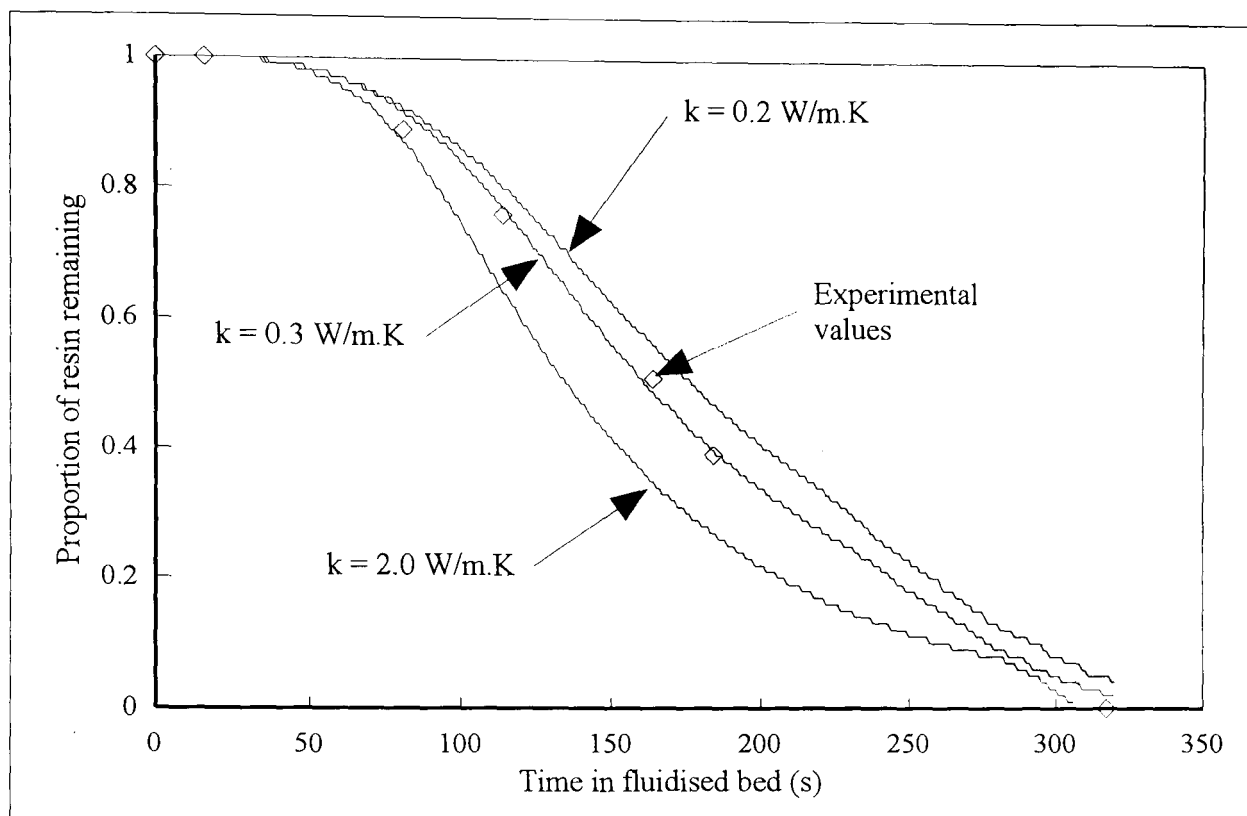
Figure 6.2   Graph of Resin Mass against Time of Composite in a Fluidised Bed.

This graph indicates the sensitivity of the model to a change in the thermal conductivity of the composite. Curves are shown for thermal conductivities of resin and filler, these are 0.2 and 2 W/m.K, respectively. The model was run for the same composition as the Sheet Moulding Compound used in the experimental work, so that comparison to experimental data could be made.

Temperature dependence of thermo-physical properties

Some data exists for the change of thermal properties of the constituents of composites with temperature, see Table 6.2. However, such information is not available for all properties or materials. The agreement between the model and experimental data, shown in figure 6.2, when the change of properties with temperature was not accounted for, lends confidence to the accuracy of the model.

6.1.4 Composite surface attrition

Calculation of the attrition of the composite surface within the fluidised bed was considered to be outside the scope of the study. Composite scrap would move with the fluidised bed sand and so the bed to particle relative velocity would be (an unknown) less than the fluidising velocity. Although, literature[63] exists on the surface erosion of composite materials. This shows that erosion rate is proportional to the nth power of the particle velocity, where n varies between 2.35 to 2.80 depending on the material type. Section 6.1.6 describes the material breakdown mechanism that was assumed in the model.

6.1.5 Fluidised bed heat transfer coefficient

The heat transfer coefficient from the bed to the composite was assumed constant within the fluidised bed. The majority of the literature (some reviewed in reference 65) dealt with heat transfer at a static heat exchanger surface within or just above the bed. A number experimental correlations are reported, e.g. the heat transfer coefficient varying between 422 and 490 $W/m^2.K^{[66]}$ for 533 μm sand bed, at temperatures of 450 and 650°C respectively. However, the majority of the reported experimental results vary between 200 and 400 $W/m^2.K^{[65]}$.

The crushed composite scrap is in the form of plates. These are not static within a fluidised bed, unlike a heat exchanger surface. Thus the relative velocity between the particles and bed will be lower than the fluidising velocity, lowering the heat transfer coefficient value. Therefore, the actual heat transfer coefficient is likely to be at the lower range of that in the literature.

A number of heat transfer coefficient values were assumed, the model output was compared with experimental data, see below.

6.1.6 Composite fibre release

When the resin at a given position in the composite had all decomposed or reduced below a certain proportion (7% was used in the model), it was assumed that the fibres at that position were released and the node effectively became part of the bed. This moved the resin surface toward the centre by a nodal spacing. The composite then continued to be modelled as a thinner section.

This is only an approximation for two reasons. Firstly, practical experience shows that loose bundles of fibres can be sieved, intact, from the bed even without the binding matrix. Secondly, this assumption implies that the fibres are all parallel to the surface; it is more likely that one end of a fibre will become exposed to the bed whilst still held to the decomposing composite at the other end. This assumption would be more applicable for short fibres, rather than the standard 25 mm chopped roving of Sheet Moulding Compound.

6.2   Thermal Model Theory

Lumped capacitance heat transfer

As the composite scrap is of relatively thin section, then the temperature gradient across the section may be uniform. If this were the case then modelling the heat transfer could be modelled by a lumped capacitance method. The measure of applicability of this method is if the Biot number is below 0.1[67]:

$$Bi = \frac{h \cdot L}{k} \leq 0.1$$

Substituting values of: heat transfer coefficient, characteristic dimension (half thickness for a slab) and thermal conductivity of: 200 W/m^2.K, 2 mm and 0.3 W/m.K respectively gives a Biot number of 1.3. This does not meet the applicability criterion. Thus, through thickness temperature variations are significant and this approximation cannot be used. A one dimensional finite difference model was applied between the composite surface and the centre line. The half thickness of the composite was split equally, creating a number of equi-spaced nodes, see figure 6.1. Each node represents a discrete material volume.

6.2.1 Heat transfer theory

The one dimensional heat transfer equation, simplified from Holman[68] is:

$$\rho C_p \frac{\partial T}{\partial t} = k \frac{\partial^2 T}{\partial x^2}$$

When terms for the decomposition of the resin are added, the equation becomes[69]:

$$\rho C_p \frac{\partial T}{\partial t} = k \frac{\partial^2 T}{\partial x^2} - Q_p \rho A e^{-\frac{E}{RT}}$$

The last term includes Qp, the endothermic energy required for decomposition of the resin.

Alumina trihydrate dehydration

Rather than include an extra term, the endothermic effect of alumina trihydrate losing water was accounted for by increasing the overall composite specific heat capacity value during the temperature range 200 to 400°C. The 150 kJ/mol[59] or 1.85 MJ/kg endothermic energy was distributed over the 200°C temperature range. This was achieved by assuming that the specific heat capacity increased by 0 kJ/kg.K at 200°C, 18.5 kJ/kg.K at 300°C and 0 kJ/kg.K at 400°C, varying linearly within the 200 to 400°C range.

6.2.2 Model plan

The flow chart in figure 6.3 shows the sequence of the completed Turbo Pascal model. The Pascal methodology of organising a programme into procedural blocks ensures ready access to a moderate programmer for future development.

Nodal spacing

The nodal spacing is calculated within the model simply by dividing half the thickness of the composite by one less than the number of nodes. The number of nodes was chosen arbitrarily so that the program run times were not excessive. Fifteen nodes were used in all the model work in this chapter.

Minimum finite difference time increment

The explicit finite difference method used is not unconditionally stable and the time increment must be specified with some care. Holman[70] gives the stability requirements as:

For an interior node:

$$Fo \leq \frac{1}{4}$$

For a convection boundary node:

$$Fo \, (\, 2 \, + \, Bi \,) \, \leq \frac{1}{2}$$

Where, the Fourier number is given by:

$$Fo \, = \, \frac{k}{\rho . \, C_p} \cdot \frac{\Delta t}{\Delta x^{\, 2}}$$

Inspection of these equations shows an interior node to have the smallest time step. In the model the time step is set for the centre node at every iteration as the thermo-physical constants change.
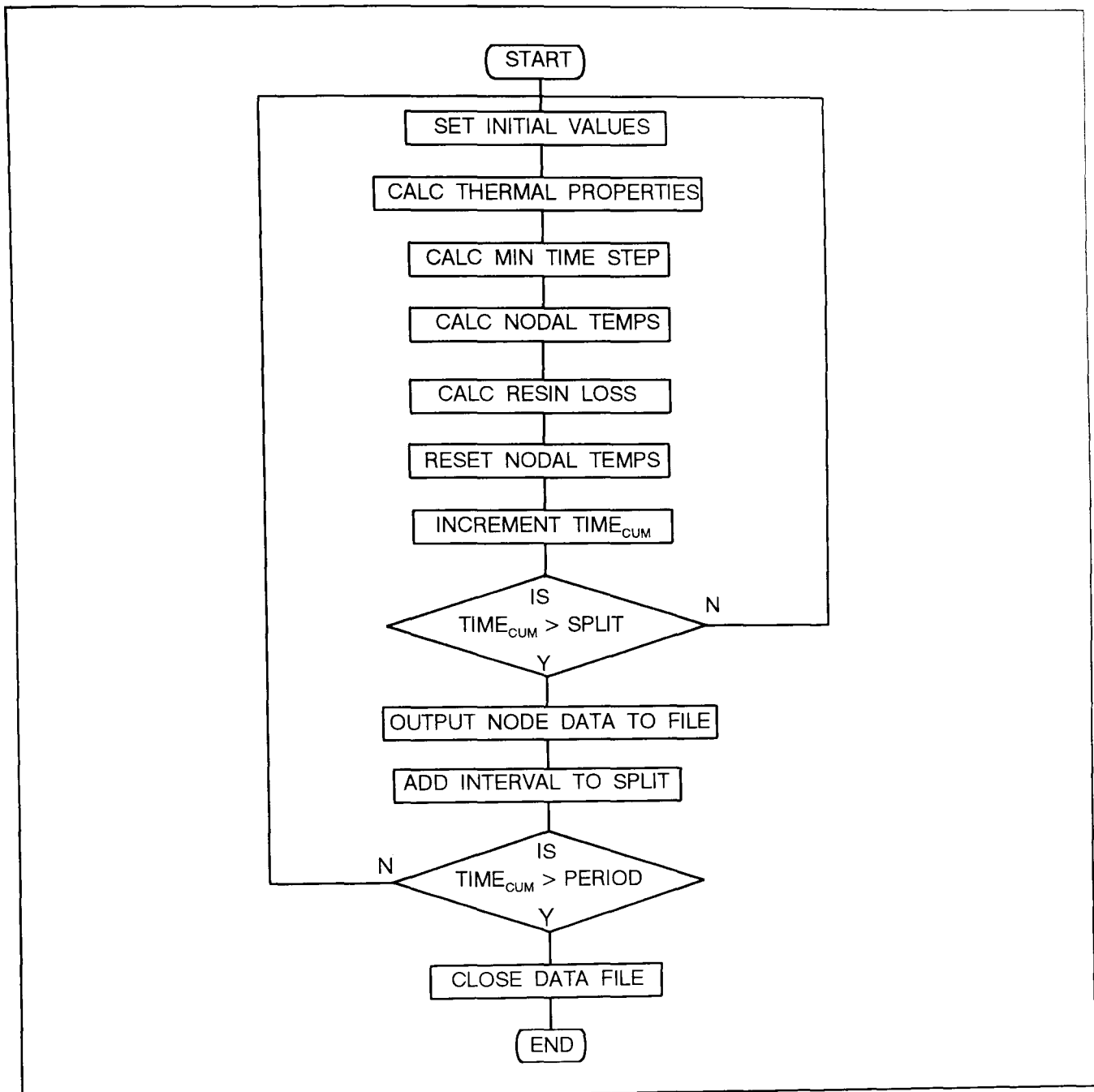
Figure 6.3   Flow Chart of Decomposition Model
This diagram shows how the various procedures are called up within the thermal model.

6.3   Calculation of Resin Decomposition Constants

The decomposition of the resin was modelled using an Arrhenius equation:

$$K = A \cdot e^{-\frac{E}{RT}}$$

This required the activation energy (E) and pre-exponential factor (A) for the resin. No values for these constants were found in the literature, so they were calculated from thermogravimetric analysis of cured polyester resin.

The governing mass loss equation is:

$$\frac{d\alpha}{dt} = K(1-\alpha)^n$$

Re-arranging[71] and assuming that the decomposition reaction is first order gives:

$$\frac{\frac{d\alpha}{dT}}{(1-\alpha)} = \frac{A}{\beta} \cdot e^{-\frac{E}{RT}}$$

Taking natural logs of both sides, then a plot of the natural log of the left hand side against (1/T) would have a gradient of (-E/R) and an ordinate intercept of $\ln(A/\beta)$.

Cured polyester resin was crushed with a pestle and mortar and sieved less than 105 μm. A sample was then processed in a thermogravimetric analyser at Leeds Metropolitan University[72], at a heating rate of 10°C/min. The thermogravimetric mass loss curves were obtained for both air and nitrogen atmospheres, to check for mass loss due to combustion, the curves were virtually identical. Figure 6.4 shows both the mass loss curve as measured in nitrogen and the (inverse) fraction decomposed (α) curve. It is the gradient of the latter curve that provides the values for calculation. Figure 6.5 shows the natural log plot having a gradient of (-E/R) and an ordinate intercept of $\ln(A/\beta)$.
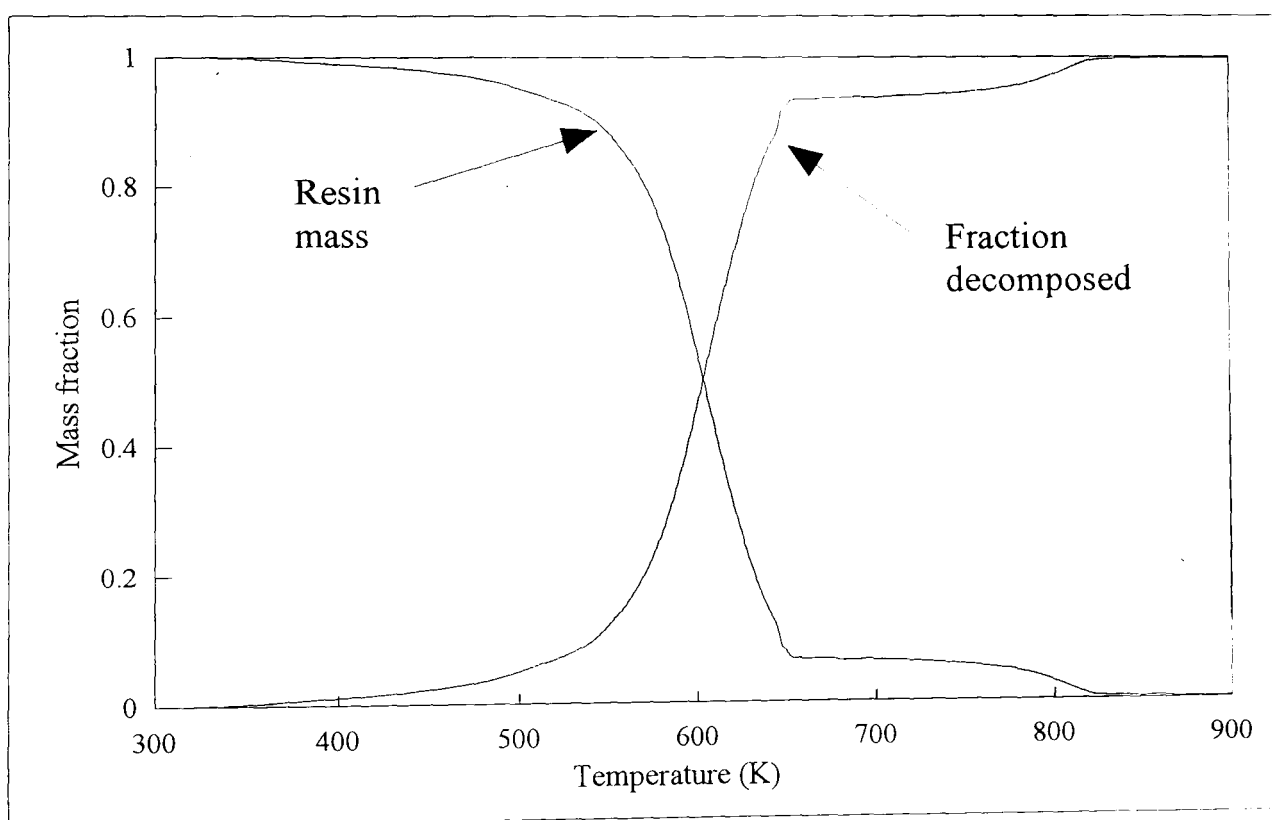
Figure 6.4   Thermogravimetric Analysis of Polyester Resin, Mass Change Against Temperature

63
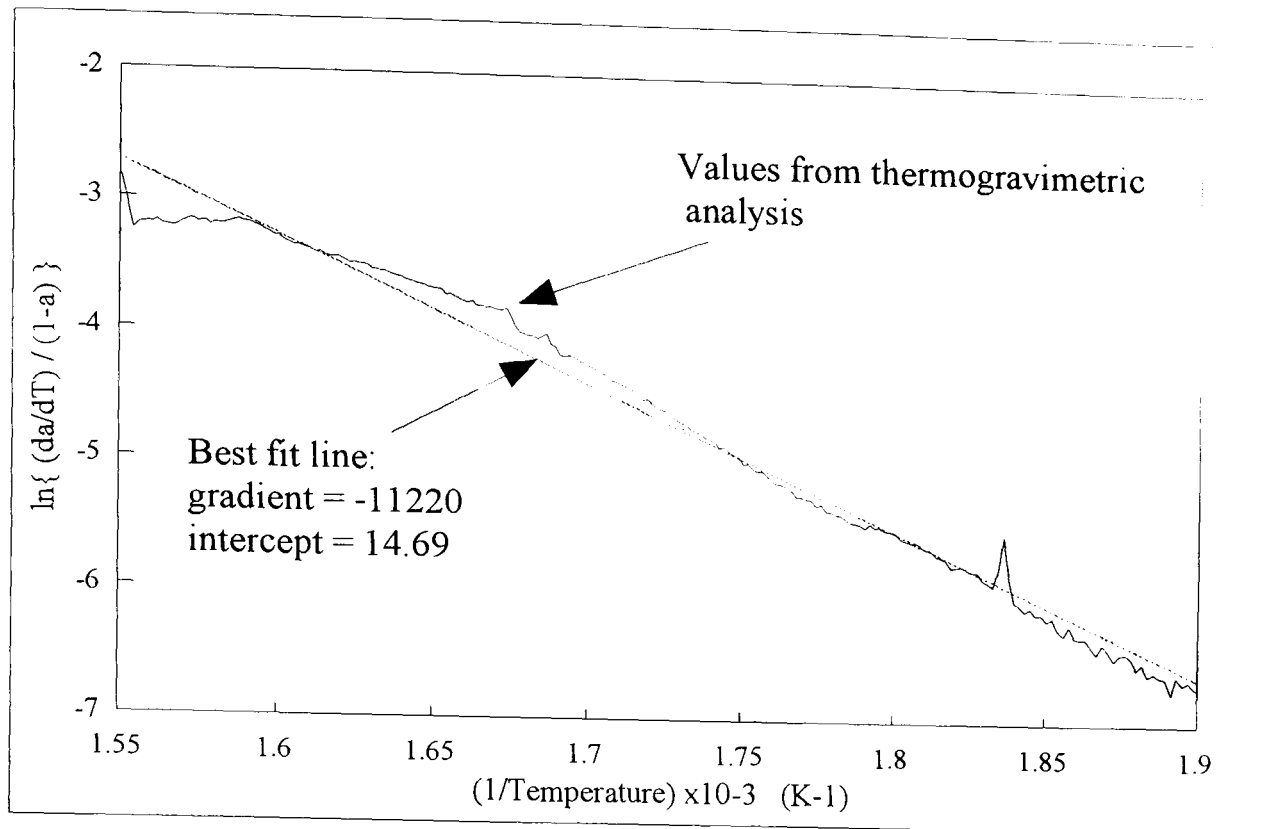
Figure 6.5 Derivation of Resin Decomposition Constants
This graph plots data derived from the mass fraction decomposed curve shown in figure 6.4. The gradient of the best fit line is (-E/R) and the ordinate intercept is $\ln(A/\beta)$. Substituting gives values of E and A as 93.3 kJ/mol.K and $A = 399.8 \times 10^3$ s^{-1} respectively.

6.4   Model Validation

Experimental validation of the numerical model was made by measuring the gas concentration from the fluidised bed as composite pieces were processed at 450°C. Numerical integration of the carbon monoxide concentrations over the test duration resulted in a resin mass loss decomposition curve. The model was applied to the thermal decomposition of the various composite scrap at the conditions tested.

6.4.1 Investigation of heat transfer coefficient

Figure 6.6 shows the total resin mass losses calculated from the model assuming different heat transfer coefficient values with a bed temperature of 450°C. These curves are compared with data for a piece of the Sheet Moulding Compound, 3.6mm thick and 50mm square.

Figure 6.6 shows that the model output assuming a fixed heat transfer coefficient of 200 $W/m^2.K$ is the best fit to the experimentally derived resin mass loss. Therefore, this value is assumed for all subsequent model work.
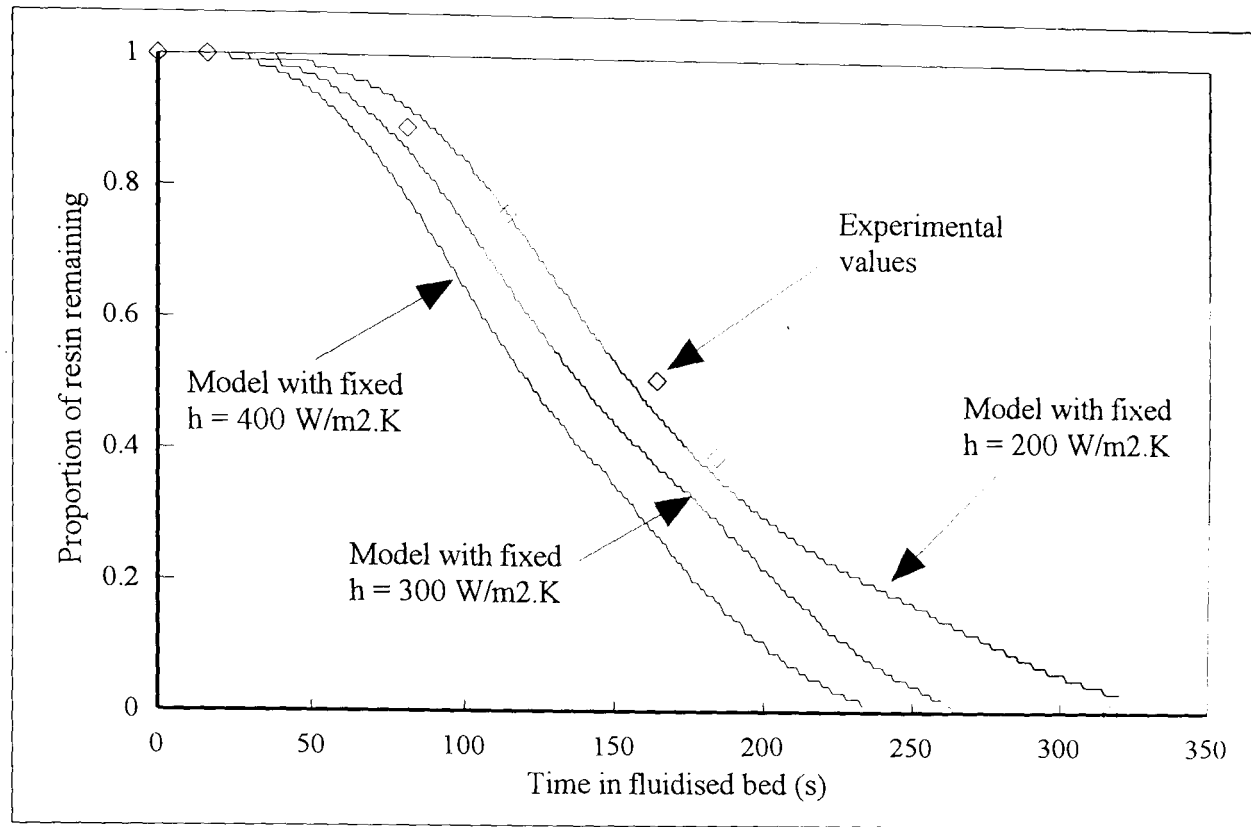
Figure 6.6 Comparison of Experimental with Model Decomposition for Different Values of Fluidised Bed Heat Transfer Coefficient

6.4.2 Testing the model with GRP of different sizes and thicknesses

The model was tested against the resin mass loss curves produced experimentally for the polyester resin composite samples detailed in Table 6.3.

Table 6.3 Polyester Composite Scrap Plates used in Model Validation

Sample	A	B	C	D	E
Type	DMC	Polyester resin and glass			
Thickness (mm)	2.65	3.75	1.99	6.27	
Plate Size (mm)	50.5×51.3	51.2×51.3	28×29.3	50.9×50.6	26.4×25.9
% Resin	17	63.2	54.9	67.7	
% $CaCO_3$	68	-	-	-	
% Glass	15	36.8	45.1	32.3	

65

Figure 6.7 compares the resin mass loss calculated by the model with an experimentally derived curve for the Dough Moulding Compound (DMC) sample. The model curve is steep compared with the experimental data, possibly due to the assumed heat transfer characteristic being too high for this highly filled material.
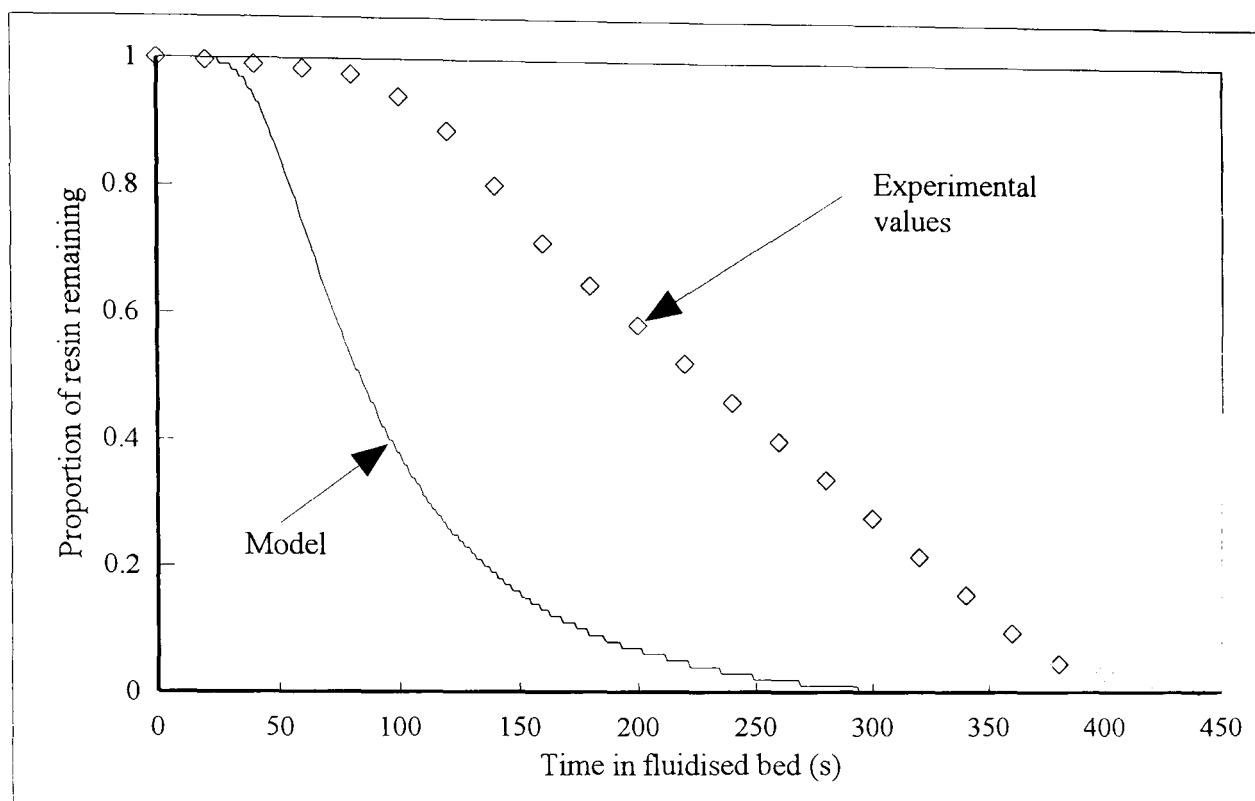
Figure 6.7   Comparison of Experimental Resin Mass Loss with Model Decomposition of Dough Moulding Compound, Sample A

The model curve for the standard thickness (3.75 mm) composite, see figure 6.8, finishes very nearly coincident with the experimentally derived mass loss data giving reasonable overall agreement. The model curve for a thin section composite scrap, see figure 6.9, shows worse agreement with experimental values than the standard composite thickness shown in figure 6.8. This indicates that the model is less accurate when applied to thin section composite scrap.

Figure 6.10 compares the experimentally derived curves for small and large composite pieces (of the same thickness) with model data. Initially, the model has good agreement with the large sample, as could be expected from the one dimensional heat transfer assumption. However, below approximately 50% resin left, the model becomes close to the experimental curve from the small sample.
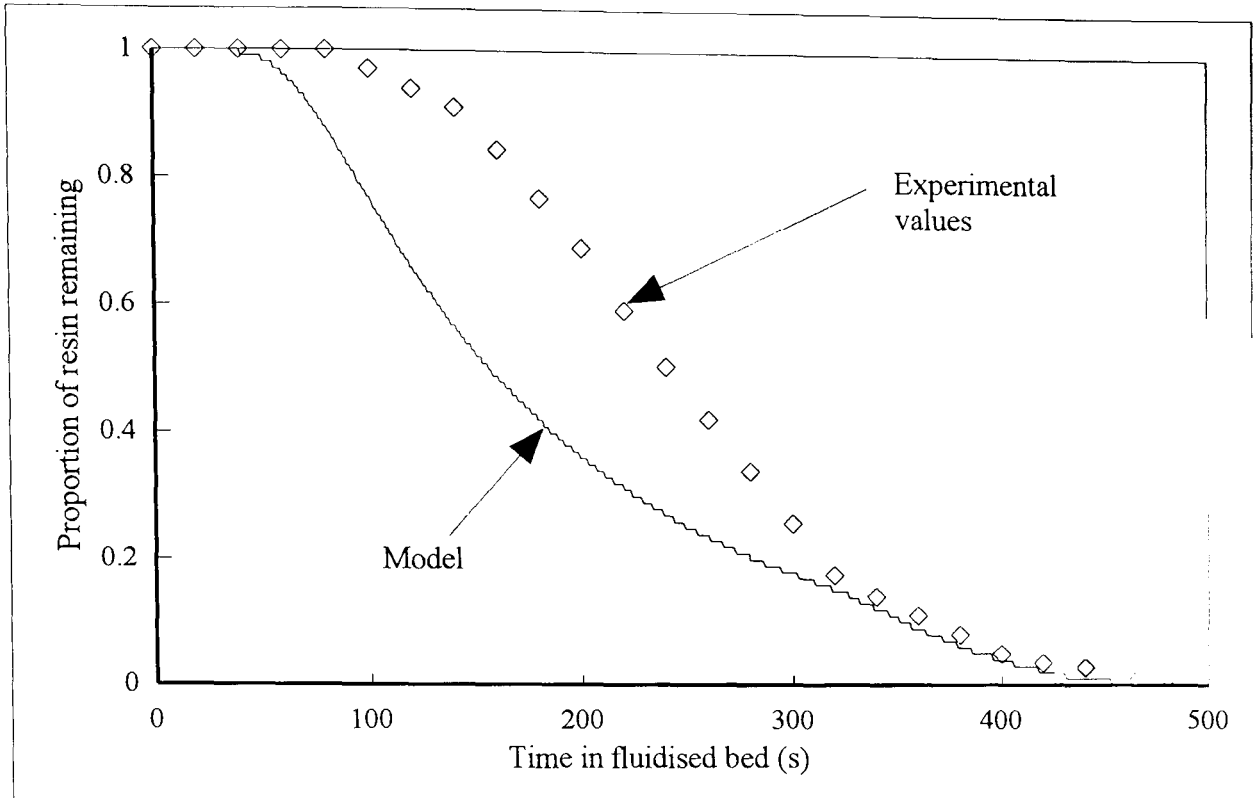
Figure 6.8   Comparison of Experimental Resin Mass Loss with Model Decomposition for 3.75 mm Thickness Composite Scrap, Sample B
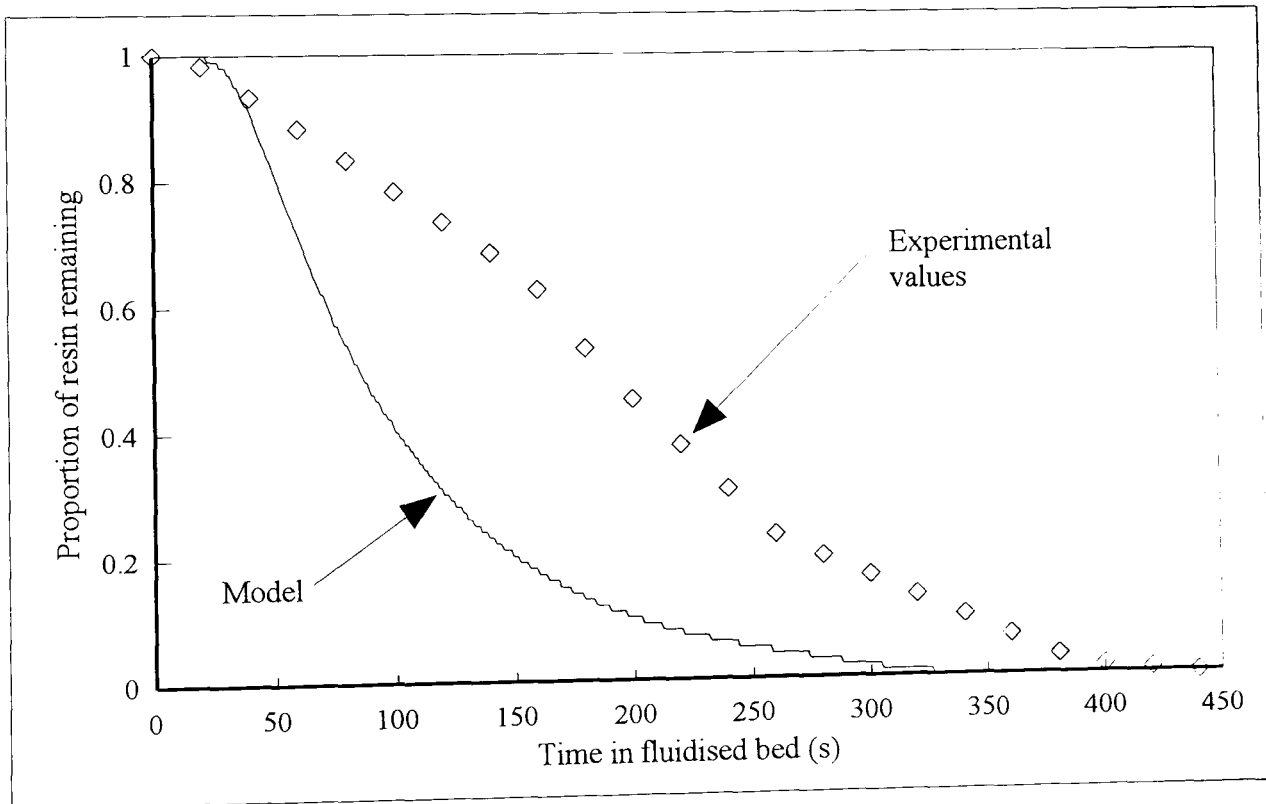
Figure 6.9   Comparison of Experimental Resin Mass Loss with Model Decomposition for 1.99 mm Thick Composite GRP, Sample C
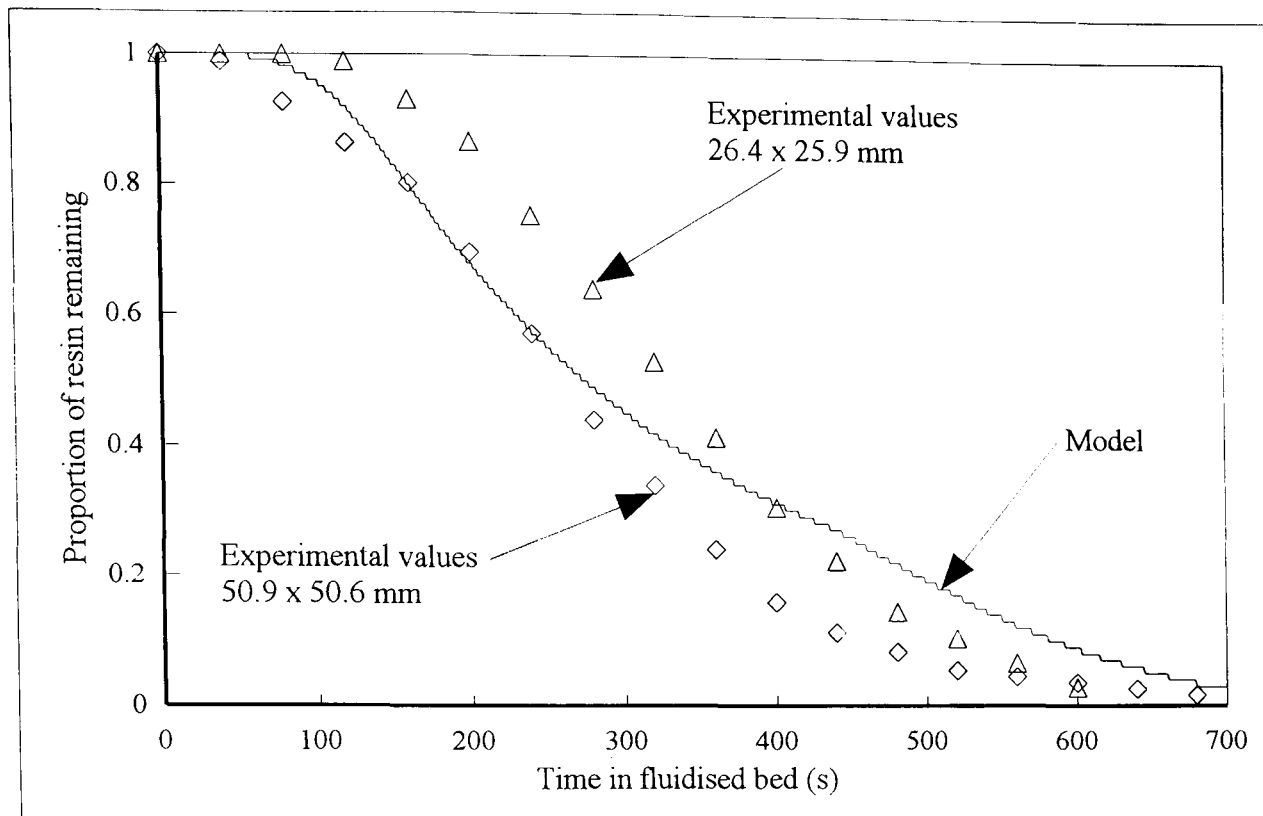
Figure 6.10 Comparison of Experimental Resin Mass Loss with Model Decomposition for 6.27 mm Thick Composite Scrap of Two Plate Sizes, Samples D and E

Considering the agreement shown for the other samples, the model output curves shown in figure 6.10 could be considered to have reasonable agreement to both the experimental curves. This implies that the one dimensional heat transfer assumption is reasonable for the sample sizes tested.

There is good agreement between the small (but thick) experimental data (Sample E) and the model in figure 6.10. However, the model curve for thin plate Sample C, of similar face dimensions to Sample E, shows poor agreement with the experimental curve. This implies that the plate thickness is the dominant factor for model accuracy, rather than face size.

6.4.3 Summary

The model output shows the best agreement with experimental data for standard to thick section composite scrap and good agreement for the Sheet Moulding Compound used in the recovery trials. The Sheet Moulding Compound has a nominal 4 mm thickness, twice that of the composite with the poor model to experimental agreement shown in figure 6.9. This lends confidence for modelling the thermal decomposition of the crushed Sheet Moulding Compound.

6.5 Prediction of Sheet Moulding Compound Fibres Bed Residence Time

The model was run for the Sheet Moulding Compound with bed temperatures covering the range tested experimentally: 450-650°C. The fibre release criteria was set at 7% to lower the end of the model output curves shown in figure 6.6. The time-temperature results are discussed in Chapter 7.

Chapter 7
RESULTS AND DISCUSSION

7.0   Overview

This chapter presents and discusses the results from the trial of both Phases of the fluidised bed test rig, analysis of the recovered fibres and temperature profiles from the thermal model.

7.1   Results and Discussion - Rig Phase 1

7.1.1 Rig parameter optimisation

The range of conditions tested during Phase 1 of the fluidised bed rig are summarised in Table 7.1. This also shows the duration of the test at each condition and the destination of the incombustible residue on completion of each test.

Figure 7.1 shows that no collection efficiency correlations can be drawn from the recovered quantities of materials. Although, at higher fluidising velocities, less material was generally left in the bed and more recovered from the cyclone and bin. In a continuous process, the quantity of material in the bed at any one time is not critical - as long as the build up reaches a steady state without affecting fluidising conditions significantly.

At the fluidising velocity of 1.7 m/s, sand was elutriated with the fillers and fibres. This was undesirable as the fibres were required to be as pure as possible for further processing. The quality of the recovered materials at each process condition was considered to be the key in optimising the process parameters.

7.1.2 Scanning Electron Microscopy of recovered fibres

Figures 7.2, 7.3 and 7.4 show micrographs of fibres recovered from the rig tests at temperatures of 450°C, 550°C and 650°C respectively. The figures show that the fibres are visually intact with smooth surfaces. Similar levels of filler contamination are apparent, irrespective of the processing temperature.

Table 7.1 Optimisation Testing on Rig - Phase 1

This table summarises the test work carried out on Phase 1 of the test rig at various bed temperatures and fluidising velocities. Also shown is the destination (see figure 4.1) of the incombustible material, on completion of each test.

Bed Temp (°C)	Bed Fluidising Velocity (m/s)	Time (min)		Recovered / recoverable incombustible mass (%)			
		Feed	Run on post feed	Bin	Other	Bed	Total
450	1.2	60	10	37.3	36.3	24.2	97.8
450	1.3	60	10	64.2	3.6	25.8	93.6
450	1.5	60	10	47.2	24.7	14.1	86
450	1.7	60	10	66.1	16	16.7	98.8
550	1.3	60	10	35	19.2	15	69.2
550	1.5	45	10	60.7	23.8	15.3	99.8
550	1.67	11	13	63.8	0	9.9	73.7
650	1.3	38	10	46.2	9.4	27.3	82.9
650	1.5	31	10	33.2	35.4	20.7	89.3
650	1.71	28	10	83.4	0	9.37	92.7
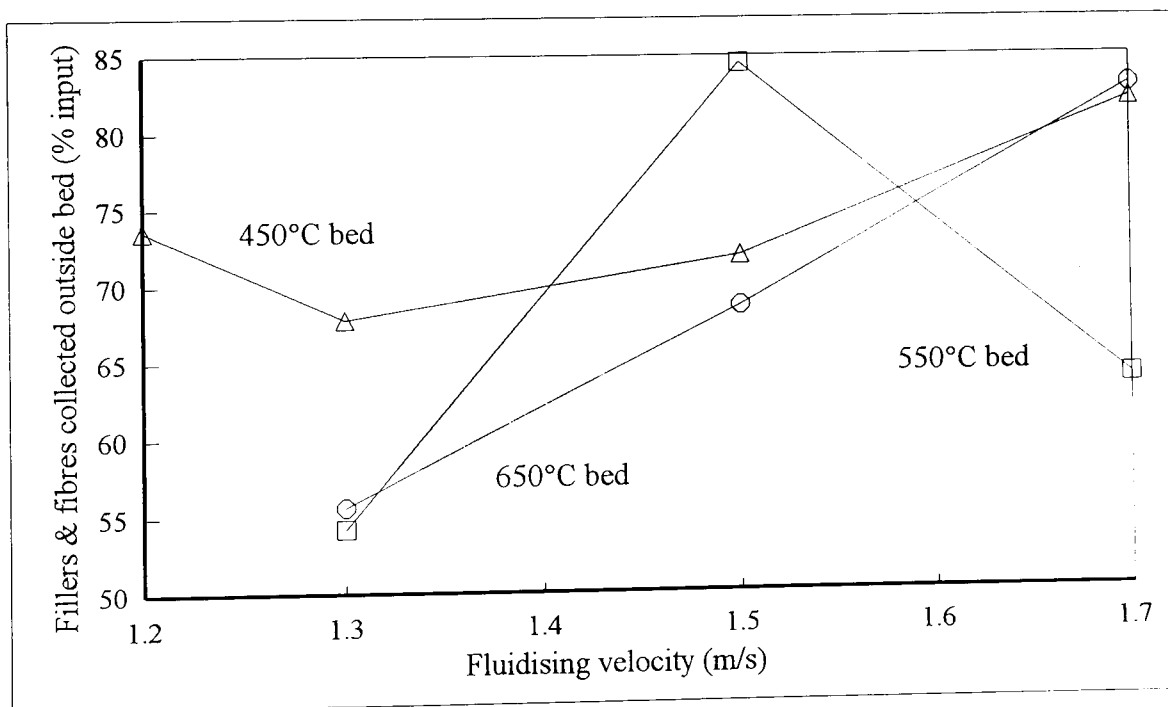
Figure 7.1   Graph of Incombustible Material Collected in the Settling Bin and Cyclone

The recovered material is expressed as a mass percentage of the recoverable, incombustible constituents of the Sheet Moulding Compound.

12KU X1600   8613   10.0U ME&MD
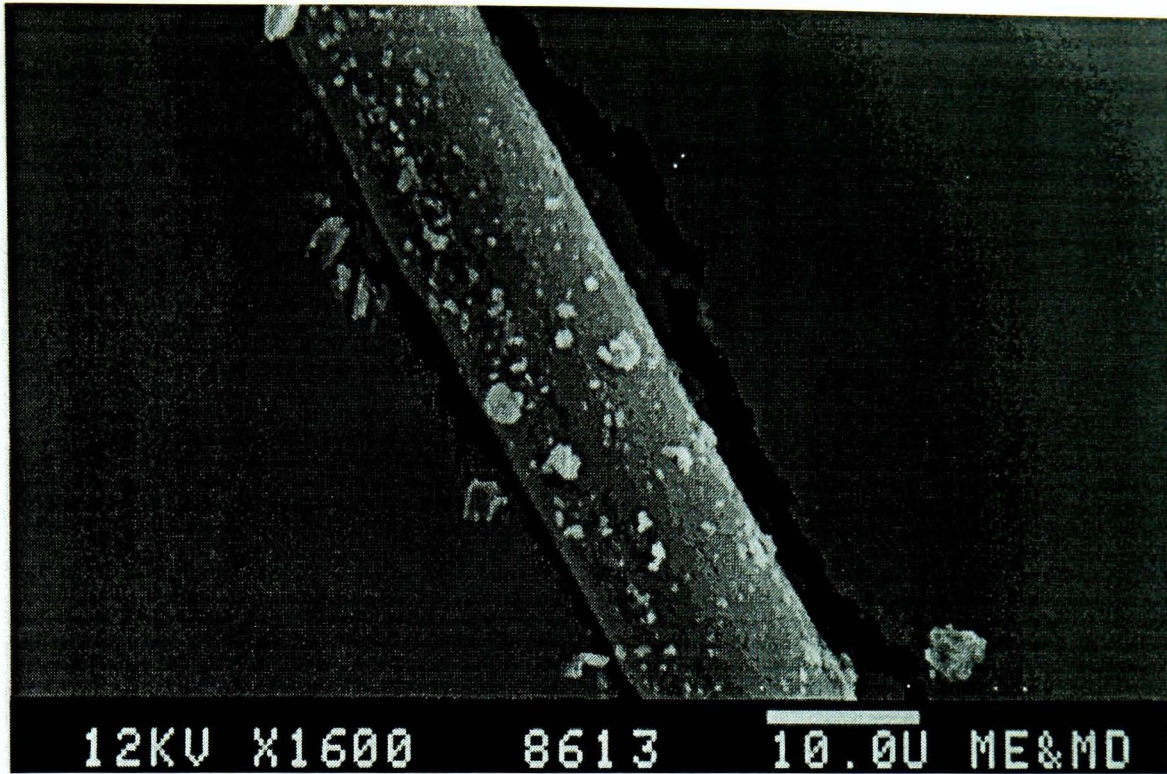
Figure 7.2   Micrograph of Glass Fibres Recovered from Sheet Moulding Compound Processed at 450°C

The legend of the micrograph shows the magnification and a 10 μm scale bar.

12KU X1600   8616   10.0U ME&MD
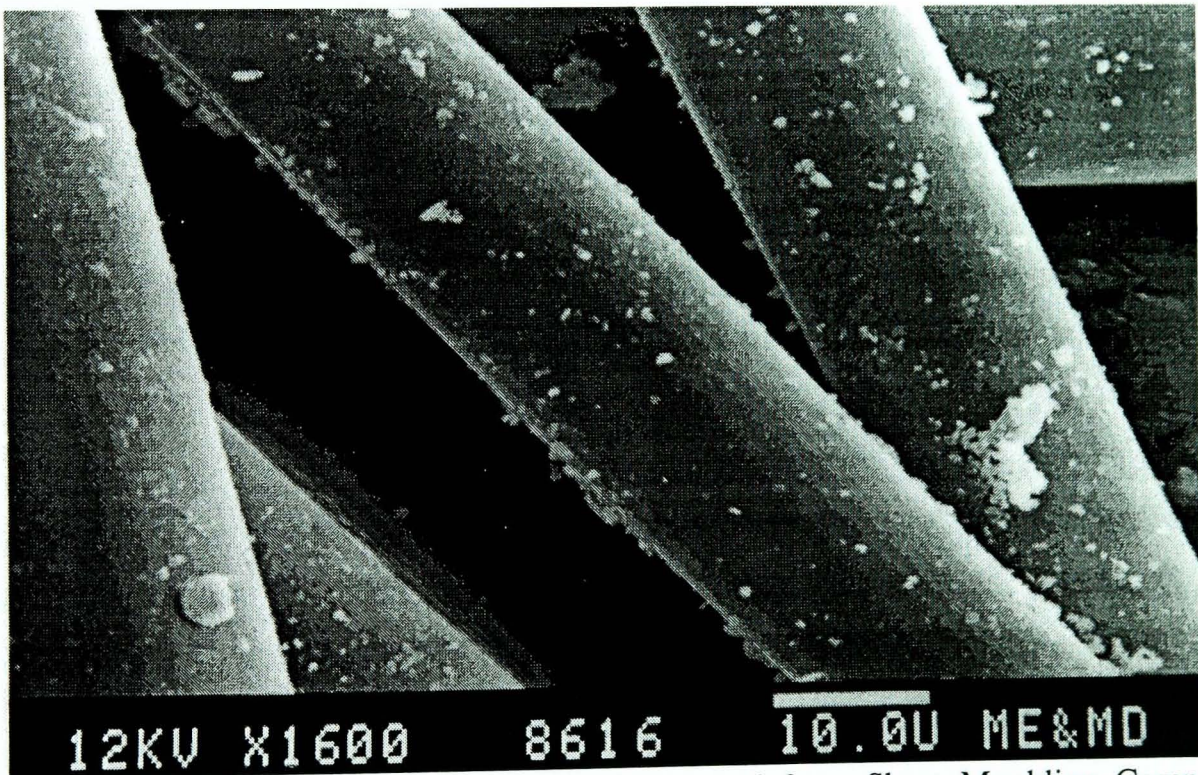
Figure 7.3   Micrograph of Glass Fibres Recovered from Sheet Moulding Compound Processed at 550°C

The legend of the micrograph shows the magnification and a 10 μm scale bar.
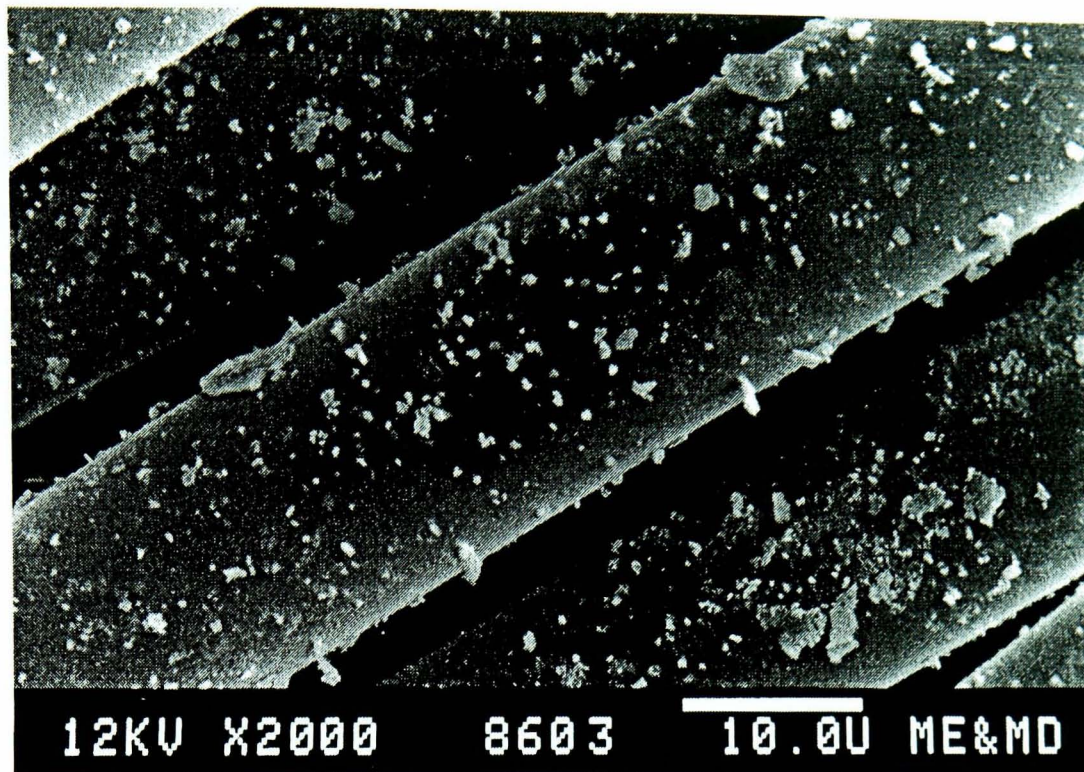
Figure 7.4 Micrograph of Glass Fibres Recovered from Sheet Moulding Compound Processed at 650°C.

The legend of the micrograph shows the magnification and a 10 μm scale bar.

7.1.3 Strength of recovered fibres[73]

The tensile strength of the recovered fibres is expressed in terms of the Weibull Modulus. Figure 7.5 shows the Weibull Modulus, expressed as a percentage of the modulus of virgin fibres for recovered fibre samples, each containing twenty fibres. These were recovered from processing at different Phase 1 rig conditions.

Weibull Analysis

Weibull Analysis is a statistical analysis technique. It can be applied to determine a characteristic strength (η) for a brittle material that fails over a range of measured strengths (s). Considering a range of strength test results, then the fraction failing (F) is given by[74]:

$$F(s) = 1 - e^{-(\frac{s}{\eta})^{\beta}}$$

By this analysis, the fraction failing is always 0.623[75] or 63.2%, i.e. the Weibull Modulus (η) is defined as the value at which 63.2% of the range fails. The shape parameter (β)

scope of this investigation.

Figure 7.5 shows that retained strength reduces with increasing temperature, in agreement with the literature review in Chapter 2. Values for processing at 1.7 m/s fluidising velocity are slightly below those at 1.3 m/s, probably due to increased fibre damage during the cyclone collection stage. However, temperature is seen to be the dominant parameter.
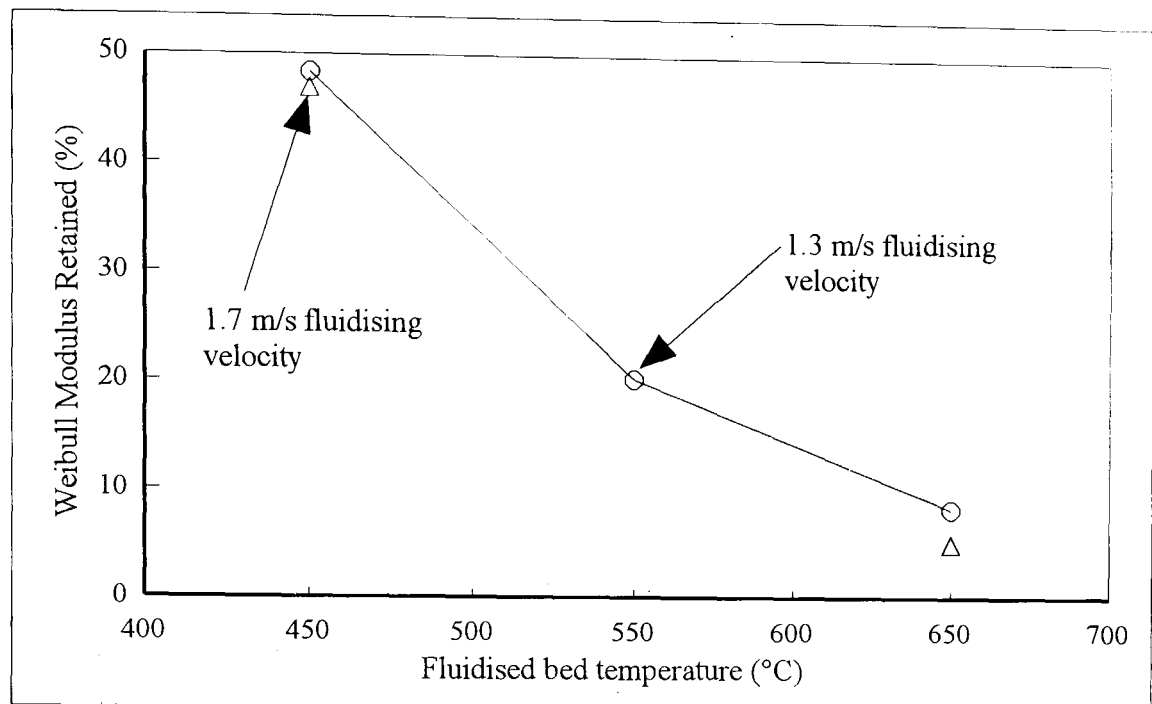
Figure 7.5   Single Fibre Retained Strength After Processing in Fluidised Bed Rig Over a Range of Temperatures[73].

This graph shows the Weibull Modulus of recovered fibres, compared with that of virgin roving, expressed as a percentage strength retained. Values are quoted for fibres recovered from processing in the test rig at different temperatures and fluidising velocities.

Figure 7.6 shows a graph of the natural logarithm of the retained Weibull Modulus against the natural logarithm of the fluidised bed temperature for data from figure 7.5 at 1.3 m/s fluidising velocity. Analysis of this graph gives the relationship between retained Weibull Modulus (Rη) and processing temperature (T):

$$R\eta \ (\%) = 2.35 \times 10^{14} . T^{-4.78}$$

This implies that 100% of fibre strength, measured as 2.77 GPa, would remain at 387°C with a fluidising velocity of 1.3 m/s. However, this is not a viable processing temperature as commissioning work showed that fibres were only released from the Sheet Moulding

Compound at a reasonable rate at temperatures in excess of 400°C.
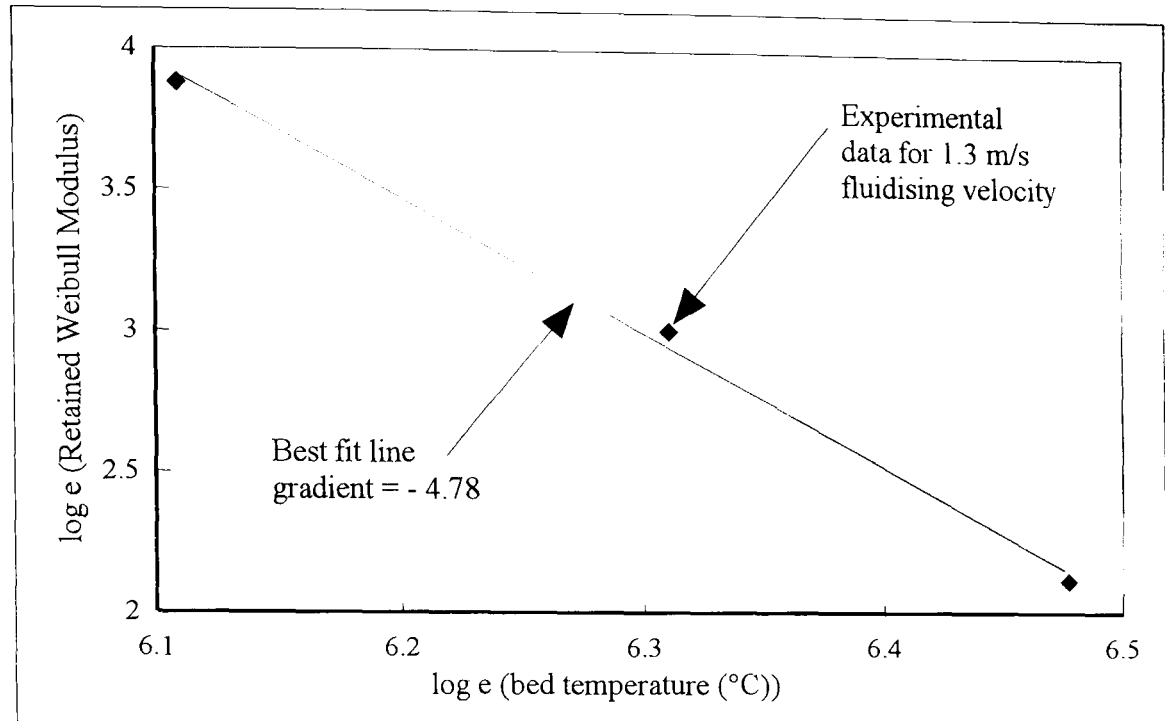
Figure 7.6 Graph of Natural Logarithm of Fibre Retained Weibull Modulus against Temperature for Fibres Processed at 1.3 m/s Fluidising Velocity

This graph is used to determine a relationship between retained Weibull modulus and bed temperature.

Kennerley[76] further investigated strengths of fibres from the Sheet Moulding Compound heated in an electric furnace for different periods at 350°C, see figure 7.7. From figure 7.7, the relationship between retained modulus ($R\eta$) and time (t) is:

$$R\eta \ (\%) = 150 \ .t^{-0.2}$$

Thus the retained strength decreases with both increasing temperature and time at a given temperature, in agreement with the literature reviewed in Chapter 2. A expression single indicating how retained strength varies with time and temperature cannot be obtained as the second assessment was after processing at a different temperature and in a furnace. It is likely that the time index would be more negative for a temperature of 450°C and larger still for processing in a fluidised bed that has a higher heat transfer coefficient than a furnace.

In order to have a high retained strength, the Sheet Moulding Compound must be processed at a low temperature, within practical limits and or have a short residence time in the bed. The actual bed residence time of fibres within the fluidised bed test rig was unknown, this led to the development of a decomposition model for composites, see

Section 7.3.
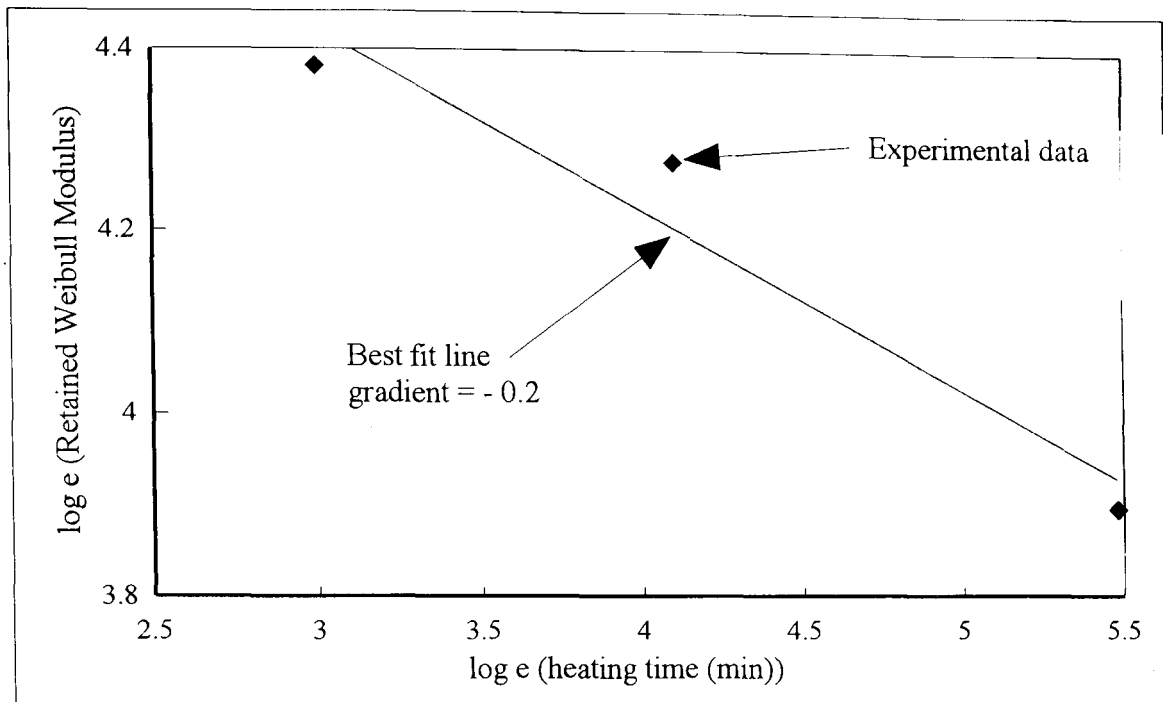
Figure 7.7   Graph of Natural Logarithm of Fibre Retained Weibull Modulus against Time
for Heating Sheet Moulding Compound at 350°C in a Furnace

This graph is used to determine a relationship between retained Weibull
modulus and time of heating.

7.1.4 Fibre contamination

Figure 7.8 shows a quantitative assessment of the macro (loose dust) contamination of the
recovered fibres. This figure includes points from Phase 2 processing, with the Rotating
Screen Filter. These are discussed below. The loose contamination made it difficult to wet
out fibres on subsequent processing or coating. The fibre bundles floated on top of water,
unless treated with significant agitation or dispersion agents.

Figure 7.8 shows that the quantity of loose contamination reduces both with increasing
temperature and decreasing fluidising velocity. It is possible that, at the low (combustion)
temperature of 450°C, the presence of residual unburnt hydrocarbons resulted in filler
particles adhering to the surface of the fibres. This effect would decrease with increasing
temperature and improving resin combustion, but at the expense of fibre strength. Another
explanation of figure 7.8 could be that as the temperature increases, the fillers modify to a
form that does not adhere to the fibres as effectively.

At high fluidising velocities, more material was elutriated from the bed, as loose

76

contamination, including bed sand at 1.7 m/s. The contamination was lower at 1.2 m/s, but less material was recovered from the collection bin, see Table 7.1. Thus an intermediate fluidising velocity of 1.3 m/s was used for subsequent test work.
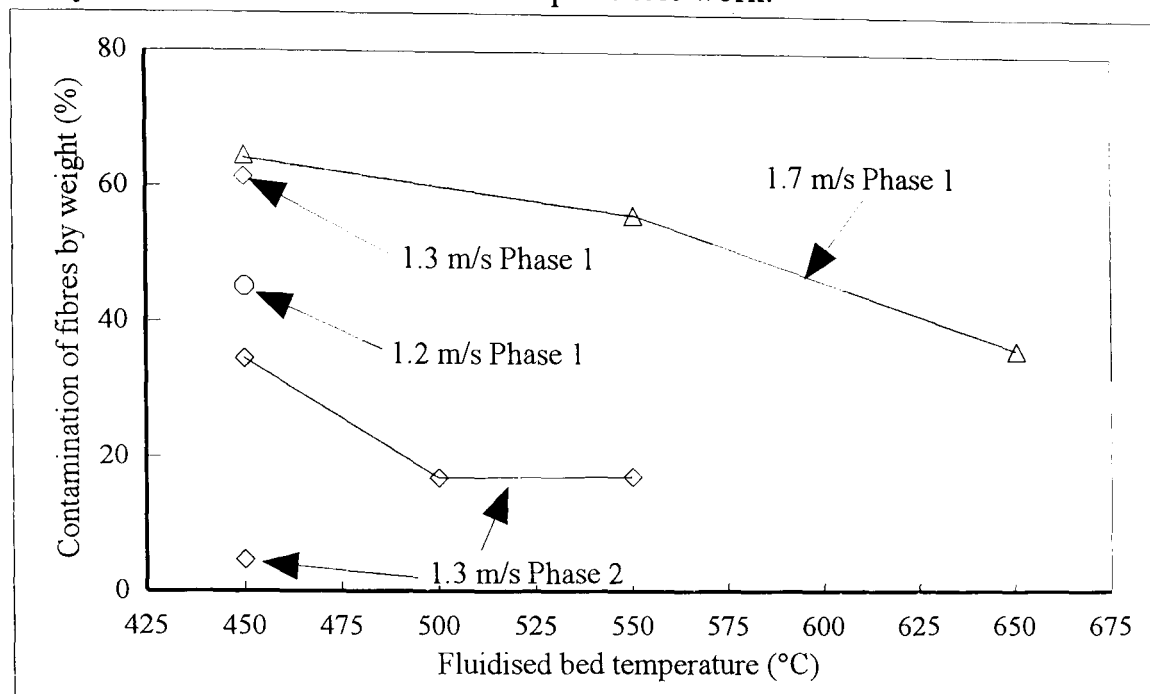
Figure 7.8   Mass Percentage of Loose Contamination Removed by Washing with Water

This graph shows the fibre contamination by weight that was washed from fibre samples recovered from fluidised bed processing at different temperatures and fluidising velocities. The contamination is expressed as a percentage of the initial total mass recovered before washing.

7.1.5 Flue Gas analysis

Measurement of the flue gas species with the electro-chemical analyser was undertaken to provide information on the quality of Sheet Moulding Compound resin combustion and or thermal decomposition. Plots of the flue gas carbon monoxide, nitrogen oxides and sulphur dioxide are shown in figures 7.9 to 7.11. The sampling point was after the fillers had been removed from the gas in the cyclone and the flue gas had cooled by typically 200°C compared with the bed temperature. The measured data, in parts per million (ppm), were converted to mg/m^3. These were then expressed as an average mass of gas evolved per mass resin input, over a whole test. This data enabled comparison between tests carried out at different processing conditions.

The presence of carbon monoxide in the flue gas is indicative of unburnt gaseous fuel that has not been fully oxidised to carbon dioxide. Evidence exists to show that carbon monoxide does not burn in a fluidised bed below 700°C[77]. It is not surprising that processing the Sheet

Moulding Compound at low temperatures, to optimise the fibre strength retention, resulted in high carbon monoxide levels in the flue gas, as the bed temperature was too low for effective combustion. Figure 7.9 shows that fluidising velocity is seen to have a significant effect on carbon monoxide levels at 550°C, but a negligible influence at 450°C.
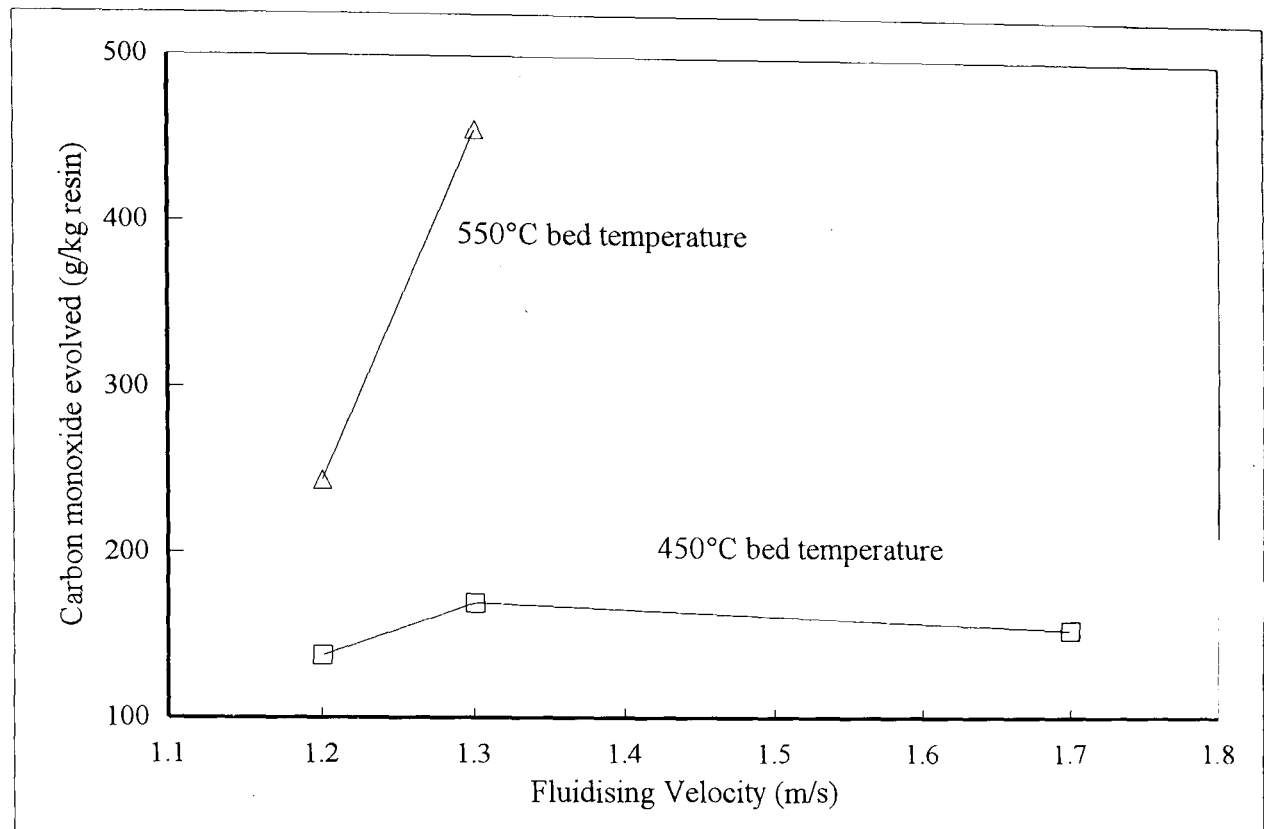
Figure 7.9   Mean Flue Gas Carbon Monoxide against Fluidising Velocity.
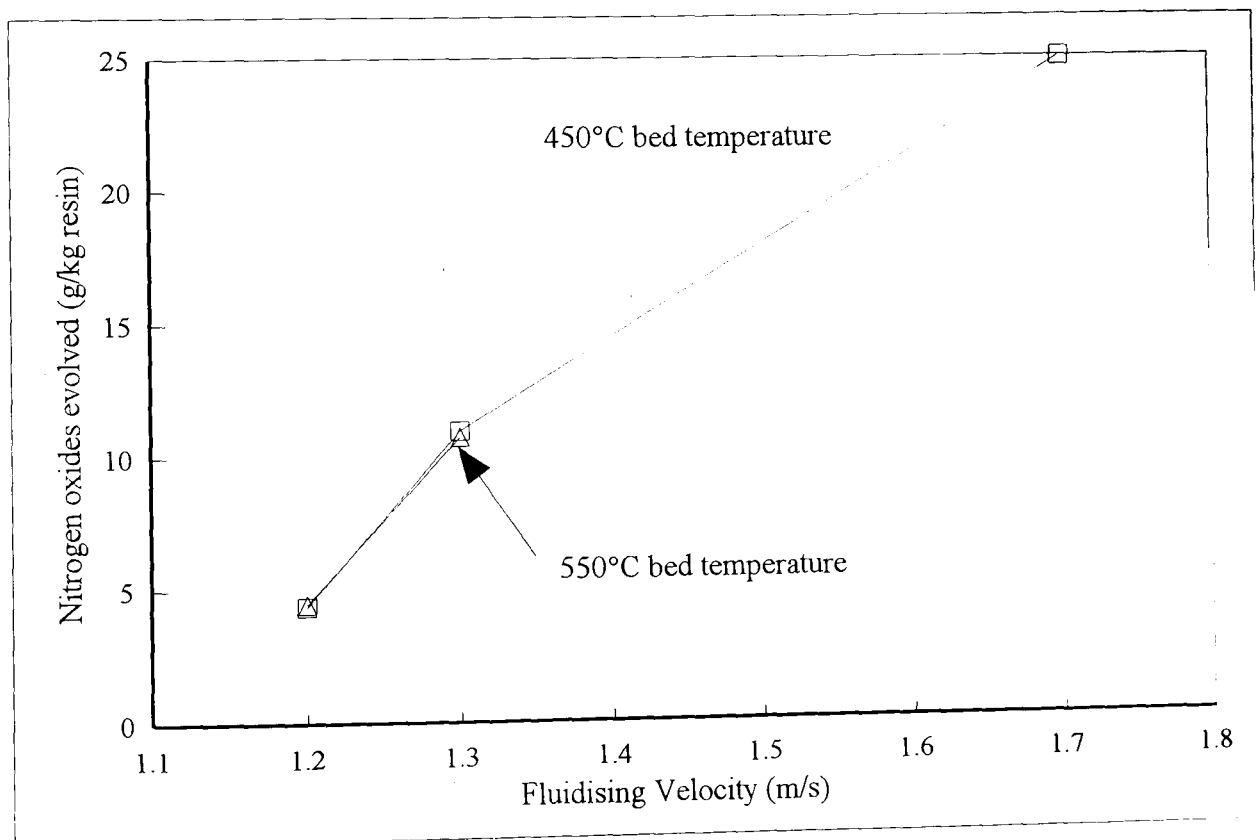
Figure 7.10   Mean Flue Gas Nitrogen Oxides against Fluidising Velocity.

The graph of nitrogen oxides in the flue gases in figure 7.10 shows low levels and little influence of bed temperature, although the nitrogen oxides evolved does increase with fluidising velocity. Since the process temperatures are much lower than those at which nitrogen oxides would be formed by oxidation of nitrogen in the combustion air, the only source of nitrogen oxides is therefore nitrogen in the resin.

Similarly, the only source of sulphur in the process is if it were present in the Sheet Moulding Compound. However, the manufacturer's formulation of the Sheet Moulding Compound does not include compounds containing either nitrogen or sulphur, unless they were present in the pigment. The quantity of sulphur dioxide evolved is low, see figure 7.11, similar to the nitrogen oxides.
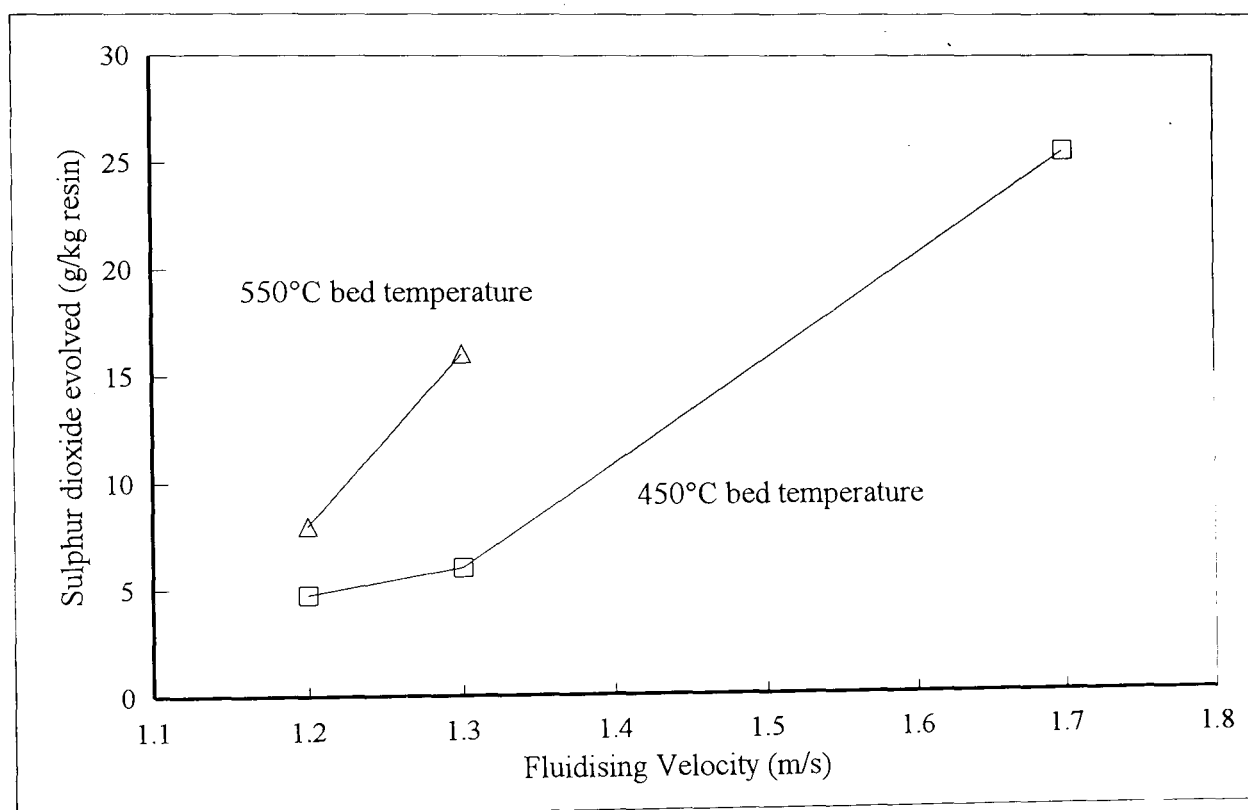
Figure 7.11   Mean Flue Gas Sulphur Dioxide against Fluidising Velocity

7.2   Results and Discussion - Rig Phase 2

The improvement expected from the second Phase of the rig was more efficient separation of the fibres and fillers and thus reduced fibre surface contamination. This would aid the wet out of the fibres on subsequent processing, as would collecting the fibres wet. It was hoped

that re-sizing the fibres immediately after fluidised bed processing would also improve fibre strength by protecting the fibre surface.

7.2.1 Optimisation of the Rotating Screen Filter

The testing carried out on the second Phase of the fluidised bed test rig is summarised in Table 7.2. This shows the duration of the tests at each condition and where the incombustible material resided on shutting down the rig. Also the mass of recovered fibres is compared with the mass of the fibres input in the Sheet Moulding Compound.

Table 7.2 Rotating Screen Collector Optimisation on Rig - Phase 2

This table summarises the test work carried out on Phase 2 of the test rig at different bed temperatures and fluidising velocities. Also detailed is where the incombustible material resided, on completion of each test run. The comparison of the recovered to input fibres gives an indication of fibre recovery efficiency.

Bed °C	Bed Fluidising Velocity (m/s)	Time (min)		Rec fibres / input fibres %	Recovered / recoverable incombustible mass (%)			
		Feed	Run on post feed		Tank (fibres)	Cyclone (fillers)	Bed	Total
450	1.3	9	0	13.8	4.8	25.4	38.5	69
450	1.3	29	8	13.4	29.2	39	27	95
500	1.3	13	0	15.4	6.1	36.7	44.4	87
550	1.3	15	8	39.7	15.8	46.9	25	88
450	1.3	22	10	44.9	16.7	42.8	32.1	92
450	1.3	162	10	57.3	28.6	47.4	20.5	96.5

The high overall recovery rate of incombustible material seen on Phase 1 of the rig was repeated with the modified collection system. The fibres recovered from the tank (less the measured contamination) represent up to 57% of the input fibres. The remainder of the fibres were collected by the cyclone, mixed with the fillers. Thus the rotating screen collector worked, in that low contamination fibres (see below) were collected, but the fibre collection efficiency was somewhat low.

7.2.2 Scanning Electron Microscopy of Recovered Fibres from Phase 2

Figure 7.12 shows that the quantity of surface contamination of the fibres collected with the rotating screen collector is similar to those collected via the Phase 1 bin. This was expected, as within the freeboard, the elutriated fibres and fillers interact freely. Firmly attached contamination of this kind has not presented any problems for reuse or further processing. The size solution forms thin film over the top of the filler contaminant particles (see figure 7.12).
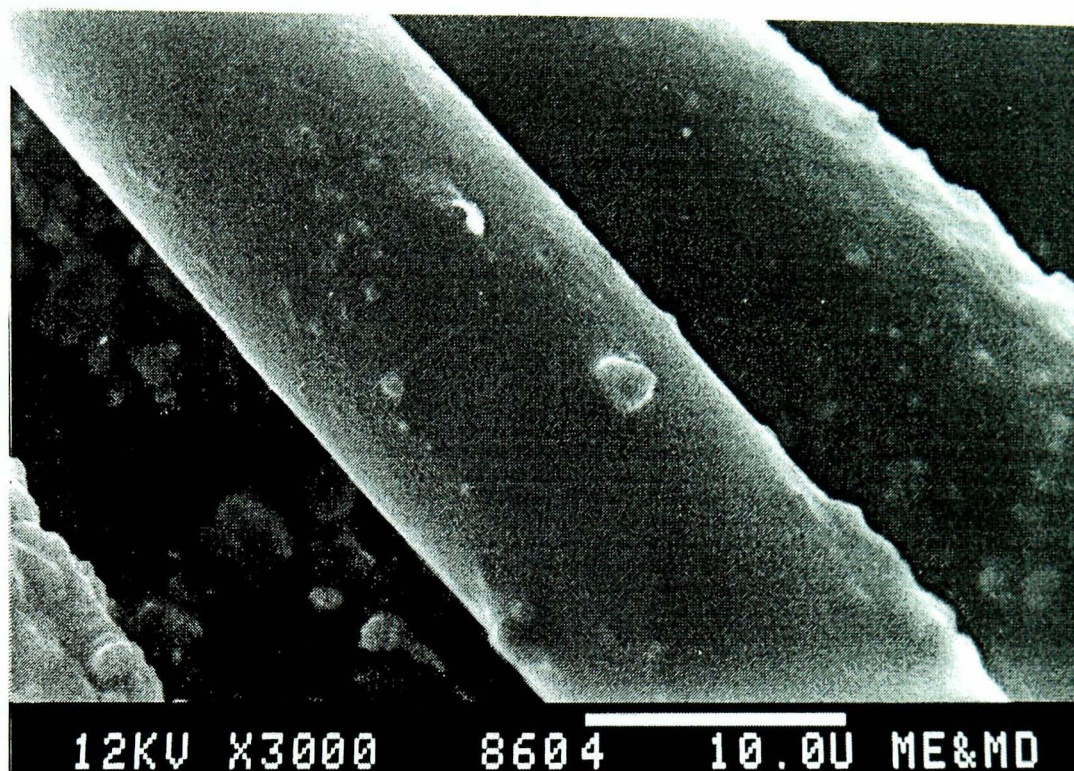
Figure 7.12 Micrograph of Glass Fibres Recovered from the Sheet Moulding Compound. The fibres were recovered from processing at 450°C bed temperature in Phase 2 of the test rig. The size film on the surface of the fibres can be clearly seen.

7.2.3 Fibre Contamination

The loose contamination on the fibres was assessed by washing, as for Phase 1. Figure 7.8 shows the macro (loose dust) contamination of the fibres recovered from the Phase 2 test work. The size spray used to treat the fibres during collection is like a continuous washing process. Figure 7.8 shows that the fibres collected via the rotating screen collector have significantly reduced contamination compared with those from Phase 1. At 450°C processing, the contamination level was approximately half that of the Phase 1 fibres and still lower at higher processing temperatures.

The point in figure 7.8 indicating very low contamination at 450°C processing, represents

fibres that were collected with the collection tank valve biased to give a small bleed flow from cold to hot i.e. counter to the fibre movement. Thus the air flow opposed the flow of fine particles, resulting in very clean fibres being collected. Unfortunately, there were very few fibres collected as the fibre movement was also opposed by the bleed flow. Further work could investigate modifying the rotating screen collector to process reasonable quantities at this minimum contamination level.

The fibres from the 550°C test were superficially very clean and it was a surprise that the contamination was higher than the 500°C value. The 550°C fibres were visually noticed to be quite short and thus some fibres may have slipped through the filter on straining after washing. If this were the case, then the contamination level would appear to be higher than it actually was.

7.2.4 Analysis of flue gas total hydrocarbons

It was expected, at the relatively low thermal processing temperatures, that the resin would not fully combust to gaseous species like carbon monoxide, but exist as vaporised hydrocarbons. This was confirmed on Phase 1 rig testing, as condensed hydrocarbons were found after the larger cyclone, which acted like a cooling chamber for the flue gases. Unburnt hydrocarbons and carbon monoxide, constitute unused fuel being wasted.

Assessment of flue total hydrocarbons was performed by sampling from the freeboard, before the flue gas cooled down below a temperature at which the hydrocarbons would condense. As the sampling was done from this position, before the rotating screen collector, then the results are indicative of both Phases of the rig. Figure 7.13 shows a graph of total hydrocarbon emissions during three tests at different temperatures on the Phase 2 rig.

The data in figure 7.13 is expressed on a time basis after the Sheet Moulding Compound feed was switched on, thus the delay within the screw is clearly seen. The total hydrocarbons present in the freeboard increases with decreasing process temperature as expected, as the resin is less well combusted at lower temperatures. In fact the total hydrocarbons value at 450°C is approximately twice that at 550°C. This again shows that the rig is operating at sub-optimum combustion conditions attempting to recover the highest strength fibres possible.

The presence of both vapour and gaseous fuel in the flue implies energy recovery will have

to be achieved in an after-burner chamber rather than relying on combustion within the bed. Such an after-burner would be operated at high temperature for high thermal efficiency and to destroy gaseous pollutants. On a commercial plant the exhaust gas could be recirculated and used to fuel the air preheater.
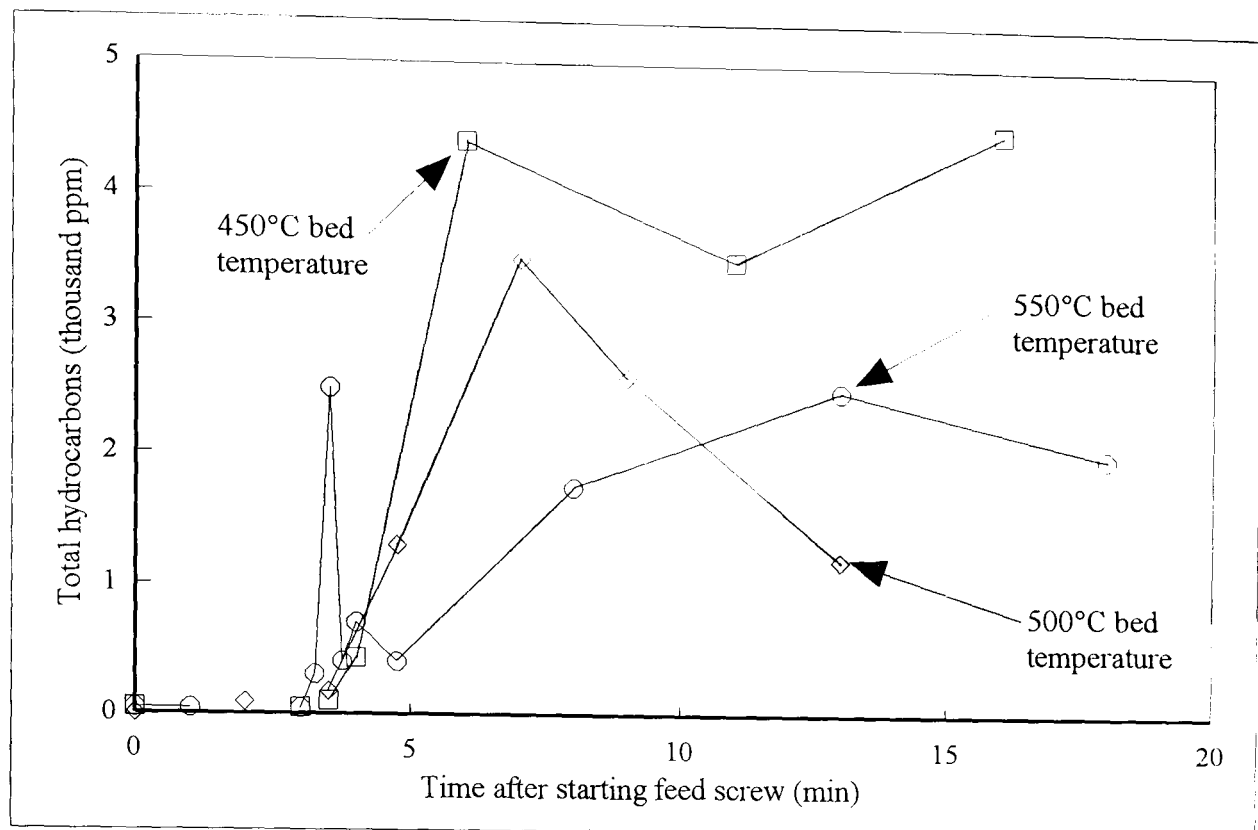
Figure 7.13   Measurement of Flue Gas Hydrocarbons

7.3   Process Modelling Results and Discussion

The model of composite decomposition, described in Chapter 6, was applied to investigate the likely temperature-time history of glass fibres during fluidised bed thermal processing. Graphs of surface, mid body and centre plane nodal temperatures for the range of bed temperatures tested experimentally are shown in figures 7.14 to 7.16.

The results from the model indicate that there is not a large temperature difference between the surface and the centre plane. This is not unreasonable considering that the Sheet Moulding Compound section is 3.8 mm thick and is exposed to heat input on both faces. Figures 7.14 to 7.16, imply that the resin decomposition occurs at temperatures below that of the bed. Within the test rig, this means that the fibres would not be exposed to the relatively high bed temperature until released into the bed.
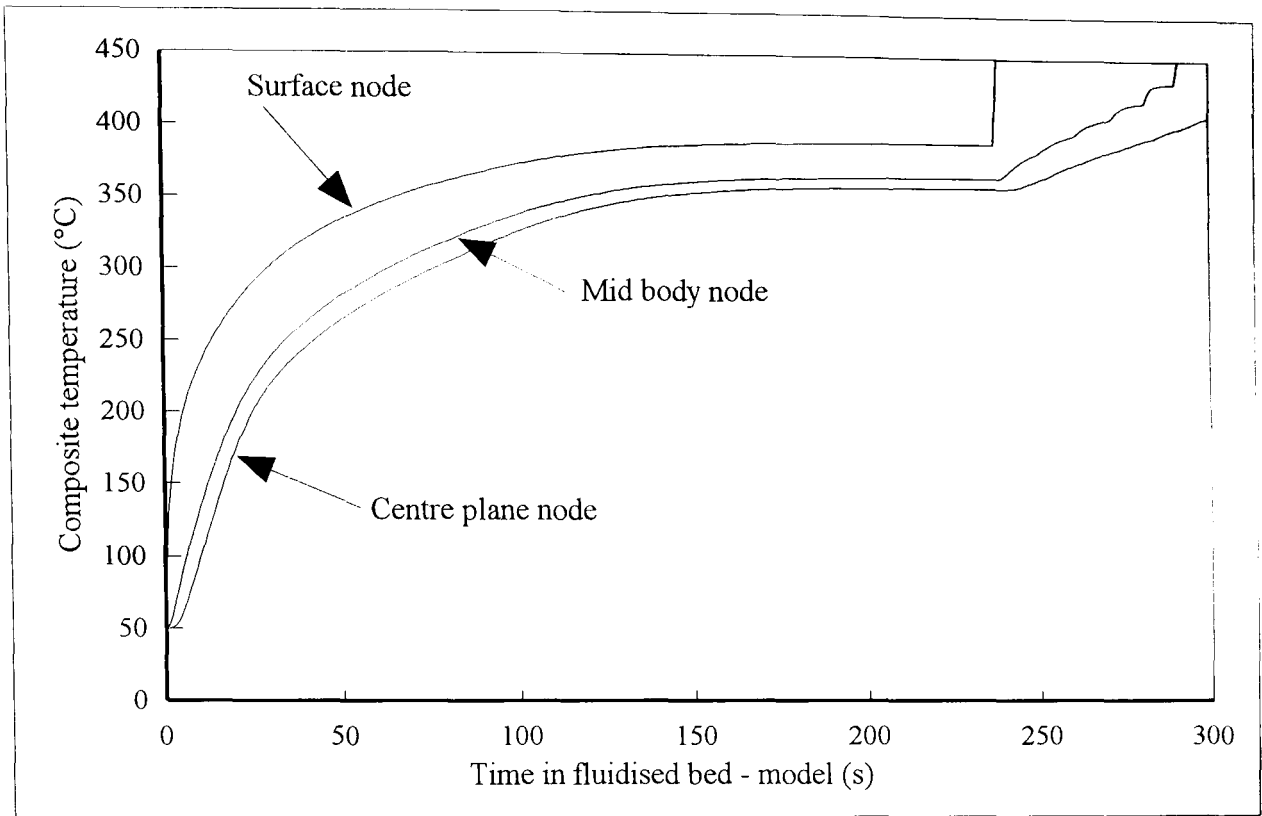
Figure 7.14 Model Predicted Surface, Mid-plane and Centre Temperatures with 450°C Bed.
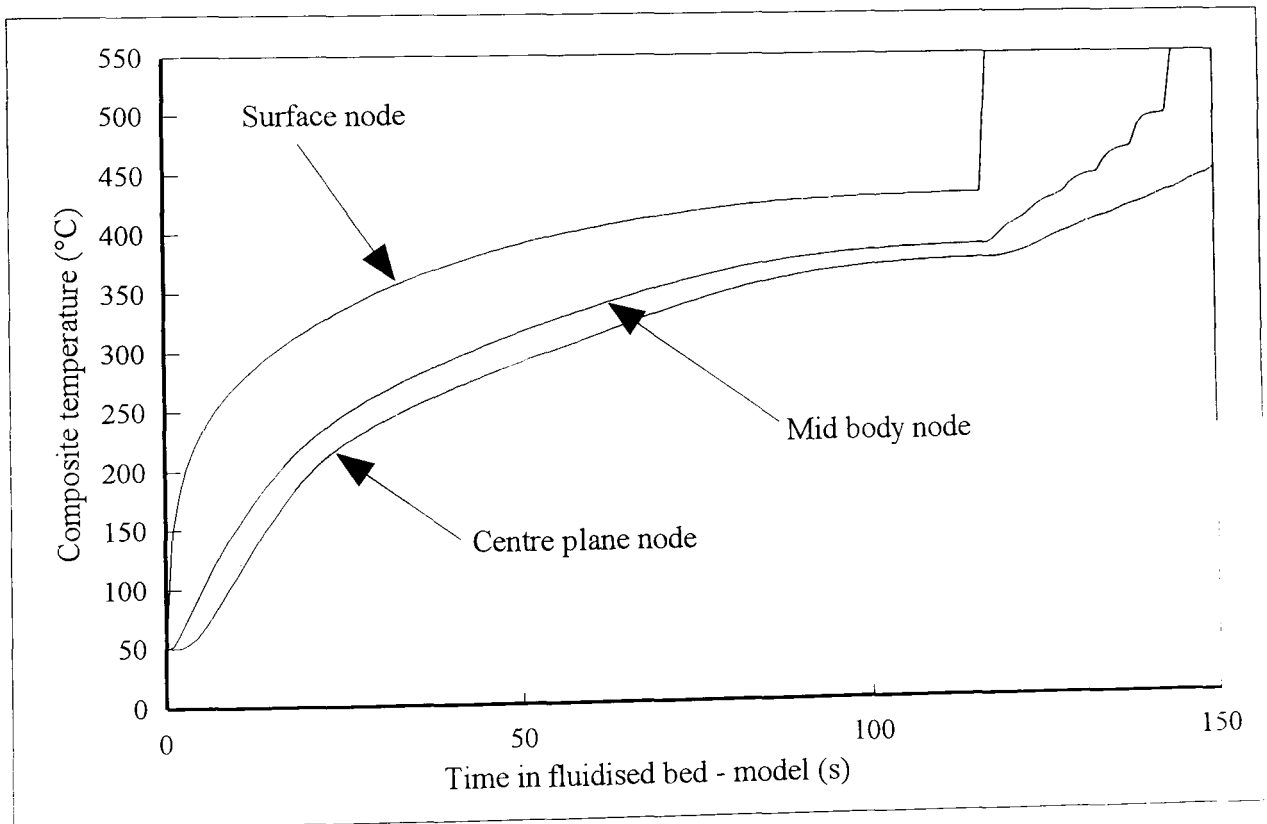
Figure 7.15 Model Predicted Surface, Mid-plane and Centre Temperatures with 550°C Bed.

The temperature curves for the mid body node, half way from the surface to the centre, show some instability after release of the surface nodal spacing of composite. This is due to the step change in temperature at the surface being transmitted through the nodal network. This implies that the fibre release mechanism assumed in Chapter 6 is too rapid and a more gradual change of the surface node to the bed temperature is required.

Considering the mid body node as an average position, then the fibres are released from this position into the 450, 550 and 650°C beds at 291, 144 and 91 seconds after input to the bed, respectively. After release, the fibres are subject to the bed temperature for a period until elutriation. Thereafter, in Phase 2 of the rig, the fibres rise through the 1.2 m high freeboard at the freeboard temperature, in approximately one second before being quenched by the secondary airflow. Thus the strength reduction is related to the temperature-time history of the fibres during these three regimes.
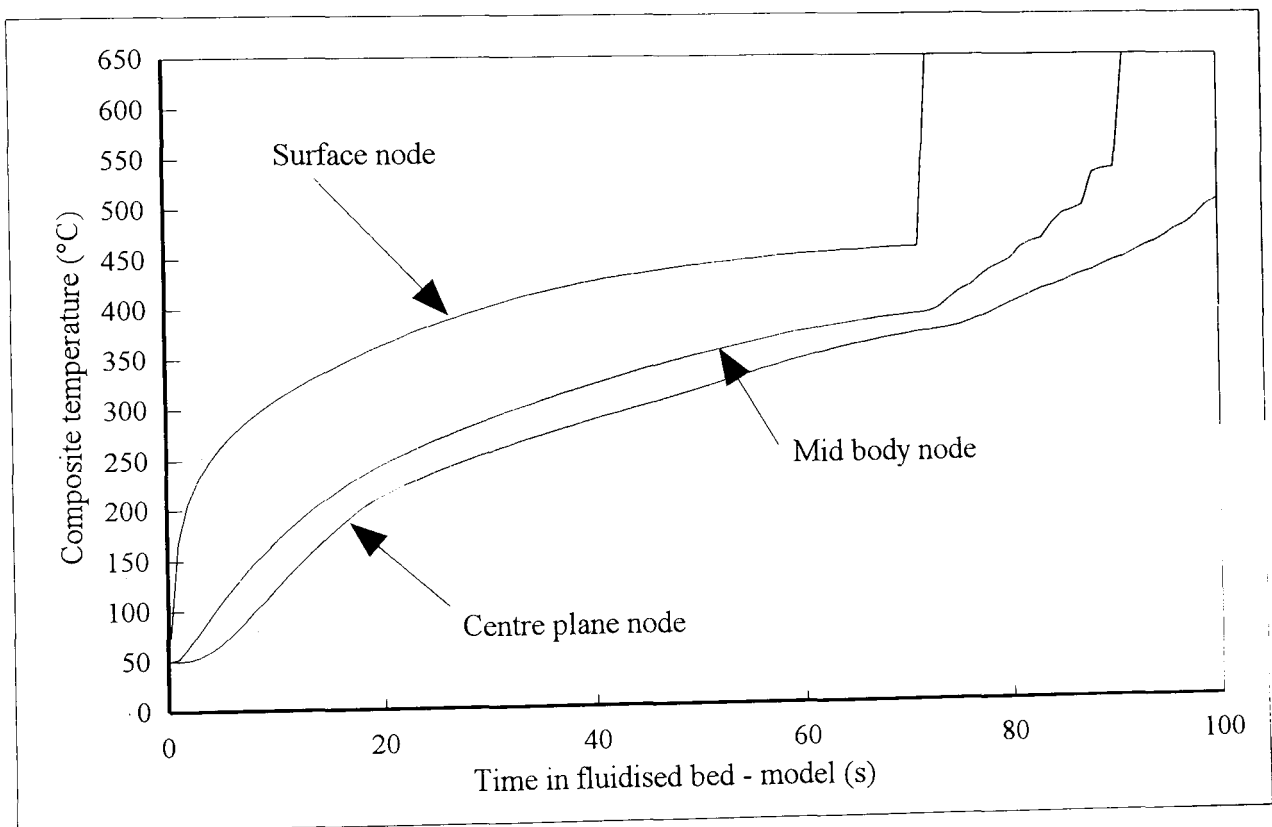
Figure 7.16 Model Predicted Surface, Mid-plane and Centre Temperatures with 650°C Bed.

For processing at 450°C bed temperature, the time-temperature history produces a 50% loss in fibre strength, compared with virgin fibres. Although some fibre strength deterioration could occur during the composite manufacturing process itself and an 8% reduction can be

estimated from Kennerley's figures[76].

The single fibre strength measurements reported above (see Section 7.1.3) imply that fibres processed in a fluidised bed below approximately 390°C would not lose any strength. The maximum temperature experienced by a surface fibre prior to release, from the 450°C model plot in figure 7.14 is 391°C. This suggests that the major influence on the recovered fibre strength is not the period during the resin decomposition, but the time spent within the fluidised bed and freeboard.

Alternatively, the fibres may not be released quickly from the composite during decomposition and a fibre could be partially joined to the decomposing Sheet Moulding Compound particle for a time period. This could be similar to the decomposition period, but at a temperature approaching that of the bed, higher than that predicted by the model.

Further modelling work on the elutriation of monofilament fibres from a fluidised bed may indicate which of the above scenarios is closest to reality.

7.4 Fluidised bed Thermal Recycling Process - Discussion

7.4.1 Success of fluidised bed test rig.

Comparing the above results with the test rig success criterion of Section 5.3, the following statements can be made:

- The incombustible constituents of the Sheet Moulding Compound were released, on thermal fluidised bed processing, during the decomposition of the resin matrix. These were collected at high recovery rates compared with the input material. The reinforcing glass fibres were elutriated as monofilaments and recovered intact from the flue gases. An assessment of the strength[73] of the fibres recovered from processing at 450°C bed indicated 50% retention of tensile strength.

- Analysis of the flue gas showed that carbon monoxide and unburnt hydrocarbons were present. This indicated that the resin was not being fully combusted within the test rig and the heat energy not recovered. Although this was not important on the laboratory trials of the recycling process, an after-burning chamber for the 'fuel' in

the flue gas would be required for assessment of heat recovery efficiency.

- The gas analysis reported above cannot be assessed against any emission standards as full combustion is clearly not taking place. However the results are useful for comparing the different process conditions. After full combustion of the resin decomposition products in a separate chamber then the exhaust gas could be assessed, with existing equipment, for atmospheric pollutants.

7.4.2 The improvements from Phase 2 of the test rig.

Phase 2 of the test rig was developed to reduce the contamination with filler particles of the recovered glass fibres.

Comparing fibre samples recovered from Phase 1 and 2, then in Phase 2, the loose contamination was reduced by 50%, when processing at 450°C bed temperature. The firmly attached surface contamination appeared similar, from Scanning Electron Microscope assessment.

The one negative aspect of using the rotating screen collector to recover fibres is the potential for blocking the filter. However, monitoring the internal pressure at different positions on the rig gives advance warning of this phenomenon. Transient blockages were cleared by manually cycling the back pressure valve open and closed. This could easily be automated on a pilot plant linked to pressure sensors.

7.4.3 Comment on economic viability

The use of scrap composite as a sorbent for sulphur dioxide from fluidised bed combustion of coal was technically successful but economically unviable (see Chapter 3), even accounting for a high landfill cost similar to that in Germany. This was due to the composite crushing operation being expensive and the cost of the raw material replaced (limestone) being very cheap. The disposal of the glass fibres, an inert material in the process, was the extra cost that made the co-combustion method economically unviable.

The thermal recycling method, developed using the fluidised bed rig, targeted the incombustible material for recovery in as high a value form as possible, i.e. the glass fibres for recycling. This process was also a technical success in that intact glass monofilaments

were collected, albeit with a 50% reduction in tensile strength.

Table 7.3 shows that, for a typical composite of 30% glass content, reuse of recovered monofilaments in glass fibre veil equates to a £0.90/(kg composite) incentive to recycle composites via this process. However, this does not account for the extra cost required to manufacture veil from the recovered fibres. This manufacturing cost would be offset by the savings in replacing virgin fibre, of £ 1.50/kg, depending on the proportion of recovered fibres in the veil.

Table 7.3   Comparison of Markets for Glass Fibres by Cost

Material	Cost	
Glass roving	1.41	£/kg[78]
Glass veil	0.2	£/m^2 [78]
Average 60 g/m^2 veil with 20% binder content	4.18	£/kg
Increase in value of glass by conversion to veil	2.77	£/kg (glass)

Thus, there is likely to be an overall economic incentive to reuse the recovered fibres within a veil, rather than attempt to densify the fibres and recycle back into composites as a replacement for (cheap) roving. If the energy recovered from the resin combustion and reuse of the mineral fillers were also accounted for; then recycling via fluidised bed thermal processing could be more economically viable than the co-combustion method.

The best economic feasibility would be realised if a fluidised bed recycling plant were integrated with veil manufacture equipment. In this scenario the recovered heat could be utilised directly, for example in the ovens for curing the veil binder.

Chapter 8

CONCLUSIONS AND RECOMMENDATIONS FOR FURTHER WORK

8.1 Introduction

The work presented in this thesis commenced with a description of the problem of the disposal of thermoset composite waste. This is particularly applicable to the automotive industry, which has the potential to generate large quantities of thermoset waste when vehicles are scrapped. This theme was developed by a thorough review of relevant literature in Chapter 2. It was found that thermal treatment of glass fibres produced a degradation of physical properties, which increased with increased processing temperature. This was a potential problem with for a thermal recycling method.

Experimental work

In an attempt to find a solution to the disposal of thermoset composite waste, two recycling methods were investigated experimentally:

- The first was an extension of previous trials on a test rig to a full commercial scale trial. This investigated the reduction of sulphur emissions from coal fluidised bed combustion by co-combustion with calcium carbonate filled composite scrap.

- The second was the medium temperature thermal processing of scrap Sheet Moulding Compound in a fluidised bed, to recover the reinforcing fibres. This required the development of a new test rig.

Both methods were technically successful.

Thermal modelling

The thermal decomposition of a polyester thermoset composite was modelled by a one dimensional finite difference method. This was undertaken to provide information on the time-temperature history of glass fibres released from composites processed in the fluidised bed test rig.

This chapter summarises the results of the experimental and modelling work before recommending further work in this field.

8.2 Conclusions from the experimental work.

8.2.1 Co-combustion of composite scrap with coal in a fluidised bed.

- No significant problems were encountered during the trial on the commercially operating boiler in terms of plant operation. This was encouraging as the test was carried out during normal operation of the boiler.

- Up to 75% of the sulphur input, in the coal, was retained based on the reduction in sulphur dioxide output.

- There were problems with the composite scrap feeding system and these resulted in a varying feed rate. This resulted in large fluctuations in the flue gas emissions[50]. More development of a suitable feeding system for the composite scrap would be required for full commercial operation.

- During size characterisation of the cyclone fines, produced when burning scrap composite scrap, some short glass fibres were identified[50]. This indicated the potential to recover the glass fibres from scrap composite materials by fluidised bed thermal processing.

- Economic analysis showed that at low landfill costs, typical of the UK, the use of composite scrap as a sulphur dioxide sorbent costs 20.3% more than for equivalent sulphur retention by limestone. Even applying a high landfill charge, typical of Germany, this difference only reduces to 9.2%.

8.2.2 Fluidised bed thermal process test rig.

Phase 1 Test Rig

The results from the work associated with the first phase of the fluidised bed test rig can be summarised as:

- The incombustible constituents of the Sheet Moulding Compound were released, on fluidised bed processing above 400°C, by the decomposition of the resin matrix. A high

proportion of these fibres and fillers were recovered. The reinforcing glass fibres were elutriated as monofilaments and recovered from the flue gases, without apparent significant degradation in length.

- Scanning Electron Microscopy showed that the recovered fibres were intact, with smooth surfaces similar to virgin fibres. However, the surfaces were contaminated with filler particles.

- Measurement of the mechanical properties of the recovered fibres[73] showed that the tensile strength was degraded during thermal processing. Approximately 50% of virgin roving tensile strength was retained from processing at 450°C, but this was reduced to below 10% strength retention at 650°C. This meant that the processing should be carried out at the lowest temperature practicable. Strength was also found to reduce with increasing time at a temperature[76].

- The contamination of the recovered fibres was identified as a problem for reuse, inhibiting fibre wet out. The loose contamination reduced with increasing processing temperature and reducing fluidising velocity. Thus a low fluidising velocity and low processing temperature are required for low contamination and high retained strength of the recovered fibres.

- Analysis of the flue gas showed that carbon monoxide was present. This indicated that the resin decomposition products were not being fully combusted (oxidised) to carbon dioxide within the test rig and the associated heat energy lost from the system. The carbon monoxide concentration increased with reducing temperature. At 450°C bed temperature, fluidising velocity had a significant influence, carbon monoxide concentration increasing with reducing velocity. The measured nitrogen oxides and sulphur dioxide concentrations were low.

Phase 2 Test Rig

The testing and analysis associated with Phase 1 showed that a low process temperature was required for the best fibre strength retention. Unfortunately, at such temperatures, the combustion of the resin was incomplete and there was significant fibre surface contamination. Reducing the fluidising velocity to improve the contamination also increased the carbon

monoxide concentration. The flue gas could be burnt in a secondary combustion chamber to give complete combustion, but the contamination remained a problem. Thus, the second phase of the test rig, incorporating the Rotating Screen Collector was developed to reduce the recovered fibre contamination. The results from the work associated with Phase 2 of the fluidised bed test rig can be summarised as:

- The Rotating Screen Collector system worked as designed, the fibres were filtered from the flue gases and recovered in the collection tank.

- The high overall recovery rate of incombustible material seen during Phase 1 of the rig was repeated on the test rig with the Rotating Screen Collector system. Fibre recovery rates of up to 57% were measured.

- The recovered fibre loose contamination was measured as 34% from 450°C processing temperature, this is a 50% reduction compared with Phase 1.

- During the Phase 2 trials, total hydrocarbons as well as carbon monoxide were also measured in the flue gases from the test rig. These total hydrocarbon measurements followed the trend of the flue gas carbon monoxide measured previously: reducing with increasing processing temperature. This again confirmed that complete combustion could not be achieved at low processing temperatures.

- Preliminary analysis indicated that the fluidised bed thermal recycling process has the potential to be more economically viable than the co-combustion disposal method.

8.3 Conclusions from the Modelling Work

- The results of the modelling indicated that the endothermic energy of decomposition of the resin maintained the temperature of the Sheet Moulding Compound pieces approximately constant during the resin decomposition in the fluidised bed. The temperatures of the composite during decomposition were approximately 60°C, 125°C and 194°C below the bed temperatures of 450°C, 550°C and 650°C, respectively.

- The degradation in strength of the fibres recovered from fluidised bed processing was similar to that measured in fibres processed at the same temperature in a furnace. However, the modelling work implies that the temperature of the composite was significantly lower than the fluidised bed temperature, during the decomposition of the resin. The fibres spend a period of time at the bed and freeboard temperatures before recovery and the degradation in strength of the fibres occurs mainly during this period.

8.4   Original Aspects of this Investigation

In addition to reducing material going to landfill it was the intention that this work was to be an engineering solution to reduce the environmental impact of vehicles. With an acceptable recycling route in place, there should be no barrier to the increased use of composites in automotive construction. This would tend to reduce vehicle mass, thus improving fuel economy and reducing emissions over the life of the vehicle.

The following main aspects of the work undertaken by the author are original and contribute to knowledge in the area of the recycling of composite materials:

- The use of a thermal fluidised bed process to breakdown the polymer in a composite and allow the fibres to be recovered by elutriation is novel. The process has been demonstrated to work. Operation of the fluidised bed at as low a temperature as possible, 450°C in the case of the Sheet Moulding Compound tested, minimises the degradation in the strength of the fibres. At such low temperatures, complete combustion of the polymer is not achieved. A secondary combustion chamber would be required to maximise energy recovery and reduce emissions.

- The design and development of the Rotating Screen Collector is a unique solution to the problem of separating the fibres and fillers from the gases leaving the fluidised bed. The Rotating Screen Collector significantly reduced the contamination of the fibres with fillers compared with conventional separation techniques such as cyclones.

- The identification of the use of recovered glass fibres in veil is an important step in devising a material recycling loop. This loop does not close with the recyclate going back into the original material type but could be technically and economically viable.

93

8.5 Recommendations for Further Work

8.5.1 Co-combustion of composite scrap with coal in a fluidised bed.

The unfavourable economic case for this recycling process means that any further work, other than purely academic investigation, could not be justified.

8.5.2 Fluidised bed thermal process test rig.

- The assessment of recovered materials has concentrated on the most valuable, the glass fibres. However, as composites are highly filled, the reuse of the fillers is vital to the overall economic viability of a recycling process. Material characterisation is required to assess potential markets. The fillers recovered from Phase 2 of the test rig contain short glass fibres and thus may be marketed as a functional filler, having some reinforcement properties.

- The susceptibility of the process to contamination of the composite scrap should be investigated. This would determine the maximum level of contamination which can be allowed, without significantly affecting the quality of the recovered fibres.

- A flue gas combustion chamber for the test rig requires commissioning. The rig operation could then simulate a full pilot plant, enabling the calculation of the efficiency of heat recovery from the resin products. This would allow a full economic assessment of the process including energy and material recovery and determination of the likely emissions.

- Subject to a favourable economic analysis of a full rig, continued work would exist as a challenge to industry to move to a pilot plant scale investigation of the process.

8.5.3 Thermal model

- To improve the understanding of composite decomposition within a fluidised bed, then the thermal model requires extension to investigate the fibre release assumption. This could include a function to model surface attrition and elutriation criteria for monofilaments within the bed to determine bed residence time. Further validation of the results of the model is also required.

REFERENCES

1) MAXWELL, J.
   Plastics in the Automotive Industry. Woodhead Publishing, 1994, p170-1.

2) DEPARTMENT OF THE ENVIRONMENT
   Indicators of Sustainable Development for the United KIngdom. HMSO, Mar 1996, p15.

3) BRITISH PLASTICS FEDERATION (BPF)
   Statistics Handbook. 1993 Edition (319/7).

4) BIRD, TONY.
   Reclamation and Recycling - The Motor Car and White Goods.
   Plastics Recycling - Future Challenges, 20-21 Sept, 1989.

5) SOCIETY OF MOTOR MANUFACTURES AND TRADERS (SMMT)
   Motor Industry of Great Britain 1994, World Automotive Statistics.

6) BURLACE, C.J.
   Plastics in Motor Vehicles, Problems and Recycling Opportunities.
   Warren Spring Laboratories Report, June 1992.

7) KRUMMACHER, B.
   Polymers in Cars, Energy Consumption and Recycling. Dow Europe report, 15 June,
   1990, p5. Dow Plastics Development, Taegerwillen, Germany.

8) ANON.
   Environmental Data Services Report 252, Jan 1996, p37.

9) BUSCH, J.V. & DIEFFENBACH, J.R.
   *Why Aren't Composites More Widely Used by the Automotive Industry: A Lifecycle Cost
   Conundrum.* Proc. 8th Advanced Composites Conf., Chicago, USA. 2-5 Nov. 1992.

10) ANON.
    Materials Recycling Week, Dec 1, 1995, p24.

11) FORD, P.
    What a Waste Recycling the Automobile. Recycling of Vehicles and Components
    Seminar, Supplementary Paper 1, IMechE, London, 2 Oct 1995.

12) ANON.
    Automotive Aluminium Recycling in 2010. Automotive Engineering, Aug 1994, p17.

13) KELDERMAN, H.
    Presentation to RRECOM progress meeting June 1995. DSM Resins, PO Box 6500,
    6401 JH Heerlen, The Netherlands.

14) ANON.
    LandfillTax Regime Takes Shape. Environmental Data Services Report 250, Nov 1995,
    p3.

15) ANON.
Environmental Data Services Report 246, Jul 1995, p23.

16) BENSON, M.
Disposal of Thermosetting Plastics. PhD thesis, The University of Nottingham, Oct 1993.

17) ROYAL COMMISSION ON ENVIRONMENTAL POLLUTION.
Seventeenth Report: Incineration of Waste. May 1993, HMSO, p97.

18) EUROPEAN COMMISION
Draft proposal on End of Life Vehicles. Reported in Environmental Data Services Report 252, Jan 1996, p42.

19) FARRISSEY, W.J.
Thermosets. in Plastics Recycling, Products and Processes.
Ehlig, R.H. (Ed) Hanser, 1992, p233.

20) PICKERING, S.J.
Personnel Communication, July 1994. The Department of Mechanical Engineering, The University of Nottingham, University Park, Nottingham.

21) HNAT, J.G. et AL
Recycling of Auto Shredder Fluff into Value Added Glass Products. Proceedings of the 8th Advanced composites Conference, Chicargo, Illinois, USA, 2-5 Nov. 1992.

22) Reference 7, p11.

23) DAY, M.
Auto Shredder Residue - a Waste or Valuable Resource?. Automobile Life Cycle Tools and Recycling Technologies, SP-966. Publ SAE, Mar 1993, p73-80.

24) CARDEW, BILL.
Personal Communication, June 1995. Croxton + Garry, Curtis Road, Dorking, Surrey.

25) PETTERSSON, J.   NILSSON, P.
Recycling of SMC. 48th Annual Conference, Composites Institute, The Society of the Plastics Industry, Inc Feb 8-11, 1993, paper 15-F.

26) KITAMURA, T.
Recycling Thermosets in Japan Update - Tertiary Report. 48th Annual Conference, Composites Institute, The Society of the Plastics Industry, Feb 8-11, 1993, paper 15-E.

27) BLEDZKI, A.K.   KUREK, K.   KASSEL, C.H.
Properties of SMC's with Regrind. Kunstoffe German Plastics 82 (1992), 11, p14-16.

28) KAWAMURA, N. ICHIKAWA, S.
Effective Re-utilisation of Material in the Field of plastic Automotive Parts Recycling. Recycle' 94, March 14-18, 1994, Davos, Switzerland. Paper 10-8.

29) KONIG, U. BUHL, D. MOBIUS LUDWIGSHAFEN, K.H.
Particle Recycling Guarantees the Future of SMCs.
Kunstoffe German Plastics, 82 (1992) 8, p21-23.

30) SCHAEFER, P.
Personal communication, 21 October 1994. ERCOM Composite Recycling GmbH, Kunststoffaufbereitung, Rastatt, Germany.

31) SIMS, B., BOOTH, C.A., LAKSHMANAN, V.I.
Process for Separating Fibres from Composite Materials. International Patent B03B 9/06, B29B 17/02.

32) KAMINSKY, W.
Re-use of Rubber and Plastics by Pyrolysis.
Proceedings Davos Recycle '93, Davos Switzerland, Mar 22-26, 1993.

33) KOMATSU, N. and USHIKOSHI, K.
Recycling of CFRP. Proceedings, 23rd FRP Symposium. Polymer & Chemical Technology Laboratory, Kobe Steel Ltd, Kobe, Japan.

34) MITSUBISHI HEAVY INDUSTRIES
    a) ANON.   *Japan Advances in FRP Recycling.* Reinforced Plastics, Feb. 1994.
    b) ANON.   *Energy Recycling.* Plast. Ind. News - Japan, May 1993.
    c) ANON.   *How to incinerate Reinforced Plastics Without Destroying the Glass Inside.* Chemical Engnrg, Mar 1994.

35) PATEL, S.H. et AL
Alternative Procedures for the Recycling of Sheet Molding Compounds.
Advances in Polymer Technology, Vol.12, No.1, 1993, p35-45.

36) HANSON, D.G.
Recovery of Fiberglas Reinforcement and Additive Materials from Scrap Circuit Board Laminates. 46th Annual Conference, Composites Institute, The Society of the Plastics Industry, Inc. Feb 18-21, 1991, Paper 18-E.

37) KITAMURA, T.
Challenge for Recycling Technologies of FRP in Japan.
Composites Plast. Renf. Fibres Verre Text, n6, Nov/Dec 1993, p17-20.

38) KITAMURA, T. HOSOKAWA, J. KOBAYASHI, Y.
Thermal Decomposition of FRP and Utilization of Residue.
Composites Plast. Renf. Fibres Verre Text, n6, Nov/Dec 1993, p21-24.

39) HAMADA, K. HOSOKAWA, J. NISHIYAMA, M.
Pyrolysis of Glass Fiber Reinforced Plastic Using Steam Stream.
Kobunshi Ronbunshu, v49, n8, Aug 1992, p661-669.

40) HAMADA, K.
Japanese Journal of Polymer Science and Technology, v49, n8, 1992, p89-91.

41) STANWORTH, J.E.
Physical Properties of Glass. Oxford University Press, 1950, p89-91.

42) THOMAS, W.F.
An Investigation of the Factors Likely to Affect the Strength and Properties of Glass Fibres. Physics and Chemistry of Glasses, v1, n1, Feb 1960, p4-18.

43) SAKKA, S.
Effects of Reheating on Strength of Glass Fibers.
Bull. Inst. Chem. Res, 1956, v34, p316-320.

44) SOH, S.K. LEE, D.K. CHO, Q. RAG, Q.
Low Temperature Pyrolysis of SMC Scrap. Proceedings of the 10th Annual ASM/ESD Advanced Composites Conference, Dearborn, Michigan, USA, 7-10 Nov 1994, p47-52.

45) J. R. KENNERLEY, N. J. FENWICK, S. J. PICKERING AND C. D. RUDD.
The Properties of Glass Fibres Recycled from the Thermal Processing of Scrap Thermoset Composites. Antec '96, Indianapolis, May 1996.

46) BLEDSKI, A., SPAUDE, R., EHRENSTEIN, G.W.
Corrosion Phenomena in Glass Fibers and Glass Fiber Reinforced Thermosetting Resins. Composites Science and Technology 23 (1985), p263-285.

47) METCALFE, A.G. GULDEN, M.E. SCHMITZ, G.K.
Spontaneous Cracking of Glass Filaments. Glass Technology, v12, n1, 1971, p15-23.

48) HONGY, LIN. et AL.
The Effect of Fibre Annealing on the Properties of an Optically Transparent PMMA Composite. Composites Science and Technology, v50, n3, 1994, p367-372.

49) PEARSON, A.G.N., VICKERS, M.A., MILNER, C.N.
Fluidised Bed Combustion Tests on Coal/GRP. Coal and Energy Services, Coal Research Establishment, Report No. 370055, July 1991.

50) COAL AND ENERGY SERVICES.
An Assessment of Gaseous and Particulate Emissions from a Fluidised Bed Boiler at Sutton Bonington. Report No. 372240/ZH09, April 1993.

51) VICKERS, M.A and MILNER, C.N.
A Commercial Demonstration of Reduced NO_x and SO_2 Emissions from a 1.8MW Industrial Fluidised Bed Boiler. FBC Technology and the Environmental Challenge, 5th UK FBC Conf, London, 1991.

52) RUBIERA, F. GARCIA, F. FUERTES, A.B. PIS, J.J. ADANEZ, J.
Characterisation of the Reactivity of Limestone with SO_2 in a Fluidised Bed Reactor. Proceedings of 11th International Conference on Fluidised Bed Combustion, Montreal, ASME 1991, p1493.

53) FENWICK, N.J. & PICKERING, S.J.
Using Waste Material to Reduce Emissions - Combustion of Glass Reinforced Plastic with Coal in a Fluidised Bed. Conference on Engineering Profit from Waste IV, 9-11 November 1994, I Mech E, London.

54) STRAUSS, W.
Industrial Gas Cleaning, Pergammon Press, 1966, p172.

55) LY, J.L.
Curing of Compression Molded Sheet Molding Compound. Polymer Engineering and Science, v21, n8, Mid-June, 1981, p483-92.

56) PUSATCIOGLU, S.Y., FRICKE, A.L., HASSLER, J.C.
Variation of Thermal Conductivity and Specific Heat during Cure of Thermoset Polymers. Journal of Applied Polymer Science, v24, 1979, p947-952.

57) KUNII, D. LEVENSPIEL, O.
Fluidization Engineering, 2ND Ed. Butterworth-Heinemann, 1991, p324.

58) GASKELL, P.
Personal communication. Croxton + Garry Technical Centre, PO Box 1, Melton, N Ferriby, North Humberside.

59) CROXTON + GARRY.
Martinal® Product Specification. Croxton + Garry Technical Centre, PO Box 1, Melton, N Ferriby, North Humberside.

60) OWENS CORNING FIBERGLAS CORPORATION
Textile Fibers for Industry, p18. Owens-Corning World Headquarters, Fiberglas Tower, Toledo, Ohio 43659, USA.

61) OTT, H. J.
Thermal Conductivity of Composite Materials. Plastic and Rubber Processing and Applications, n1, 1981, p9-24.

62) DODDS, N.
Personal communication. Materials Division, Herschel Building, University of Newcastle-upon-Tyne, Newcastle.

63) MIYAZAKI, N., TAKEDA, N.
Solid Particle Erosion of Fiber Reinforced Plastics. Journal of Composite Materials, v27, n1, 1993, p21-31.

65) Reference 57, p314-318.

66) HOWARD, J. R. (Ed)
Fluidized Beds Combustion and Applications. Applied Science Publishers, 1983, p25.

67) HOLMAN, J.P.
Heat Transfer. McGraw-Hill, 1989, p134.

68) Reference 67, p159.

69) SULLIVAN, R.M.
A Coupled Solution Method for Predicting the Thermostructural Response of Decomposing, Expanding Polymeric Composites. Journal of Composite Materials, v27, n4, 1993, p408-434.

70) Reference 67, p165.

71) KEATTCH, C.
Introduction to Thermogravimetry. UMI, Michigan, 1994, p42-3.

72) THERMAL ANALYSIS CONSULTANCY SERVICE
Leeds Metropolitan University, Calverley Street, Leeds.

73) KENNERLEY, J.R.
RRECOM Progress Report, Dec 1995, p51.

74) ABERNATHY, R.B.
The New Weibull Handbook. 536,Oyster Road, North Palm Beach, Florida 33408, USA, 1993, p2-3.

75) Reference 74, p2-5.

76) KENNERLEY, J.R.
Strength of Fibres taken from SMC Heated at 350°C.
RRECOM Progress Report, June 1996, p32.

77) MLADEN S. LLIĆ, SIMEON N. OKA, DRAGOLJUB V. DAKIĆ.
Combustion Kinetics of Coal Chars in a Fluidised Bed.
Fluidised Bed Combustion, ASME 1995, v2, p1463-1468.

78) THYS, E.
Personal communication, Nov. 1995. European Owens-Corning Fiberglas SA, Route de Charneux 59, 4651 Battice, Belgium.

79) VERWYEN, N., RENZ, U., REINARTZ, A.
Measurements and Modeling of SO_2 Emissions from a Pressurised Fluidised Bed Combustor. Proceedings of 11th International Conference on Fluidized Bed Combustion, Montreal, ASME 1991. p1402.

80) SENARY, M. K.
NO_x Emission Studies in Fluidized-Bed Combustion. Proceedings of 11th International Conference on Fluidized Bed Combustion, Montreal, ASME 1991. p1399.

81) BARRON, L.S., WANG, J.C.Z., SCHÆFER, J.L., JONES, T.M., HASLER, J.R., COLLINS, D.J., ROBL, T.L.
AFBC Pilot Plant Test of Six Kentucky Limestones. Proceedings of the 9th International Conference on Fluidized Bed Combustion. v1, 1987, p476.

82) DAM-JOHANSEN, K., OSTERGAARD, K.
Kinetics of the Reaction Between Sulphur Dioxide and Limestone Particles in Fluidised Beds. Proc. 5th Eng. Found. Conf. on Fluidization, 1986, p571-8.

83) CHRISTOFIDES, N.J., BROWN, R.C.
Calcination and Sulphation of Coal-Water-Limestone Mixtures, Proceedings of 11th International Conference on Fluidized Bed Combustion, Montreal, ASME 1991. p1498.

84) HAMER, C.A.
Evaluation of SO_2 Sorbents in a Fluidised-Bed Reactor. Proceedings of the 9th International Conference on Fluidized Bed Combustion. v1, 1987, p459.

85) LOWRY, H.H. (Ed)
Chemistry of Coal Utilisation. Wiley, 1963, p883-4.

86) KHAN, W.U.Z., GIBBS, B.M.
The Effects of Bed Temperature and Oxygen Stoichiometry on Sulphur Dioxide Capture by Limestone in a Fluidised Bed Combustor. Proceedings of 11th International Conference on Fluidized Bed Combustion, Montreal, ASME 1991, p1503-10.

87) BOYTON, R.S.
Chemistry and Technology of Lime and Limestone. Wiley, 1980, p160-1.

88) LYNGFELT, A., LECKNER, B.
Sulphur Capture in Fluidised-Bed Combustors: Temperature Dependence and Lime Conversion. Journal of the Institute of Energy, Mar. 1989, p62-72.

89) BORGWARDT, R.H., BRUCE, K.R.
Effect of Specific Surface Area on the Reactivity of CaO with SO_2. AIChE Journal (v32, n2), Feb 1986, p239-246.

90) HAJI-SULAIMAN, M.Z., SCARONI, A.W.
Evaluation of the Properties for Fluidized-Bed Combustion. Proceedings of the 9th International Conference on Fluidized Bed Combustion, v1, 1987, p481-6.

91) DOUGLAS, E., SAYLES, C.P.
Dry Sorting Using Pneumatically Fluidized Powders. AIChE Symposium Series, n116, v67, p201-209.

92) NIENOW, A.W., ROWE, P.N., CHIBA, T.
Mixing and Segregation of a Small Proportion of Large Particles in Gas Fluidised Beds of Considerably Smaller Ones. AIChE Symposium Series, n176, v74, p45-53.

93) NIENOW, A.W., ROWE, P.N.
Fluidised Bed Mixing and Segregation in Solid Refuse Treatment. First International Symposium on Materials and Energy Recovery from Refuse, Antwerp, 1976, p131-42.

94) NAKAYAMA, J.
Operating Experience and Data on Revolving Type Fluidised Bed Incineration Plants. 14th Biennial National Waste Processing Conference, 3-6 June 1990, Longbeach, USA. ASME 1990, p211-220.

101

95) GREEN, D.W. (Ed)
Perry's Chemical Engineers' Handbook, 6th Edition. McGraw-Hill, 1984, p20-82 - 20-121.

96) WARD, J.
Control of Particulate Emissions from Industrial Furnaces and Boilers.
C.I.T lecture notes, 1989.

97) KUMAR, A., CHANDRA, Y., RAO, N.J.
Continuous Classification in Fluidized Beds.
J. Inst. Eng. India, Jun 1981, 61, CH3, p59-61.

98) STESSEL, R.I., PEIRCE, J.
Cyclones in Waste-to-Energy Production Facilities.
Journal of Energy Engineering, A. Soc. Civ. Enginrs, v110, n3, Sep 1984.

99) SYRED, N., BIFFIN, M., WRIGHT, M.
Vortex Collector Pockets to Enhance Dust Separation in Gas Cyclones.
Filtr. and Sep., Nov/Dec 1985, p367-370.

100) SCHMIDT, P.
Unconventional Cyclone Separators. Int. Chem. Eng., v33, n1, Jan 1993, p9-17.

101) ANON.
Proposal for a Council Directive on the Incineration of Hazardous Waste.
Official Journal of the European Communities, (92/C 130/01), Mar 1992.

Appendix 1
LITERATURE REVIEW OF THE USE OF SULPHUR DIOXIDE SORBENTS IN FLUIDISED BED COMBUSTION

A1.1 Coal Fluidised Bed Combustion Desulphurisation Sorbents.

Commercially, crushed and graded limestone or dolomite is added to a fluidised bed to capture sulphur dioxide from the combustion of coal.

A1.1.1 Sulphur dioxide reduction mechanism

On heating, calcium carbonate releases carbon dioxide during calcination to form calcium oxide as:

$$CaCO_3 \rightarrow CaO + CO_2$$
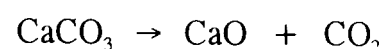
Subsequent sulphur capture from any available sulphur dioxide follows either of the following reactions[77]:

$$CaO + \tfrac{1}{2} O_2 + SO_2 \rightarrow CaSO_4$$

$$CaCO_3 + \tfrac{1}{2} O_2 + SO_2 \rightarrow CaSO_4 + CO_2$$
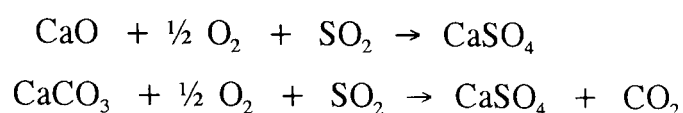
However, the reaction with lime takes place much faster than with calcium carbonate.

A1.1.2 Sorbent types

Commercial sulphur dioxide sorbents are either limestones or dolomites depending upon local availability. Limestones, although varying in composition, calcine on heating to produce more calcium oxide (percentage by mass) than dolomites[79,80], which contain significant quantities of magnesium oxide. However, some testing indicates that trace impurities found in dolomites act as a catalyst for the formation of calcium sulphate. Thus, some dolomites perform better than limestones, based on sulphur captured per unit weight of sorbent used[81].

A1.1.3 Sorbent particle size

Sorbents used in commercial operations (including pilot plants) referred to in the literature typically have particle sizes of: 1.0 to 3.0 mm[79], 0.85 to 1.00mm[81] and 0.80mm[49]. Whilst those tested in rig or laboratory scale experiments are quoted at: 0.78 to 2.00 mm[82], 3.125×0.600 mm[80], 1.59 mm to 1.0×0.5 mm[83] and 0.85 to 1.00 mm[84]. The

greater range merely reflecting the testing of different particle sizes.

Obviously, smaller particle sizes give a larger surface area, so that utilisation of small particles is more effective than that of larger particles. However, when the sorbent size is reduced, elutriation is more probable, leading to reduction of sulphur dioxide emissions in the freeboard rather than the bed itself. However, this effect will be small due to the short residence time in the freeboard[79], as fluidising velocities are typically 1 to 2 m/s.

A1.1.4 Boiler tube deposits

The theory of deposition formation within boiler tubes is well documented as follows[85]:

i) A thin oxide of the boiler tube metal forms on the tube surface between 315 and 427°C.

ii) Alkali-metal oxides, i.e. fuel impurities, react with sulphur trioxide to form sulphates, these are 'sticky' and adhere to the oxide layer.

iii) As the layer of sulphate deposits increase in thickness, the surface exposed to the flue gas becomes hot (being a poor conductor) and very sticky such that ash adheres to it. The high local temperature evolves sulphur trioxide in the ash layer.

iv) The sulphur trioxide defuses to the oxide or sulphate interface and reacts with the tube wall oxide, typically forming $Na_3Fe(SO_4)_3$. Such a reduction in the oxide layer results in the tube wall corroding further.

v) A further layer of sulphates stick to the outside of the ash and so the cycle continues.

This is confirmed by the analysis of the deposits formed on the boiler tubes at Sutton Bonington during previous testing by the Coal Research Establishment[49], which contained 14-18% sodium sulphate and 31-51% calcium sulphate.

A1.1.5 Nitrogen oxides emissions

A natural conflict exists between reducing sulphur dioxide and nitrogen oxides emissions. This is because nitrogen oxides emissions are decreased by combustion under reducing (i.e. no excess air) bed conditions and staged combustion. However, whilst calcium sulphate formation, or sulphur dioxide capture, is promoted by excess oxygen. There is a difference of opinion in the literature over the effect on nitrogen oxides emissions by reducing sulphur dioxide via the addition of limestone, which seems to be linked to a size effect moving from a laboratory to a pilot or full scale fluidised bed. For example, experiments with a 0.3 m

square fluidised bed rig[86], run with a calcium to sulphur ratio of 3:1 produced the following results:

Staged Air

This method (splits the required stoichiometric plus any excess combustion air between a primary and secondary injection) without limestone reduced nitrogen oxides emissions. However, as the ratio of secondary over-fire air to primary bed air was increased, sulphur dioxide gas emissions increased and became increasingly temperature dependent. Thus, increasing bed temperature from 830-850°C, with a sub-stoichiometric primary air-fuel (PAF) ratio of 0.84, increased the original sulphur dioxide gas emissions by 20%.

Air staging and limestone addition

The sulphur retention (in the ash or particulates) decreased as the PAF was reduced, for example sulphur dioxide gas emissions increased by 20% as the PAF decreased from 0.95 to 0.84. The testing on the Sutton Bonington boiler[49] at a bed temperature of 840°C and Ca/S of 3:1 had a sulphur dioxide reduction efficiency of 50%. Increasing the over-fire air from 16% to 30% made no difference to sulphur retention. Although, with a bed temperature of 900°C the limestone became ineffective at sulphur dioxide retention with over 16% overfire air. This demonstrates some complex size to temperature to PAF relationship.

A1.1.5 Calcium to sulphur (Ca/S) ratio

This is a molar ratio, the relative mass quantities of sorbent to coal feed rate depend upon the chemical composition. The Ca/S ratio will vary depending upon the stringency of emission standards, values of 2:1[49] up to 4.9[79] are quoted for commercial boilers.

Figure A1[52] shows the diminishing return in sulphur retention on increasing the Ca/S ratio, (the sulphur retention was calculated from the flue gas concentration of sulphur dioxide with and without sorbent addition into the fluidised bed combustion). Such a trend is typical throughout the literature. The high experimental retention percentages were obtained in this case in a small rig of 0.14 m internal diameter.
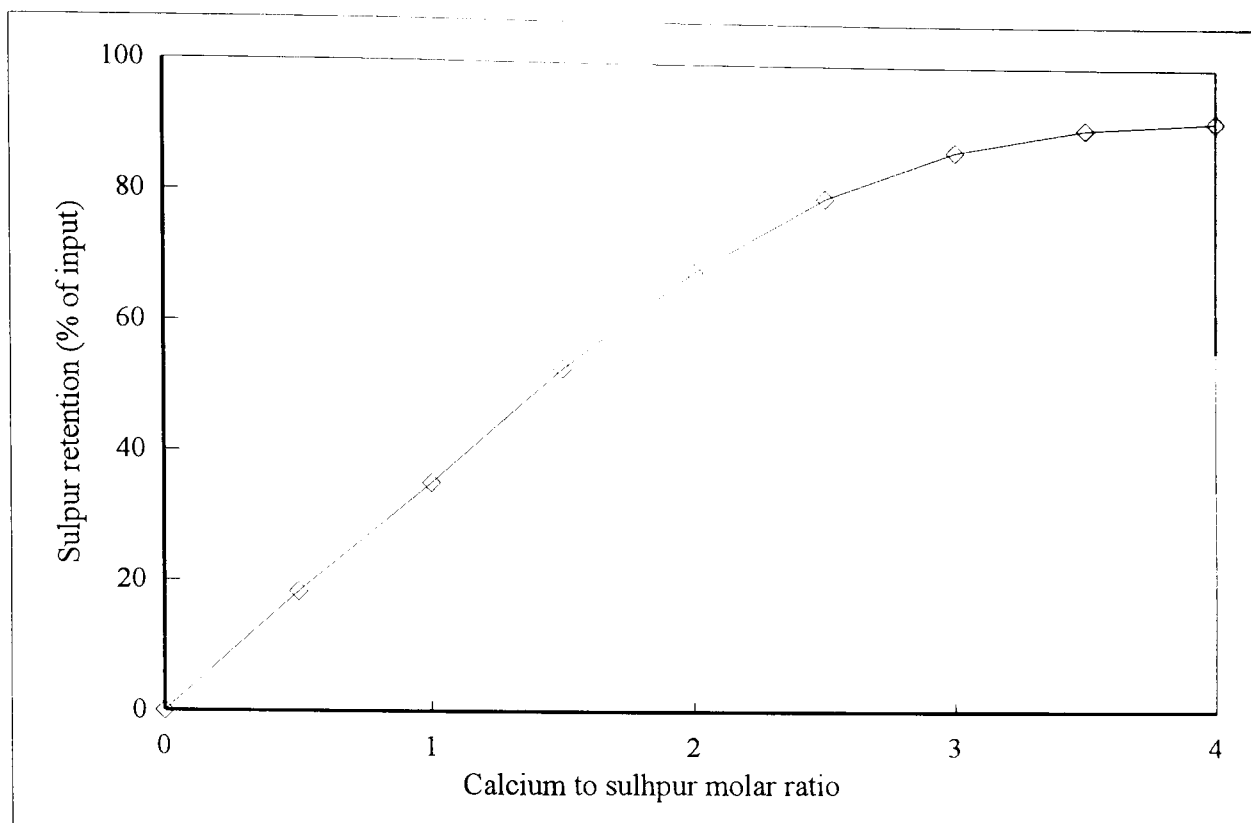
Figure A1   Sulphur Retention by Limestone as a Function of Ca/S Ratio[52]
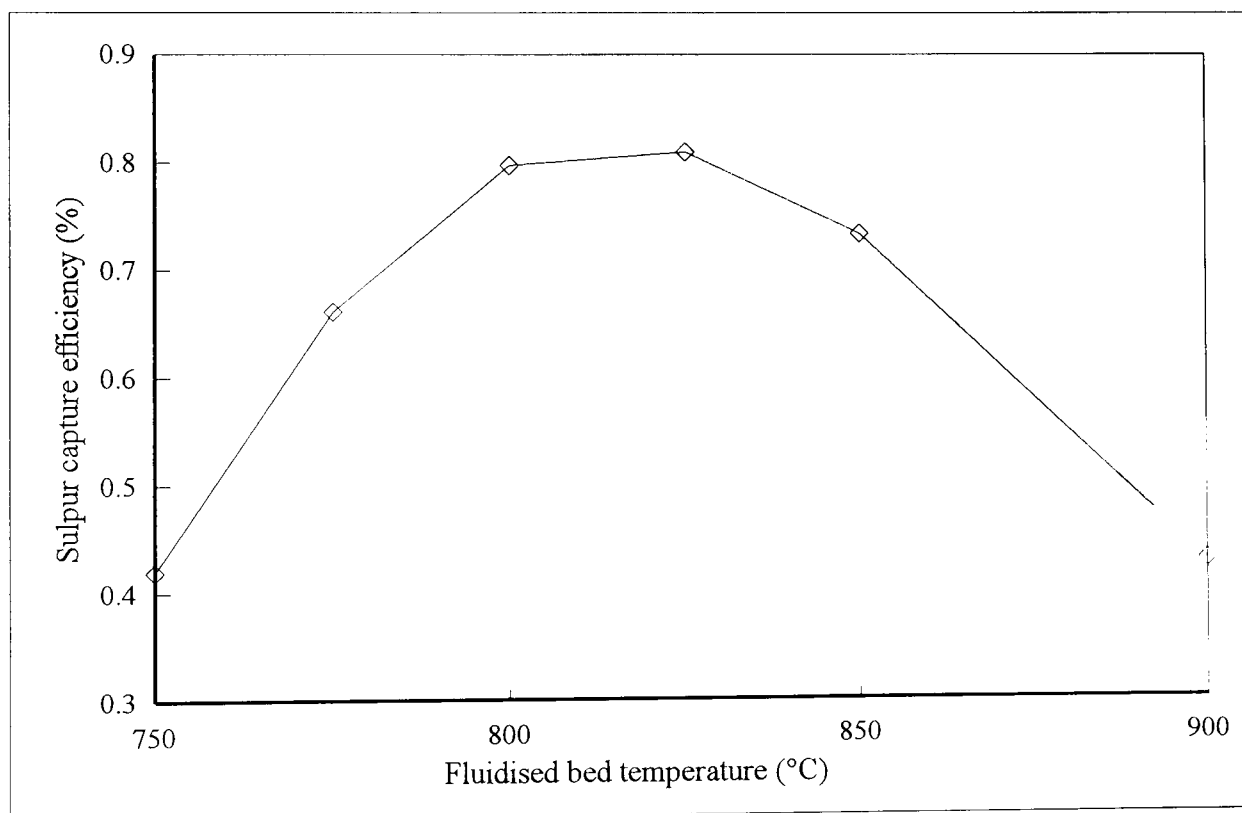
Figure A2   Fluidised Bed Sulphur Capture: Efficiency as a Function of Temperature[88]

A1.1.6 Temperature effects

The recognised dissociation temperatures for calcite and magnesite in 100% carbon dioxide atmosphere at one atmosphere pressure are 898°C and 725°C respectively[87]. However, these standards are misleading in that limestones and dolomites contain both minerals in varying quantities together with trace impurities which will all influence the minimum calcination temperature. Also, the rate of calcination is in part determined by the speed of diffusion of carbon dioxide from the solid surface. Thus the carbon dioxide partial pressure of the surrounding gas will be a rate influencing factor. The carbon dioxide partial pressure within a fluidised bed combustion will be much less than 100%, again changing the calcination temperatures.

Above the minimum calcination temperature, the sulphur capture efficiency of limestone is reported as having a strong temperature dependency, best illustrated by the review of previous literature[88], shown in figure A2. This shows that there is a rapid fall off in efficiency below 800°C and above 850°C bed temperatures. The Sutton Bonington boiler fluidised bed now operates between the target temperatures of 835° to 839°C to limit nitrogen oxides emissions and approximately at the optimum for sulphur dioxide emissions from figure A2.

A1.2 Composite Scrap as a Sulphur Dioxide Sorbent

- Depending on how the composite decomposes, the mineral filler could be much smaller than the commercial sorbents, influencing both reaction rate and particle residence time.
- The sulphur dioxide absorption is likely to occur in the freeboard which may be at a non-optimum temperature.
- The catalytic nature of naturally occurring mineral impurities is reduced due to the high quality of the filler.

A1.2.1 Introduction

No literature was found on the use of composites for the direct sorption of sulphur dioxide during combustion processes. The calcium carbonate filler in a composite matrix is likely to have significantly different reaction properties compared with crushed and graded limestone.

A1.2.2 Physical properties

The composite calcium carbonate filler is much more finely divided, at a mean particle size of 3 μm (range of 0 to 10 μm), than the crushed limestone utilised in most of the literature

(see above). Thus the reaction surface area will be much larger. However, the composite scrap decomposition process was unknown

One series of laboratory testing[89] considered the significance of the $CaCO_3$ grain size and the resulting specific surface area on the reactivity of lime with sulphur dioxide. The specific surface area being given by:

$$S_g = \frac{3}{r_g \cdot d_{CaO}}$$

Thus a composite filler particle of 3 μm with a maximum effective grain radius of 1.5 μm. Comparing this with 225 to 600 μm for limestones and 13 to 43 μm for dolomites[81], the composite filler has a specific area one order of magnitude greater than dolomites and three orders greater than limestones. However, mineral grain sizes vary widely depending on the origin of the mineral.

A1.2.3 Fluidised Bed Residence time

As mentioned above, the fine particles potentially produced on the break down of the shredded composite are expected to have a short bed residence time. This effect will be accelerated by calcination which reduces the particle density[83], thus increasing the likelihood of elutriation.

Figure A3[89] shows the percentage conversion to lime for small, 3.4 to 14 μm, limestone particles and how it varies with residence time. Although the conversion only appears to be in the order of 20%, this may well be compensated for by the potentially large surface area of lime for reaction compared with a limestone sorbent.

One method of increasing effective residence time within the bed or freeboard is to recirculate the elutriated particles. Analysis of particulate samples before flue gas cleaning would determine the proportion of free lime and or calcium carbonate available in the fines.

A1.2.3 Temperature effects

With reference to figure A2, it must be remembered that the bulk of sulphur dioxide capture is expected to take place within the freeboard. The freeboard temperature at Sutton Bonington has been measured as being 15 to 45°C above bed temperature[49]. Thus the sulphation

108

efficiency may be reduced by the reaction taking place at a temperature above optimum.
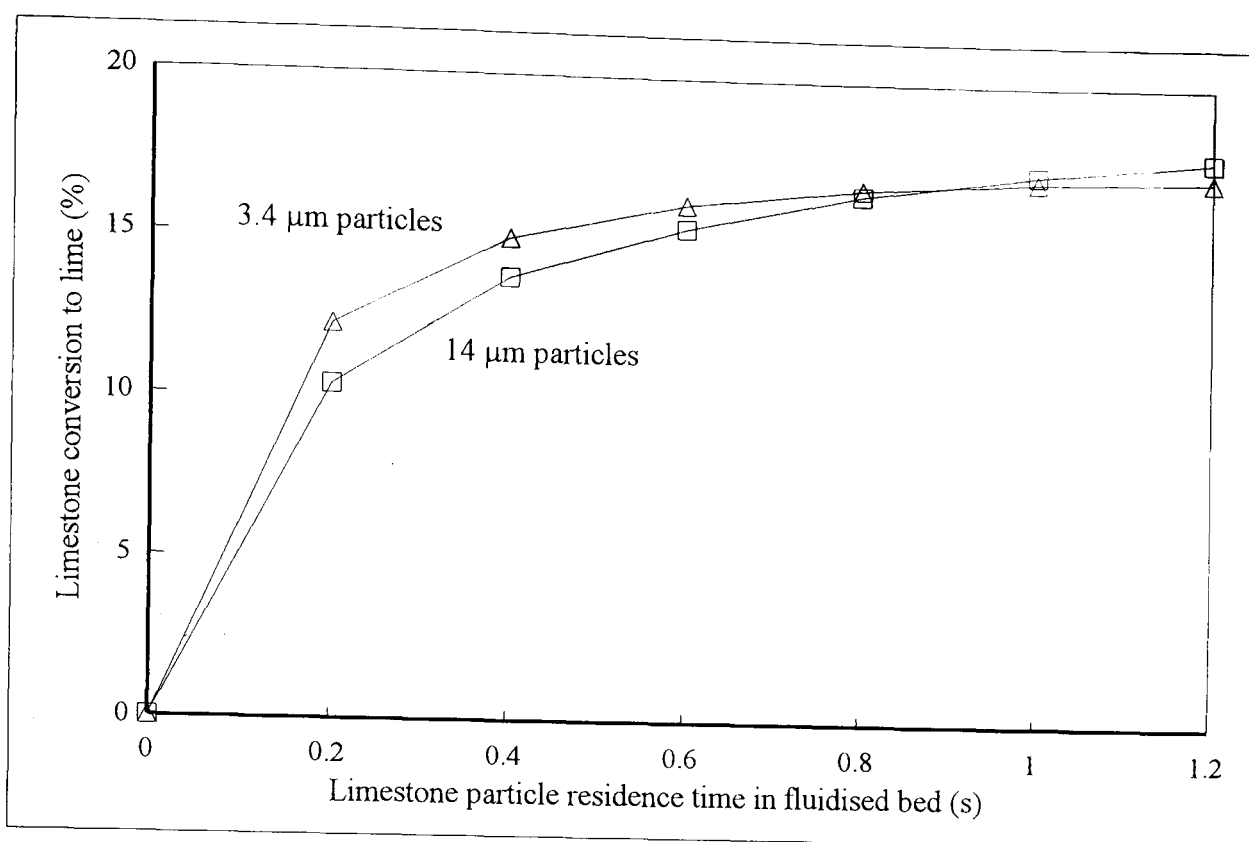
Figure A3   Fine Particle Limestone Conversion to Lime against Residence Time[89]

A1.2.4 Chemical composition

The high purity of the calcium carbonate filler may well prove to be a disadvantage, as impurities such as iron oxide (Fe_2O_3) effectively catalyses the sulphation reaction. It is thought that the impurities delay the blocking of the calcine surface pores by $CaSO_4$, thus enabling greater penetration by the sulphur dioxide to the unreacted lime[90]. The composite filler contains 0.02% iron oxide compared with 0.12 to 1.09% in the literature[90] for limestones.

A1.2.5 Deposition

The increased flow of particulates, elutriated filler and glass ash, through the boiler tubes is likely to escalate the formation of deposits. This was the case when testing with limestone injection[49]; although, that testing lasted for six weeks before significant build up occurred. It is suggested that the formation of sodium sulphate could be avoided by the addition of Kaolin or China Clay[49] into the fluidised bed which would react preferentially with the sodium oxide. The alumina trihydrate fire retardant present in some composites may perform a similar function.

109

Appendix 2

ECONOMIC ANALYSIS OF REDUCTION OF SULPHUR EMISSIONS USING COMPOSITE AS A SORBENT

Table A1   Cost Analysis Based on Low UK Landfill Charges (1994)

(costs based on high German landfill charges in parenthesis)

	Coal Fired	Coal + Limestone	Coal + composite
Coal input (tonne)	1.0	1.0	0.94
Coal cost (£)	**51**	**51**	**47.9**
Inert ash (kg)	25	25	23.5 + 66.7 glass
Inert Ash Disposal cost @ 2.9p/kg (£) **(12.6p/kg) (£)**	**0.73** **(3.15)**	-	-
Sulphur input (kg)	12.8	12.8	12.03
Ca/S ratio	0	4.1:1	4.23:1 initial 4.5:1 final[(i)]
Sorbent required (kg)	0	128	285
Sorbent cost (£)	**0**	**1.8**	**12.7[(ii)]** **(-14.91)**
Heat input compared with 1t coal (%)	0	0	6
Coal input reduction (kg)	0	0	60
Sulphur retained (%)	0	69	69
Sulphur dioxide emitted (kg)	25.6	7.94	7.46
Active ash (kg)	$CaSO_4$	0	38	35.3
	CaO	0	18.5	61.3
	Total (inc. inert)	0	81.5	186.8
Active Ash Disposal cost @ 3.3p/kg (£) **(25.2p/kg) (£)**	**0**	**2.69** **(20.54)**	**6.16** **(47.07)**

Notes

i: The heat content of the composite (assumed to be an average of the Sheet Moulding

110

Compound and Dough Moulding Compound used during the Sutton Bonington test work) reduces the coal demand slightly. This effectively increases the Ca/S ratio, therefore a lower ratio, than required to achieve a retention similar to the limestone case, was initially assumed.

ii: The sorbent cost for the crushed composite includes the cost of crushing at £73.7/tonne, this would probably reduce under commercial operation. Also included is the cost saving of not landfilling the scrap composite at inert waste rates.

Appendix 3
LITERATURE REVIEW - FLUIDISATION AND SEPARATION TECHNIQUES

A3.1 Introduction

This review was undertaken to appraise fluidised bed processing for simultaneous combustion and material separation of composite scrap. The basis of this search followed two separation concepts: in-bed separation of residues from thermally treated composites and particulate separation from combustion gases including cyclone designs. It was recognised that the most appropriate material recovery methods may be different at different operating conditions and could well be a combination of in-bed and gas separation techniques.

A3.2 In-bed Separation

Since the bed material effectively behaves as a fluid, particle density governs the vertical distribution within the bed for bed material and any added solids. If the composite were processed at relatively low temperatures, the burnt-off volatiles could be combusted separately (at high temperatures for higher combustion efficiency) to provide process heat. The remaining fibres and fillers may be induced to sink or float within the fluidised bed, enabling the separation and potential collection at different bed heights[91,92,93]. This incombustible fraction would be intact, subject to in-bed attrition. This depends upon the fluidising velocity and the residence time of the incombustible materials. A number of parameters are cited in the literature as being relevant to fluidised beds as a separation medium:

Density
If the density of the fluidising medium is between the densities of the constituents of a two component mixture (e.g. fibre and filler), then one component will tend to float and the other will collect on the bottom of the bed.

Size
The initial size of the composite feedstock is not critical as the fluidised bed attrition will help the material breakdown[94]. The bed material size is a critical parameter, together with density,

the bed material size governs the fluidising conditions. For example, a small size will readily fluidise at gas velocities too low to cause appreciable elutriation and thus enhance in-bed separation.

Shape

Plate-like material (e.g. crushed panels) of low density will tend to float on a bubbling bed surface like a raft[91]. However, a vigorously bubbling bed will throw sand on top of such a raft, sinking it to a lower level. Large plates (25 mm square) were found to float at the density directed height in the vertical plane, but sink to and stay on the bottom in a horizontal attitude[92]. This need not be a problem, as on volatiles mass loss, the plates will break down into fillers and fibres, aided by the bed circulation. The breakdown will occur from the exterior inwards - smoothing the plates into lozenge shapes, that would behave differently from plates. No literature was found on the behaviour of needles or fibres within fluidised beds.

Fluidising Conditions

Reduced fluidising velocity results in reduced turbulence, this increases the viscosity and aids separation[91].

A3.3 Solid Collection and Separation from Exhaust Gases

The collection of elutriated fillers and fibres the outlet gas stream should be possible by standard gas cleaning equipment[95,96]. Several types of equipment may be used depending on particle size. The smaller the particle size to be collected - the greater the installation and running costs.

Table A2   Comparison of Gas Cleaning Equipment

Equipment Type	Practical Duty Limits[95,96]
Gravity settling chamber	size $> 43\mu$m, speed < 3m/s
Fabric Filter	size to 1μm
Impingement separator	size > 10-20μm
Cyclone	5-20μm $<$ size $< 200\mu$m

The size distribution of the cyclone fines, with and without composite addition, was determined from samples taken during the Sutton Bonington tests. The fines, calculated via mass balance, attributable to incombustible residue from the composite secondary fuel were sized at 23 μm.

An extension of particulate collection could be simultaneous separation or classification. The simplest form of which is to collect solids at different heights within the freeboard[97].

A3.3.1 Cyclones

Cyclones are compact, low capital and operating cost devices. The contaminated air enters tangentially at the top of the cyclone, spirals downward in an annular vortex, before returning up the centre in a cylindrical vortex, leaving axially near the inlet. Particles are separated by from the gas flow by loss of momentum, often by contacting the cyclone inner wall and sliding down within the boundary layer to a collection hopper. The actual flow regime within a cyclone is contested and different theories, often empirical in nature, apply with varying accuracy to different applications[98].

The lower particle separation size limit or 'cut' is defined when the centrifugal force acting on a particle is balanced by the drag force of the centre vortex. A cylindrical shell, the same diameter as the outlet, of such border-line particles can be imagined. Larger or heavier particles would not be able to approach the exterior of the shell, being centrifuged toward the wall. Smaller or lighter particles would be swept through the shell with the cleaner gases and exit the cyclone.

Cyclone design for elutriated filler and fibre separation

It can be seen from the above table that cyclones are usually thought of as being unable to capture material of small sizes. This may exclude the calcium carbonate filler of 3 micron average grade. Also, the behaviour of a fibre, of small diameter and mass, but large aspect ratio is uncertain. One report[98] exposes the inadequacy of classical cyclone design theory when applied to the large, low density and irregular output from a domestic rubbish incinerator, away from the often assumed granular particulates. Re-entrainment of large particles is cited as the biggest problem for this application.

Research into extending the use of cyclones and increasing efficiencies at the operating limits

is reported in the literature. This work concentrates on removing particles from the cyclone wall to prevent re-entrainment[99] via "collector pockets". These are effectively secondary cyclones joined to the main via a slit inlet. Other work aims to improve separation at the cut shell[100] via a cylindrical insert (of slotted or mesh construction). Such devices work well with uniform material but are untested on airborne fibres of varying length - the likely output from crushed composite.

Differently sized, sequential cyclones could be designed to collect different size fractions from the elutriated incombustible residue. Whilst incorporation of more than one vortex collector pockets[99] at different heights within a cyclone, could classify in a single device. It is probable that the optimisation of a material recovery system would be a trial and error process.

However, such material recovery equipment alone is unlikely to satisfy flue gas emission regulations. For example EC guidelines for the incineration of hazardous waste[101] report that a cyclone is inadequate as a final stage for particulate clean-up. Thus for commercial operation some bag filter stage would probably be required downstream of the material recovery stage.

Appendix 4
TECHNICAL RIG DESIGN

A4.1 Fluidisation Theory

A fluidised bed is formed by the upward flow of a fluid, often air, through a layer of particles (e.g. sand). If the flow is sufficient, the particles are suspended in the air stream and the layer of solids behaves similarly to a fluid. This layer has a high heat transfer rate, due to transient solid to solid conduction over a large surface area. This, combined with the churning action produced by the air bubbles passing through the bed, makes it an ideal combustion medium.

A4.2 Fluidised Bed Distributor Design

The fluidised bed reactor was designed as laid out in Kunii (reference 57 from page 69), starting with finding the minimum fluidisation velocity, U_{mf} from:

$$\frac{1.75}{\varepsilon^3 . \phi_s} \left(\frac{dp . U_{mf} . \varrho_g}{\mu} \right)^2 + \frac{150 . (1-\varepsilon)}{\varepsilon^3 . \phi_s^2} \left(\frac{dp . U_{mf} . \varrho_g}{\mu} \right) = \frac{dp^3 . \varrho_g . (\varrho_s - \varrho_g) . g}{\mu^2}$$

At the design point of bed temperature of 600°C, quadratic solution of this equation gives a minimum fluidising velocity of 0.22 m/s. In practice, commercial beds operate between 1 and 2 m/s. Therefore a design operating velocity of 1.5 m/s was chosen. Such an increase above the minimum ensures that the bed will be fully and evenly fluidised during operation.

The bed pressure drop is given by:

$$\Delta P_{bed} = h . (1-\varepsilon) (\varrho_s - \varrho_g) . g = 2.3 \ kPa$$

The distributer pressure drop is usually 0.3 of the bed pressure drop (reference 57, p102), increasing this value will provide more even air distribution. A factor of four times this rule of thumb (i.e. 1.2 times) was arbitrarily chosen to ensure good distribution. Thus, the distributor pressure drop is:

$$\Delta P_{dist} = 6.2 \ kPa$$

Calculation of the distributer jet velocity is as follows:

The distributor Reynolds number:

$$Re_{dist} = \frac{D.1.3.U_{mf}.\varrho_g}{\mu} = 6190$$

The distributor orifice coefficient:

$$Cd_{orif} = 0.7 + (Re_{dist} - 300)\left(\frac{0.68 - 0.7}{200}\right) = 0.111$$

The distributor orifice velocity:

$$U_{orif} = Cd_{orif}\sqrt{\frac{2.\Delta P_{dist}}{\varrho_g}} = 13.1 \ m/s$$

The jet velocity should be kept below 40 m/s to avoid excessive in bed attrition. Keeping the jet velocity down will also keep the attrition of the fibres to a minimum. Even at a nominal maximum temperature of 840°C, the softening temperature of E-glass, and a high fluidising velocity (2 m/s) the jet velocity is calculated as 22.4 m/s.

The operating velocity to orifice velocity ratio is:

$$\frac{U_{op}}{U_{orif}} = 0.114$$

This ratio is also the required porosity of the distributor (11.4%). For simplicity, a perforated plate was chosen for the distributer, this meant that the jet hole size had to be smaller than the bed particle diameter to prevent the particles falling through. Commercially available perforated plate did not have holes that small - thus a plate assembly was devised. The assembly was formed of two stainless steel plates with 3.17 mm diameter holes and a porosity of 32%. These sandwiched a layer of stainless wire mesh of 0.51 mm aperture (37% porosity) giving a combined porosity of 0.11%.

A4.3 Cyclone Design

Textbook designs of cyclones begin with the assumption that the particles to be removed from an air stream are approximately spherical. This may be the case for elutriated filler particles,

117

but is not the case for fibres.

A4.3.1 Design point particle size

Ideally, the design of a cyclone would follow on from accurate determination of the sizes of elutriated particles or fibres. Without this information, a cyclone design was investigated with the following particle sizes:

3 μm: Minimum size of calcium carbonate filler in the Sheet Moulding Compound tested.

10 μm: Maximum size of calcium carbonate filler in the Sheet Moulding Compound tested.

15 μm: Average diameter of reinforcing fibres.

23 μm: Size of particles in Sutton Bonington cyclone fines from combustion of composite scrap.

By comparison, the spherical particle size having a mass equivalent to a fibre 13 mm long of 15 μm diameter would be 0.44 mm. N.B. the cyclone collection efficiency for such a large particle would be 100%.

A4.3.2 Cyclone design

One semi-empirical design methodology[96] for a Stairmand type cyclone separator is governed by the equations:

Pressure coefficient,
$$Z = \frac{2 \cdot \Delta p}{\rho_g \cdot u^2}$$

(Z=5.2 for high efficiency, Z=6.0 for high throughput)

Stokes number,
$$N_{st} = \frac{d^2 \cdot \rho_s \cdot u}{9 \cdot \mu \cdot D}$$

The collection efficiency of a cyclone design can be found by equating the Stokes number for the design to a standard design that has been tested experimentally. The efficiency, for a given particle diameter is then read from the experimental curves. The inlet velocity is limited to a maximum of 25 m/s for applicability of this design method. The design parameters of:

device pressure drop, particle size and air flow rate are investigated in figures A4 and A5 at a gas temperature of 300°C.
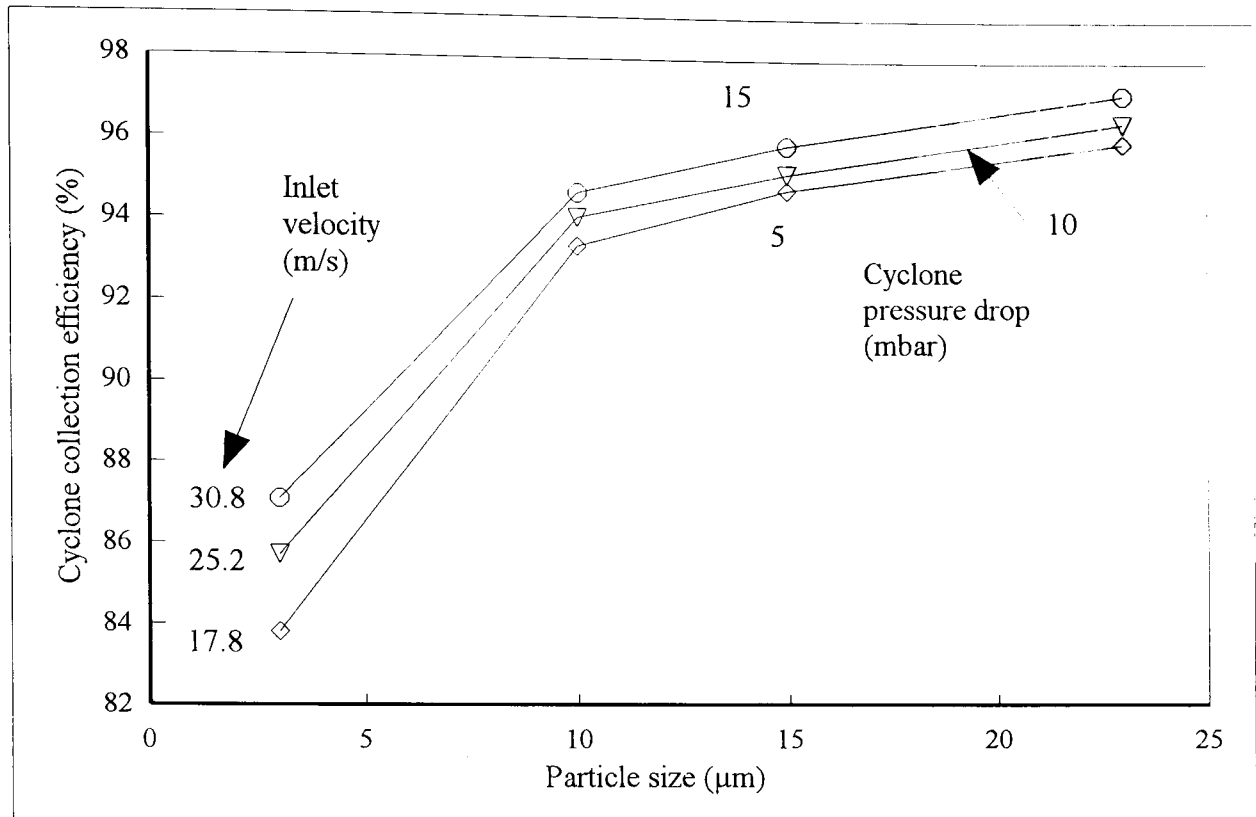
Figure A4   Cyclone Collection Efficiency Variation with Particle Size for 0.02kg/s Mass Flow
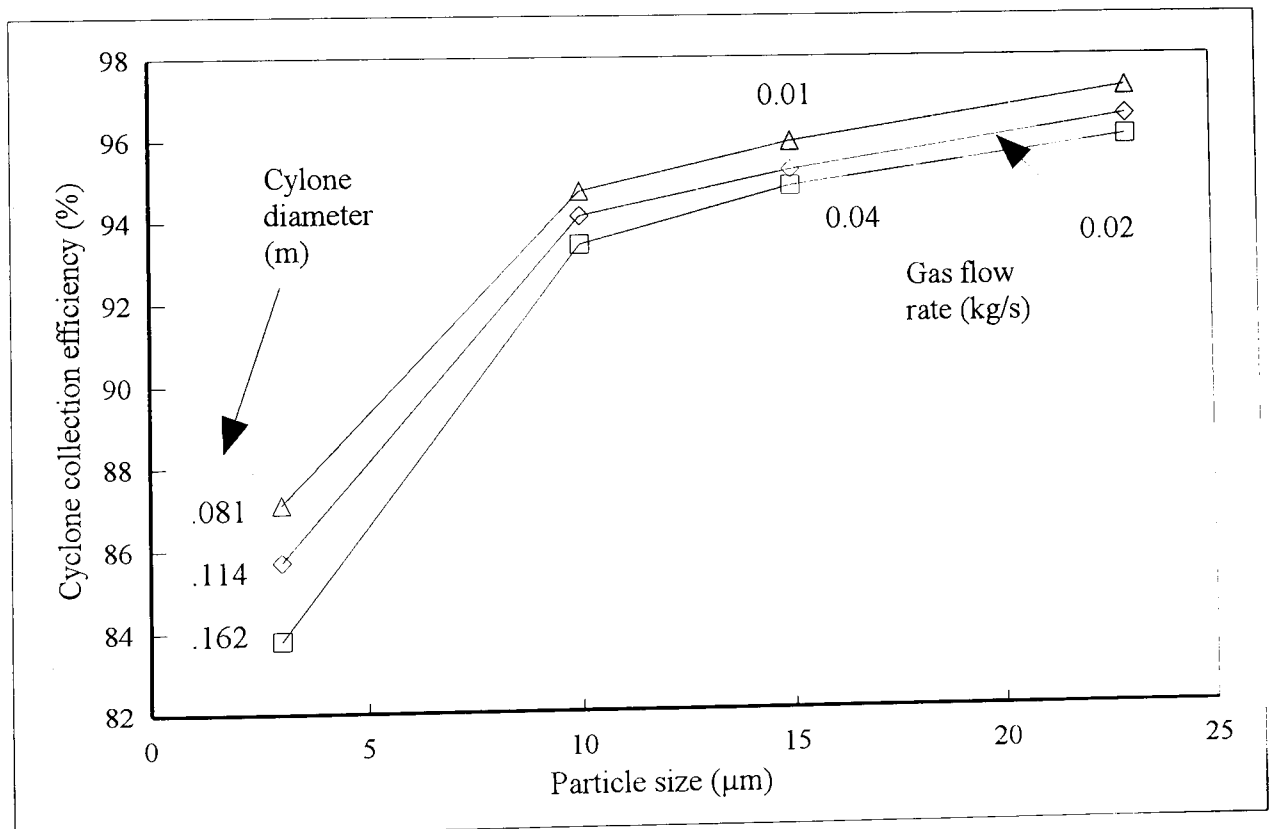
Figure A5   Cyclone Collection Efficiency Variation with Particle Size for 10mbar Pressure Drop

Figure A4 shows how cyclone collection efficiency varies with particle size. The efficiency increases with increasing particle size and pressure drop. For the inlet velocity to be below the design maximum 25 m/s, it can be seen in figure A4 that the pressure drop must be maintained below approximately 10 mbar. This limits the maximum collection efficiency to 95% for a 15 μm particle. The apparent further increase in efficiency above 10mbar is questionable, as the Stokes equation is no longer valid at such velocities. The velocity into the cyclone separator should be limited from a practical point of view, to avoid excessive wear or damage of the fibres.

Figure A5 investigates the effect of varying gas flow rate at the 10mbar maximum pressure drop, identified from figure A4, for the assumed particle size range. With a fixed pressure drop, the collection efficiency reduces slightly with increasing gas flow. The effect on cyclone diameter is also shown, for a larger flow rate, a larger diameter is required to result in the same cyclone pressure drop. A reasonable cyclone diameter is recommended to prevent the clogging of the tapered outlet of the cyclone. Only for the very small particle size of 3 μm does the collection efficiency tail off. However, all the efficiencies calculated are above 80%.

A cyclone, was designed from figures A4 and A5 for a gas mass flow rate of 0.02 kg/s at 300°C with a pressure drop of 10 mbar. The internal diameter was 114 mm and height was 456 mm. This was constructed at an early stage in the experimental investigations. During the test work described in Chapter 5 the small cyclone was operating far from the design point conditions. The actual mass flow was over twice the design at bed conditions of 450°C: 1.3 m/s. Thus the inlet velocity was above the 25 m/s limit, such that the theoretical collection efficiencies could not be calculated.

However, the above figures show that collection increases with increasing flow and device pressure drop. This was confirmed by the high rates of incombustible material achieved experimentally. Thus the cyclone was used on both phases of the test rig.

Appendix 5
FLUIDISED BED COMBUSTION TEST RIG
OPERATING PROCEDURE

A5.1 Pre - Run Checks

- Rig only to be run in combustion mode during the normal staff working hours of 08:00 to 18:00.

- Inform the L4 superintendent or technician staff prior to commencing running.

- Check that a fire extinguisher is in position outside the test cell area. Ensure that a respirator is available in the test cell and you know how to use it.

- Ensure that the data logger is switched on in the observation cell and all the rig thermocouples or parameters are being monitored. Plug in the data logger alarm output signal transformer.

- Ensure that the preheater isolation switch is off.

- Check the setting of the heater element over-temperature safety controller, maximum setting 800°C.

- Shut, lock and remove the keys from the control cabinet.

- Check that the test cell air valve is in the off (horizontal) position.

- Switch on the power supply to the pressure transducers.

- Visibly check the condition of the rig seals.

- Check that the exhaust gate valve is open.

A5.2 Running the Rig

- Start the compressor (ear defenders required in the compressor plant room), refer to the compressor plant operating procedure.

- Start the air extraction fan.

- Open valve for hopper cooling air bleed.

- Switch on the heater control panel.

- Adjust the temperature controller parameters as required.

- Open the air valve slowly until the 'Air-On' light is illuminated. (The air-on pressure switch trip level can be adjusted by a screw on the back of the pressure switch housing).

- Adjust air flow rate for required orifice plate pressure drop.

- Visibly check that the bed is fluidised.

- When ready, press the 'Heater-On' buttons on the control panel, the relays should latch audibly.

- Stabilise at the temperature set point as required.

- During running, check frequently: - orifice plate pressure drop.

  - feed screw (if used) is rotating.

- Keep test cell light on except when checking bed.

- Complete the planned test work. The rig must be manned during the input of any composite material.

A5.3   Shutting Down the Rig

- Switch off the screw feed (if used).

- Isolate heater control panel.

- Allow a suitable period with airflow on to purge the system and cool down.

- Turn off air with the test cell valve.

- Shut down the compressor, refer to the compressor plant operating procedure.

- Shut off extraction fan.

- Inform the L4 superintendent or technician that rig testing is complete.